

AD A058827

LEVEL II

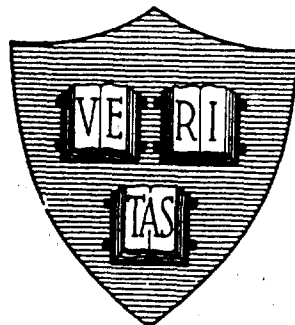
12

Office of Naval Research

Contract N00014-75-C-0848

NR-372-012

**ELECTRICALLY SMALL LOOP ANTENNA LOADED BY A
HOMOGENEOUS AND ISOTROPIC FERRITE CYLINDER-PART II**



By

D.V. Giri and R.W. P. King

July 1978

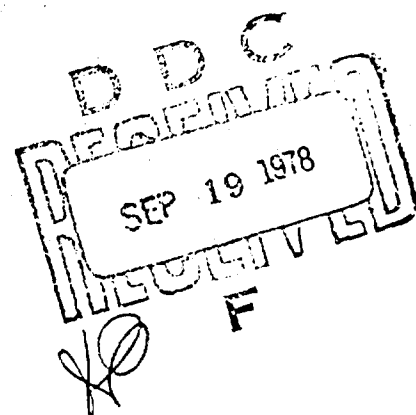
Technical Report No. 668

This document has been approved for public release
and sale; its distribution is unlimited. Reproduction in
whole or in part is permitted by the U. S. Government.

Division of Applied Sciences

Harvard University

Cambridge, Massachusetts



DDC FILE COPY

AD A058827 046

Unclassified

SECURITY CLASSIFICATION OF THIS PAGE (When Data Entered)

REPORT DOCUMENTATION PAGE		READ INSTRUCTIONS BEFORE COMPLETING FORM	
1. REPORT NUMBER Technical Report No. 668 ✓ (14) TR-668		3. RECIPIENT'S CATALOG NUMBER	
4. TITLE (and Subtitle) ELECTRICALLY SMALL LOOP ANTENNA LOADED BY A HOMOGENEOUS AND ISOTROPIC FERRITE CYLINDER. PART II.		5. TYPE OF REPORT & PERIOD COVERED Interim Report	
7. AUTHOR(s) D. V. /Giri R. W. P. King		6. PERFORMING ORG. REPORT NUMBER	
9. PERFORMING ORGANIZATION NAME AND ADDRESS Division of Applied Sciences Harvard University Cambridge, Massachusetts		8. CONTRACT OR GRANT NUMBER(s) N00014-75-C-0648 N00014-67-A-0298- 12 124p	
11. CONTROLLING OFFICE NAME AND ADDRESS		10. PROGRAM ELEMENT, PROJECT, TASK AREA & WORK UNIT NUMBERS	
14. MONITORING AGENCY NAME & ADDRESS (if different from Controlling Office)		12. REPORT DATE July 1978	
		13. NUMBER OF PAGES 125	
		15. SECURITY CLASS. (of this report) Unclassified	
		15a. DECLASSIFICATION/DOWNGRADING SCHEDULE	
16. DISTRIBUTION STATEMENT (of this Report) This document has been approved for public release and sale; its distribution is unlimited. Reproduction in whole or in part is permitted by the U.S. Government.			
17. DISTRIBUTION STATEMENT (of the abstract entered in Block 20, if different from Report)			
18. SUPPLEMENTARY NOTES			
19. KEY WORDS (Continue on reverse side if necessary and identify by block number) magnetic current on finite ferrite-rod antenna approximate 3-term solution numerical solution of coupled integral equations experimental verification			
20. ABSTRACT (Continue on reverse side if necessary and identify by block number) Two theoretical approaches are developed to determine the magnetic current distribution on a ferrite cylinder of finite length that is center-driven by an electrically small loop antenna carrying a constant current. The first method makes use of the analogy between the ferrite rod antenna and the conducting cylindrical dipole antenna to derive an integral equation for the magnetic current on an infinitely permeable ($\mu_r = \infty$) ferrite antenna that corresponds to the integral equation for the electric current on a perfectly conducting electric di- (Continued)			

Unclassified

SECURITY CLASSIFICATION OF THIS PAGE(When Data Entered)

20. Abstract (Continued)

pole antenna. In the limit $h \rightarrow \infty$, this integral equation is shown to agree with that obtained previously in Part I for the infinite ferrite rod antenna. Continuing to parallel the treatment of the electric dipole antenna, the integral equation is modified by the introduction of an internal impedance per unit length of the magnetic conductor to account for values of μ_r that are large but not infinite, and finally an approximate, three-term expression is derived for the current on an 'imperfectly conducting' magnetic conductor. The second, more rigorous theoretical approach obtains two coupled integral equations in terms of the tangential electric field and the tangential electric surface current from independent treatments of the interior (ferrite) and exterior (free space) problems. The coupled equations are then solved numerically by means of the moment method. Finally the results of the two theories are compared with experimental measurements made on eleven different antenna configurations. The agreement is good.

ACCESSION	DATE	BY	✓
NIS			
DOC			
UNCLASSIFIED			
JUL 11 1964			
BY DISSEMINATION AUTHORITY			
COPIES			
A			

Unclassified

SECURITY CLASSIFICATION OF THIS PAGE(When Data Entered)

Office of Naval Research

N00014-75-C-0648

NR-372-G12

ELECTRICALLY SMALL LOOP ANTENNA LOADED BY A
HOMOGENEOUS AND ISOTROPIC FERRITE CYLINDER - PART II

By

D. V. Giri and R. W. P. King

Technical Report No. 668

This document has been approved for public release and sale; its distribution is unlimited. Reproduction in whole or in part is permitted by the U. S. Government.

July 1978

The research reported in this document was made possible through support extended the Division of Engineering and Applied Physics, Harvard University by the U.S. Army Research Office, the U.S. Air Force Office of Scientific Research, and the U.S. Office of Naval Research under the Joint Services Electronics Program by Contracts N00014-67-A-0298-0005 and N00014-75-C-0648.

Division of Applied Sciences
Harvard University • Cambridge, Massachusetts

018

TABLE OF CONTENTS

	<u>PAGE</u>
1. INTRODUCTION.	1
2. PROBLEM OF A FINITE FERRITE ROD ANTENNA	1
3. FERRITE AS A PERFECT MAGNETIC CONDUCTOR	2
4. MAGNETIC CURRENT ON AN INFINITE ANTENNA	8
5. FERRITE AS AN IMPERFECT MAGNETIC CONDUCTOR.	10
6. THE LIMITATIONS OF THE THEORETICAL FORMULATION.	24
7. A MORE RIGOROUS TREATMENT OF THE FINITE ANTENNA	32
8. NUMERICAL SOLUTION BY THE MOMENT METHOD OF THE COUPLED INTEGRAL EQUATIONS.	45
9. EXPERIMENTAL MEASUREMENT OF THE MAGNETIC CURRENT.	52
10. SUMMARY	72
APPENDIX A.	75
APPENDIX B.	77
APPENDIX C.	81
APPENDIX D.	106
ACKNOWLEDGMENT.	117
REFERENCES.	117

ELECTRICALLY SMALL LOOP ANTENNA LOADED BY A
HOMOGENEOUS AND ISOTROPIC FERRITE CYLINDER - PART II

By

D. V. Giri and R. W. P. King

Division of Applied Sciences
Harvard University, Cambridge, Massachusetts 02138

ABSTRACT

The problem of a finite, ferrite-rod antenna has been treated theoretically by recognizing an analogy between the ferrite antenna and the conducting cylindrical dipole antenna which has been studied extensively. Initially the ferrite is idealized to be a perfect magnetic conductor and an Hallén type of integral equation [1] is obtained for the magnetic current. By allowing the antenna height to approach infinity, the formulation is shown to be consistent with previously obtained results for the infinitely long ferrite antenna [2]. Subsequently, the integral equation is modified appropriately to treat the ferrite as an imperfect magnetic conductor, and the current is obtained in the three-term form of King and Wu [3]. Because this treatment relies rather heavily on a mathematical equivalence of the two problems under idealized driving conditions, an alternative, more rigorous formulation is presented. The result is a pair of coupled integral equations in the tangential electric field (or magnetic current) and the circumferential electric current. The coupled integral equations are solved numerically. An experimental apparatus was fabricated to verify the solutions. Good agreement is obtained for a range of parameters. The experiments were performed for three values of $\Omega = 2 \ln(2h/a) = 8.5534, 7.4754$ and 6.089 . The electrical radius ak_0 ranged from .00132 to .01662.

1. INTRODUCTION

In an earlier report on this subject [2] the magnetic current on a ferrite-rod antenna was derived explicitly in the form of an inverse Fourier integral. The driving loop loaded by an infinitely long, homogeneous and isotropic ferrite rod was assumed to be electrically small so that it carried an essentially constant current I_0^e . When the ferrite rod is assumed to be of infinite length, the magnetic current is equal to a definite integral which is suitable for numerical evaluation. Two values of electrical radii, viz., $ak_0 = 0.05$ and 0.1 , were considered and for one of the cases the magnetic current was plotted [2] for several values of the permeability of the ferrite rod ranging from 10 to 200. The total magnetic current can be interpreted in terms of a sum of transmission and radiation currents. If μ_r and ϵ_r of the ferrite rod are assumed to be real, the transmission current can be associated with an unattenuated, rotationally symmetric TE surface wave. It was further found that the cutoff condition for this wave is that the electrical radius ak_1 be greater than 2.405.

In a practical situation, however, the antenna is of necessity finite and electrically short as well, so that a new mathematical formulation along with an experimental investigation is needed for the problem of a finite ferrite-rod antenna. Sections 2 through 8 present the two different theoretical approaches used to determine the magnetic current distribution on the finite ferrite antenna; Section 9 describes the experimental apparatus and results.

2. PROBLEM OF A FINITE FERRITE-ROD ANTENNA

The present formulation is based on the analogy between the cylindrical dipole antenna and the ferrite-rod antenna. The dipole antenna is made up of a wire, rod or tube of high electrical conductivity and may be driven by a

two-wire line. Equivalently, a monopole antenna fed by a coaxial line corresponds to a dipole antenna through its image in a ground plane. In either configuration, the driving source is represented by an idealized voltage or electric field generator which mathematically takes the form of a delta function. Similarly, the ferrite rod antenna is fabricated from a material of high magnetic permeability and is driven by an electrically small loop antenna carrying a constant current. The loop is, correspondingly, represented by an idealized current or magnetic field generator and takes the form of a delta function. These similarities suggest approaching the problem of the ferrite antenna by treating the ferrite rod as a good magnetic conductor. Initially, however, the ferrite is idealized to be a perfect magnetic conductor ($\mu_r = \infty$) and, later, appropriate changes are made to account for the finiteness of the value of the permeability of the ferrite material.

3. FERRITE AS A PERFECT MAGNETIC CONDUCTOR

The analogy between the ferrite antenna and the dipole antenna is based on the dual property of electric and magnetic field vectors in Maxwell's equations

$$\begin{aligned} \nabla \times \vec{E} &= -\vec{B} \\ \nabla \times \vec{H} &= \vec{J} + \vec{D} \\ \nabla \cdot \vec{B} &= 0 \\ \nabla \cdot \vec{D} &= \rho \end{aligned} \tag{1}$$

Figure 1(a) shows an electrically small loop antenna of diameter $2a$. The loop carries a constant current and is assumed to be made up of a wire of infinitesimally small radius. The wire loop is loaded by a ferrite cylinder of height $2h$. The ferrite is assumed to have an infinite permeability, in which

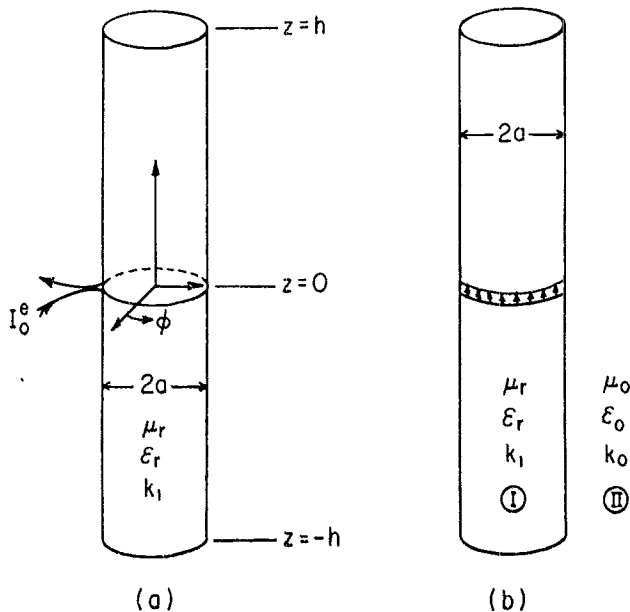


FIG. 1 (a) ELECTRICALLY SMALL LOOP ANTENNA OF DIAMETER ' $2a$ ' LOADED BY A FERRITE CYLINDER OF HALF HEIGHT ' h ' AND SURROUNDED BY FREE SPACE.

(b) MATHEMATICALLY EQUIVALENT BUT PHYSICALLY UNAVAILABLE MODEL FOR THE ANTENNA SHOWING THE IDEALIZED CURRENT GENERATOR $\oint I_0^e \delta(\rho - a) \delta(z)$.

case the value of its dielectric constant ϵ_r is immaterial in view of the nature of the driving source. Figure 1(b) shows the mathematical model of the antenna. Region I is the ferrite with parameters μ_r , ϵ_r , k_1 and region II is free space with constitutive parameters μ_0 , ϵ_0 and wave number k_0 . Because of the nature of the driving source and azimuthal symmetry, the non-zero components of the fields are H_z , H_ρ and E_ϕ . A time dependence of the form $\exp(-i\omega t)$ is assumed. Because of the assumption $\mu_r = \infty$, H_z and H_ρ vanish in region I. The ferrite is also assumed to be homogeneous and isotropic. Thus the idealized driving source is taken into account by setting

$$H_z = -I_0^e \delta(z) \quad (\text{for } \rho = a \text{ and } |z| \leq h) \quad (2)$$

Since both regions I and II have vanishing electrical conductivity and there is no free charge, Maxwell's equations reduce to

$$\nabla \times \vec{E} = -\vec{B} \quad (3a)$$

$$\nabla \times \vec{H} = \vec{D} \quad (3b)$$

$$\nabla \cdot \vec{B} = 0 \quad (3c)$$

$$\nabla \cdot \vec{D} = 0 \quad (3d)$$

It is required to solve (3a-d) for the fields subject to the condition (2) which states that the tangential component of \vec{H} is discontinuous by the true electric surface current at $\rho = a$ and for $|z| \leq h$. In order to obtain an integral equation for the magnetic current on the antenna, an electric vector potential \vec{A}^e and a magnetic scalar potential ϕ^* are defined and used.

$$\vec{D} = -\nabla \times \vec{A}^e \quad (4)$$

The definition of \vec{A}^e is incomplete unless its divergence is also specified.

Using (4) in (3b) gives $\nabla \times (\vec{H} + \vec{A}^e) = 0$, from which the scalar magnetic

potential is defined by setting

$$\vec{H} + \vec{A}^e = -\nabla\phi^* \quad (5)$$

In terms of the potentials, the fields are now given by

$$\vec{E} = (-1/\epsilon)\nabla \times \vec{A}^e \quad (6a)$$

$$\vec{H} = -\nabla\phi^* - \vec{A}^e \quad (6b)$$

Substitution of (6a,b) into Maxwell's equations (3c) and (3a) gives

$$\nabla^2\phi^* + \nabla \cdot \vec{A}^e = 0 \quad (7a)$$

$$\nabla^2\vec{A}^e - \mu\epsilon\vec{A}^e = \nabla[\nabla \cdot \vec{A}^e + \mu\epsilon\phi^*] \quad (7b)$$

Equation (7) is a set of coupled equations for the potentials which may be decoupled by defining the dual Lorentz gauge

$$\nabla \cdot \vec{A}^e + \mu\epsilon\phi^* = 0 \quad (8)$$

Upon using (8), (7) becomes

$$\nabla^2\phi^* - \mu\epsilon\phi^* = 0 \quad (9a)$$

$$\nabla^2\vec{A}^e - \mu\epsilon\vec{A}^e = 0 \quad (9b)$$

If (9) is solved for the potentials, subject to suitable boundary conditions, then the electromagnetic field is known everywhere by making use of (6). However, for the problem at hand, a \hat{z} -component of electric vector potential is adequate for a complete solution so that $\vec{A}^e = \hat{z}A_z^e$. On the surface ($r = a$, $|z| \leq h$) of the antenna, (6b) then becomes

$$H_z = -1/\epsilon \delta(z) = -(\partial\phi^*/\partial z) + i\omega\lambda_z^e \quad (10)$$

Using (8), one can rewrite (10) as

$$\left(\frac{d^2 \Lambda_z^e}{dz^2} + k_0^2 \Lambda_z^e \right) = i(k_0/v_0) I_0^e \delta(z) \quad (11)$$

where k_0 is the free space wave number and v_0 the velocity of light in free space. This equation is identical to that for the z-component of the magnetic vector potential in the case of the dipole antenna [1, eq.(3.2.4)] and, therefore, has a complete solution - like [1, eq.(3.2.12)] - which is given by

$$\Lambda_z^e(z) = (i/v_0) [C \cos k_0 z + (I_0^e/2) \sin k_0 |z|] \quad (12)$$

Equation (12) is an expression for the z-component of electric vector potential in terms of the driving current I_0^e . However, the general formula for $\vec{A}^e(\vec{r})$ due to an arbitrary distribution of magnetic surface current $\vec{K}^*(\vec{r})$ can be written as

$$\vec{A}^e(\vec{r}) = (\epsilon_0/4\pi) \int_{S_1} \vec{K}^*(\vec{r}') (e^{ik_0 R}/R) dS_1$$

In general, $\vec{K}^*(\vec{r}) = \vec{K}^*(\vec{r}) + \vec{n} \times \vec{P}^*(\vec{r})$, but because of the nature of the driving source $\vec{P}^*(\vec{r}) = 0$, so that $\vec{K}^*(\vec{r}) = \vec{K}^*(\vec{r}) = (\vec{n} \times \vec{E}) =$ magnetic surface current. Since rotational symmetry obtains, the total axial magnetic current can be introduced with thin antenna approximation so that $I_z^*(z) = 2\pi a K_z^*(\vec{r})$

$$\Lambda_z^e(z) = \Lambda_z^e(\vec{r}) = (\epsilon_0/4\pi) \int_{-h}^h I_z^*(z') dz' \int_{-\pi}^{\pi} (e^{ik_0 R_s}/R_s) d\theta'/2\pi$$

where

$$R_s = [(z - z')^2 + (2a \sin \theta'/2)^2]^{1/2}$$

Letting

$$K_s(z, z') = \int_{-\pi}^{\pi} (e^{ik_0 R_s}/R_s) d\theta'/2\pi$$

gives

$$\Lambda_z^e(z) = (\epsilon_0/4\pi) \int_{-h}^h I_z^*(z') K_s(z, z') dz' \quad (13)$$

$A_z^e(z)$ was previously obtained in (12). Equations (12) and (13) together lead to the required integral equation,

$$\int_{-h}^h I_z^*(z') K_s(z, z') dz' = 14\pi\zeta_0 [C \cos k_0 z + (I_0^e/2) \sin k_0 |z|] \quad (14)$$

with $\zeta_0 = (\mu_0/\epsilon_0)^{1/2}$ = the free space characteristic impedance.

The integral equation (14) for the magnetic current on a finite, infinitely permeable, ferrite rod antenna can be identified formally with the similar integral equation [1, eq.(3.2.23)] for the electric current on a finite dipole antenna made up of a perfect metallic conductor. Comparing the integral equations for the two cases, one finds that the driving voltage V_0^e and the free space characteristic impedance ζ_0 in the electric dipole case are replaced by the driving current I_0^e and the free space characteristic admittance $(1/\zeta_0)$ in the magnetic case. Commonly used metals like copper and brass are found to have sufficiently large electrical conductivities to justify the assumption of vanishing electric field inside the material of the dipole antenna so that an integral equation of the form (14) is adequate and has been used to obtain the electric current distributions. Furthermore, if more accuracy is required, theories do exist for imperfectly conducting cylindrical transmitting antennas. However, it is questionable whether the integral equation (14) is directly applicable to the practical ferrite rod antenna due to the relative permeability ranges of available ferrites. Whereas the treatment of the imperfectly conducting dipole antenna is done for reasons of improved accuracy, a similar treatment (μ_r large but not infinite) for the ferrite antenna appears to be a necessity. This forms the subject of Section 5.

4. MAGNETIC CURRENT ON AN INFINITE ANTENNA

The magnetic current $I_z^*(z)$ obtained by solving the integral equation (14) may be called a zeroth-order solution because of the assumption $\mu_r = \infty$. The integral equation (14) is for a finite antenna from which the zeroth-order solution $I_z^*(z)$ for an antenna of infinite length may be obtained. For the sake of convenience, the integral equation is rewritten as

$$\int_{-h}^h I_z^*(z') K_s(|z - z'|) dz' = (4\pi/\epsilon_0) A_z^e(z) = i4\pi\epsilon_0 [C \cos k_0 z + \frac{I_0^e}{2} \sin k_0 |z|]$$

As $h \rightarrow \infty$, the vector potential $A_z^e(z)$ is a traveling wave which may be obtained by setting $C = I_0^e/2i$. In this case,

$$\int_{-\infty}^{\infty} I_z^*(z') K_s(|z - z'|) dz' = 2\pi\epsilon_0 I_0^e e^{ik_0 |z|} \quad (15)$$

Taking Fourier transforms of both sides of (15), one obtains

$$\int_{-\infty}^{\infty} e^{-i\zeta z} dz \int_{-\infty}^{\infty} I_z^*(z') K_s(|z - z'|) dz' = 2\pi\epsilon_0 I_0^e \int_{-\infty}^{\infty} e^{-i\zeta z} e^{ik_0 |z|} dz$$

The left side of the above equation is a convolution integral and on the right side, the integration may be performed to obtain

$$\bar{K}(\zeta) \bar{I}_\omega^*(\zeta) = 2\pi\epsilon_0 I_0^e [2ik_0 / (k_0^2 - \zeta^2)]$$

$$\text{With } \gamma_0^2 = k_0^2 - \zeta^2$$

$$\bar{I}_\omega^*(\zeta) = 4i\pi\epsilon_0 I_0^e k_0 / \gamma_0^2 \bar{K}(\zeta) \quad (16)$$

By recalling

$$K_s(|z - z'|) = \int_{-\pi}^{\pi} (e^{ik_0 R_s} / R_s) d\theta' / 2\pi$$

with $R_s = [(z - z')^2 + (2a \sin \theta'/2)^2]^{1/2}$, it can be shown [3] that the Fourier transform $\bar{K}(\zeta)$ of the kernel $K_s(z, z')$ is given by

$$\bar{K}(\xi) = \int_{-\infty}^{\infty} e^{-i\xi z} K_g(z) dz = i\pi J_0(a\gamma_0) H_0^{(1)}(a\gamma_0) \quad (17)$$

Using (17) in (16), one obtains

$$\bar{I}_{\infty}^*(\xi) = 4\epsilon_0 I_0^e k_0 / \gamma_0^2 J_0(a\gamma_0) H_0^{(1)}(a\gamma_0)$$

The inverse Fourier transform may now be taken.

$$\begin{aligned} I_{\infty}^*(z) &= \frac{1}{2\pi} \int_{-\infty}^{\infty} \bar{I}_{\infty}^*(\xi) e^{i\xi z} d\xi \\ I_{\infty}^*(z) &= \frac{2}{\pi} I_0^e \epsilon_0 k_0 \int_{-\infty}^{\infty} \frac{e^{i\xi z} d\xi}{2 J_0(a\gamma_0) H_0^{(1)}(a\gamma_0)} \quad \text{volts} \end{aligned} \quad (18)$$

Equation (18) is thus an explicit expression in the form of an infinite integral for the current on an infinitely long, infinitely permeable, ferrite rod antenna.

The problem of infinitely long ferrite rod antennas was formulated previously [2] in terms of differential equations and the Fourier transform of this current was obtained, from [2, eq.(23)], to be

$$\bar{I}_{\infty}^*(\xi) = \frac{-i\omega a (\nu_r - 1) I_0^e \nu_0 2\pi a h_1^{(1)}(a\gamma_0) J_1(a\gamma_1)}{a [\gamma_1 J_0(a\gamma_1) H_1^{(1)}(a\gamma_0) - \gamma_0 \nu_r J_1(a\gamma_1) H_0^{(1)}(a\gamma_0)]} \quad (19)$$

where $\gamma_1^2 = k_1^2 - \xi^2$ and $\gamma_0^2 = k_0^2 - \xi^2$, ξ is the Fourier transform variable, and k_1 and k_0 are the wave numbers in the ferrite and the surrounding free space medium, respectively. The zeroth-order current on the infinite antenna may be obtained from (19) by taking the limit $\nu_r \rightarrow \infty$.

First, (19) may be rewritten as

$$\bar{I}_{\infty}^*(\xi) = (-i\omega a I_0^e \nu_0 2\pi) \left[\frac{\gamma_1 J_0(a\gamma_1)}{(\nu_r - 1) J_1(a\gamma_1)} - \frac{\gamma_0 \nu_r H_0^{(1)}(a\gamma_0)}{(\nu_r - 1) H_1^{(1)}(a\gamma_0)} \right]^{-1}$$

As $\mu_r \rightarrow \infty$, the ratio $[J_0(a\gamma_1)/J_1(a\gamma_1)]$ is finite so that the first term within the brackets approaches zero. In this case

$$\tilde{I}_\infty^*(\xi) = \frac{4\epsilon_0 I_0^e k_0}{\gamma_0^2 J_0(a\gamma_0) H_0^{(1)}(a\gamma_0)} [a\gamma_0 \frac{\pi i}{2} H_1^{(1)}(a\gamma_0) J_0(a\gamma_0)]$$

Furthermore, for a thin antenna, a small argument approximation may be used for the Bessel functions in the numerator so that $\tilde{I}_\infty^*(\xi)$ reduces to

$$\tilde{I}_\infty^*(\xi) = \frac{4\epsilon_0 I_0^e k_0}{\gamma_0^2 J_0(a\gamma_0) H_0^{(1)}(a\gamma_0)}$$

from which

$$I_\infty^*(z) = \frac{2}{\pi} I_0^e \epsilon_0 k_0 \int_{-\infty}^{\infty} \frac{e^{i\xi z} d\xi}{\gamma_0^2 J_0(a\gamma_0) H_0^{(1)}(a\gamma_0)} \quad \text{volts} \quad (20)$$

Thus, equations (20) and (18) are both independently derived explicit expressions for the zeroth-order ($\mu_r = \infty$) magnetic currents on an infinitely long ferrite rod antenna. In the limit of infinite permeability the two formulations give the same result. This limit is, however, physically unrealizable since a magnetic material with $\mu_r = \infty$ does not exist and, hence, a modification of the formulation which treats the ferrite as an imperfect magnetic conductor is required. This modification has, once again, an analogue in the electric case in the treatment of the imperfectly conducting cylindrical transmitting antenna [3], [4].

5. FERRITE AS AN IMPERFECT MAGNETIC CONDUCTOR

In order to account for the fact that the relative permeability is large but not infinite, the concept of 'internal impedance' is useful and suffi-

cient. With reference to Fig. 2, the internal impedance per unit length of a cylindrical magnetic conductor of circular cross section of radius a with its axis along the z -axis of a system of cylindrical coordinates (ρ, ϕ, z) may be defined by

$$Z_m^i = (r_m^i - iX_m^i) = H_z(\rho = a)/I_z^* \quad (21)$$

where $H_z(\rho = a)$ is the tangential magnetic field at the surface, $\rho = a$, of the conductor and I_z^* is the total axial magnetic current. Recalling the expressions of electric and magnetic fields in terms of the potentials

$$\vec{H} = -\nabla\phi^* - \vec{A}^e \quad (22a)$$

$$\vec{D} = -\nabla \times \vec{A}^e \quad (22b)$$

$$\nabla \cdot \vec{A}^e + \mu\epsilon\phi^* = 0 \quad (22c)$$

the electric vector potential satisfies

$$(\nabla^2 + k^2)\vec{A}^e = 0 \quad (23)$$

where k is replaced by k_1 and k_0 for the two regions I and II shown in Fig. 2. For the problem of a thin cylindrical conductor, the axial component of electric potential is sufficient to satisfy Maxwell's equations and the relevant boundary conditions. Thus, the electromagnetic fields everywhere can be obtained by setting $\vec{A}^e = \hat{z}A_z^e$. With the vector potential being entirely axial and also because of azimuthal symmetry, (23) becomes

$$\left[\frac{\partial^2}{\partial z^2} + \frac{1}{\rho} \frac{\partial}{\partial \rho} \left(\rho \frac{\partial}{\partial \rho} \right) + k^2 \right] A_z^e(\rho, z) = 0 \quad (24)$$

A product solution to (24) is sought in the following form:

$$A_z^e(\rho, z) = f_z(z)R_z(\rho) \quad (25)$$

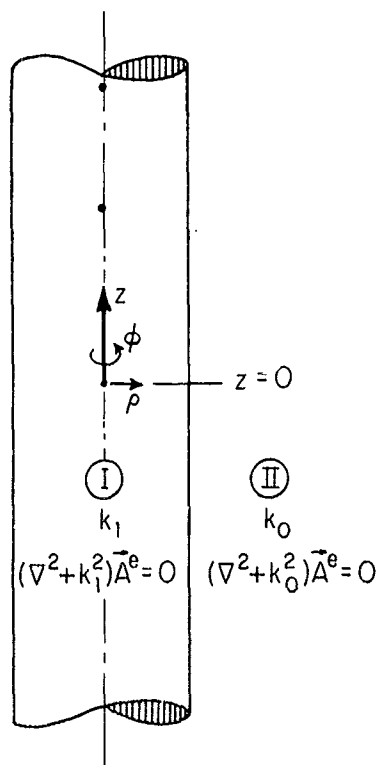


FIG. 2 A CYLINDRICAL MAGNETIC CONDUCTOR CARRYING A TOTAL AXIAL MAGNETIC CURRENT OF I_z^* AND IMMERSSED IN FREE SPACE.

Substitution of (25) into (24) leads to

$$R_z \frac{d^2 f_z}{dz^2} + f_z \frac{1}{\rho} \frac{d}{d\rho} \left(\rho \frac{dR_z}{d\rho} \right) + k^2 f_z R_z = 0 \quad (26)$$

Equation (26) may be rewritten as

$$\frac{1}{f_z} \frac{d^2 f_z}{dz^2} + k^2 = - \frac{1}{R_z} \frac{1}{\rho} \frac{d}{d\rho} \left(\rho \frac{dR_z}{d\rho} \right) \quad (27)$$

The left side of (27) is a function of z alone, while the right side is a function of ρ alone. Hence, they can be equal to each other for all possible values of ρ and z only if they are both equal to a constant (say ζ^2) which may, however, be multivalued. Therefore,

$$\frac{d^2 f_z}{dz^2} + (k^2 - \zeta^2) f_z = 0 \quad \text{and} \quad \frac{1}{\rho} \frac{d}{d\rho} \left(\rho \frac{dR_z}{d\rho} \right) + \zeta^2 R_z = 0$$

After solving the foregoing differential equations for f_z and R_z , the axial vector potential in the two regions can be written down as

$$A_{z1}^e(\rho, z) = C_1 J_0(\zeta_1 \rho) \exp(i \sqrt{k_1^2 - \zeta_1^2} z) \quad \text{in region I}$$

$$A_{z2}^e(\rho, z) = C_2 H_0^{(1)}(\zeta_0 \rho) \exp(i \sqrt{k_0^2 - \zeta_0^2} z) \quad \text{in region II}$$

Boundary conditions that are useful in determining the unknown constants in the solution require the continuity of tangential \vec{E} and \vec{H} across the surface $\rho = a$; that is

$$E_{\phi 1} \big|_{(\rho = a)} = E_{\phi 2} \big|_{(\rho = a)}$$

$$\nu_1 B_{z1} \big|_{(\rho = a)} = \nu_2 B_{z2} \big|_{(\rho = a)}$$

In terms of the vector potential, the boundary conditions at the surface

$\rho = a$ are

$$\frac{1}{\epsilon_1} \frac{\partial A_{z1}^e}{\partial \rho} = \frac{1}{\epsilon_0} \frac{\partial A_{z2}^e}{\partial \rho}$$

$$\frac{i\omega}{\nu_1} \frac{\tau_1^2}{k_1^2} A_{z1}^e = \frac{i\omega}{\nu_0} \frac{\tau_0^2}{k_0^2} A_{z2}^e$$

Application of the boundary conditions yields

$$\frac{1}{\epsilon_1} C_1 \tau_1 J_0'(\tau_1 a) \exp(i\sqrt{k_1^2 - \tau_1^2} z) = \frac{1}{\epsilon_0} C_2 \tau_0 H_0^{(1)}(\tau_0 a) \exp(i\sqrt{k_0^2 - \tau_0^2} z) \quad (28)$$

$$\frac{i\omega}{\nu_1} \frac{\tau_1^2}{k_1^2} C_1 J_0(\tau_1 a) \exp(i\sqrt{k_1^2 - \tau_1^2} z) = \frac{i\omega}{\nu_0} \frac{\tau_0^2}{k_0^2} C_2 H_0^{(1)}(\tau_0 a) \exp(i\sqrt{k_0^2 - \tau_0^2} z) \quad (29)$$

Since (28) and (29) are valid for all values of z at all times, it follows that

$$\sqrt{k_1^2 - \tau_1^2} = \sqrt{k_0^2 - \tau_0^2} = q \text{ (say)} \quad (30)$$

so that $\tau_1 = \sqrt{k_1^2 - q^2}$ and $\tau_0 = \sqrt{k_0^2 - q^2}$. Dividing (29) by (28) and rearranging, one obtains

$$\tau_0 a \frac{H_0^{(1)}(\tau_0 a)}{H_0^{(1)}(\tau_0 a)} = \frac{\epsilon_1 \nu_0}{\epsilon_0 \nu_1} \frac{k_0^2}{k_1^2} \tau_1 a \frac{J_0(\tau_1 a)}{J_0'(\tau_1 a)} \quad (31)$$

Although, in general, an explicit solution is not possible, equations (30) and (31) are theoretically sufficient to determine the unknowns τ_1 and τ_0 . The two unknowns will be determined here by two methods.

Method 1:

An approximate solution is possible by allowing k_1 to become very large. Since q is finite, $\tau_1 \rightarrow k_1$ and, therefore, τ_1 is also large. Using this on the right side of (31) gives

$$i \frac{\epsilon_1 \mu_0}{\epsilon_0 \mu_1} \frac{k_0^2}{k_1^2} \zeta_1 a \rightarrow 0$$

Therefore,

$$\zeta_0 a \frac{H_0^{(1)}(\zeta_0 a)}{H_0^{(1)}(\zeta_0 a)} \sim 0 \quad (32)$$

Equation (32) is satisfied by $\zeta_0 = 0$ since it can be shown that the ratio $H_0^{(1)}(\zeta_0 a)/H_0^{(1)}(\zeta_0 a)$ remains finite as ζ_0 approaches the value of zero. It then follows from (30) that

$$\zeta_1 = \sqrt{k_1^2 - k_0^2} = k_1 \sqrt{1 - (1/\mu_r \epsilon_r)} \sim k_1$$

Thus the solutions are $\zeta_1 \sim k_1$ and $\zeta_0 \sim 0$.

Method 2:

Method 1 may seem to be an oversimplification and hence, a slightly more rigorous method may be needed in some cases. It is observed that (31) may be identified with a similar equation obtained by Sommerfeld [5] in the problem on 'waves on wires.' Sommerfeld has developed an iterative form of solution which may be used here.

In the limit of large ζ_1 , the right side of (31) becomes

$$i \frac{\epsilon_1 \mu_0}{\epsilon_0 \mu_1} \frac{k_0^2}{k_1^2} \zeta_1 a = i \frac{\epsilon_r}{\mu_r} \frac{k_0^2}{k_1^2} a \sqrt{k_1^2 - k_0^2} \sim i \frac{\epsilon_r}{\mu_r} \frac{k_0^2}{k_1^2} a = i \frac{a k_0}{\mu_r} \sqrt{\epsilon_r / \mu_r}$$

and is small. Since the left side of (31) also has to be small, we have

$$(\zeta_0 a)^2 \ln(\gamma \zeta_0 a / 2i) = -\frac{2}{\gamma} u \ln u \quad \text{with} \quad u = (\gamma \zeta_0 a / 2i)^2$$

where $\gamma = 1.781$.

Equation (31) finally becomes

$$u \ln u = v \quad \text{with} \quad v = -\frac{iy^2}{2} \frac{ak_0}{\mu_r} \sqrt{\epsilon_r / \mu_r}$$

Since $\ln u$ varies slowly in comparison with u , it is possible to write

$$u_{n+1} \ln u_n = v$$

where u_n is the n^{th} approximation to u . The method is best illustrated by an example. In the later part of this report, eleven different antenna configurations were used in the experimental determination of the magnetic current. The example chosen here (antenna #1) corresponds to the lowest value of the $|\epsilon_r \epsilon_r|$ product for the eleven cases.

Example: $ak_0 = 0.00166$, $\mu_r = (18 + i.036)$, $\epsilon_r = 11.0$.

$$\text{Let } u_0 = v = -\frac{iy^2}{2} \frac{ak_0}{\mu_r} \sqrt{\epsilon_r / \mu_r} \approx -i(1.1 \times 10^{-4})$$

This gives

$$u_1 = \frac{v}{\ln u_0} = \frac{-11.1 \times 10^{-4}}{(-9.115 + i4.712)} = -10^{-4}(.049 - i.095)$$

$$u_2 = \frac{v}{\ln u_1} = \frac{-11.1 \times 10^{-4}}{(-11.445 + i2.047)} = -10^{-4}(.0167 - i.0931)$$

Continuing the iteration

$$u_3 = \frac{v}{\ln u_2} = \frac{-11.1 \times 10^{-4}}{(-11.5684 + i1.7478)} = -10^{-4}(.0140 - i.0930)$$

$$u_4 = \frac{v}{\ln u_3} = \frac{-11.1 \times 10^{-4}}{(-11.5748 + i1.7208)} = -10^{-4}(.0138 - i.0930)$$

and finally

$$u_5 = \frac{v}{\ln u_4} = \frac{-11.1 \times 10^{-4}}{(-11.5748 + i1.7184)} = -10^{-4}(.0138 - i.0930)$$

It is seen that this iterative procedure is rapidly converging and using the above value of u ,

$$(\epsilon_0 a)^2 = -\frac{4}{\gamma^2} u^2 = 10^{-10} (1.062 + i.3225)$$

Furthermore, from (30)

$$\begin{aligned} (aq)^2 &= (ak_0)^2 - (a\epsilon_0)^2 \\ &= 2.7556 \times 10^{-6} - 10^{-10} (1.062 + i.3225) \end{aligned}$$

from which $a\epsilon_1$ may be calculated using

$$\begin{aligned} (a\epsilon_1)^2 &= (ak_1)^2 - (aq)^2 = (ak_1)^2 - (ak_0)^2 + (a\epsilon_0)^2 \\ &= ak_1^2 \left[1 - \frac{1}{\nu_r \epsilon_r} + \left(\frac{a\epsilon_0}{ak_1} \right)^2 \right] \\ &= ak_1^2 [1 - (.0056 - i.00001) + 10^{-7} (2.159 + i.651)] \end{aligned}$$

From the calculated values of $(a\epsilon_0)^2$ and $(a\epsilon_1)^2$, it is seen that the approximate solutions, i.e., $\epsilon_0 = 0$ and $\epsilon_1 \approx k_1$, are quite satisfactory even when $|\nu_r \epsilon_r|$ is as low as 180.

Therefore, the vector potential in the interior of the conductor is given by

$$\Lambda_{z1}^e(\rho, z) = \Lambda_{z1}^e(\rho) \Lambda_{z1}^e(z) = C_1 J_0(k_1 \rho) \exp(i \sqrt{k_1^2 - \epsilon_1^2} z)$$

where ϵ_1 in the argument of the Bessel function is replaced by k_1 in view of the calculations of "Method 2." The constant C_1 can be written in terms of the potential on the surface so that

$$\Lambda_{z1}^e(\rho) = \Lambda_{z1}^e(a) J_0(k_1 \rho) / J_0(k_1 a)$$

Since H_z is proportional to Λ_z ,

$$H_{z1}(\rho) = H_{z1}(a) J_0(k_1 \rho) / J_0(k_1 a)$$

The magnetization is then given by

$$\dot{M}_z(\rho) = (\mu_r - 1) \dot{H}_{z1}(\rho) = (\mu_r - 1) \dot{H}_{z1}(a) J_0(k_1 \rho) / J_0(k_1 a)$$

from which the magnetic current can be obtained as

$$\begin{aligned} I_z^*(\rho) &= 2\pi \int_0^\rho \mu_0 \dot{M}_z(\rho') \rho' d\rho' \\ &= 2\pi \mu_0 (\mu_r - 1) \frac{\dot{H}_{z1}(a)}{J_0(k_1 a)} \int_0^\rho J_0(k_1 \rho') \rho' d\rho' \end{aligned}$$

Performing the integration gives

$$I_z^*(\rho) = \frac{2\pi \mu_0 (\mu_r - 1) \dot{H}_{z1}(a)}{J_0(k_1 a)} \frac{\rho}{k_1} J_1(k_1 \rho) \quad (33)$$

The total magnetic current carried by the conductor is, however, given by

$$I_z^*(a) = 2\pi \int_0^a \mu_0 \dot{M}_z(\rho) \rho d\rho$$

which becomes

$$I_z^*(a) = \frac{2\pi \mu_0 (\mu_r - 1) \dot{H}_{z1}(a)}{J_0(k_1 a)} \frac{a}{k_1} J_1(k_1 a) \quad (34)$$

From (33) and (34) the radial distribution of the magnetic current in the interior of the conductor is given by

$$I_z^*(\rho) = I_z^*(a) \frac{\rho}{a} \frac{J_1(k_1 \rho)}{J_1(k_1 a)} \quad (35)$$

Furthermore, having obtained the total axial magnetic current of (34), the

internal impedance per unit length defined in (21) can be written as

$$z_m = r_m - i x_m = H_{z1}(0=a)/I_z^*(a) \\ = \left[\frac{i}{2\omega} \frac{1}{\mu_0 \chi_m} \frac{1}{\pi a^2} k_1 a \frac{J_0(k_1 a)}{J_1(k_1 a)} \right] \Omega/m \quad (36)$$

where $\chi_m = (\mu_r - 1)$ = magnetic susceptibility;

ω = radian frequency;

$\mu_0 = 4\pi \times 10^{-7}$ h/m = permeability of free space;

πa^2 = cross-sectional area of the conductor;

$k_1 = \beta_1 + i\alpha_1 = k_0(\beta_{1N} + i\alpha_{1N})$ = wave number in the material of the conductor.

With $v_r = (v_r' + i v_r'') = |v_r| e^{i\theta_v}$ and $\epsilon_r = (\epsilon_r' + i\epsilon_r'') = |\epsilon_r| e^{i\theta_\epsilon}$,

$$k_1 = k_0 |v_r \epsilon_r|^{1/2} \exp[i(\theta_v + \theta_\epsilon)/2]$$

so that

$$\beta_1 = k_0 |v_r \epsilon_r|^{1/2} \cos[(\theta_v + \theta_\epsilon)/2] \quad (37a)$$

and

$$\alpha_1 = k_0 |v_r \epsilon_r|^{1/2} \sin[(\theta_v + \theta_\epsilon)/2] \quad (37b)$$

One may now use the internal impedance per unit length of a magnetic conductor carrying an axial magnetic current to find an integral equation for the magnetic current on a finite ferrite rod antenna. The axial component $A_z^0(z)$ on the surface of a cylindrical antenna that has an internal impedance per unit length z_m^i , carries an axial current $I_z^*(z)$, and is driven at $z = 0$ by a delta-function generator with an mmf of 1_0^0 , satisfies the following differential equation:

$$\left(\frac{d^2}{dz^2} + k_0^2\right) A_z^e(z) = -\frac{ik_0^2}{\omega} [z_m I_z^*(z) - I_0^e \delta(z)] \quad (38)$$

If the antenna were made of a perfect magnetic conductor, $z_m^i = 0$ because $\chi^m = \infty$ so that (38) will reduce to (11). If the radius a of the antenna and the free-space wave number $k_0 = \omega/v_0 = 2\pi/\lambda_0$ satisfy the inequality

$$ak_0 \ll 1$$

then the vector potential is given approximately by

$$A_z^e(z) \sim \frac{\epsilon_0}{4\pi} \int_{-h}^h I_z^*(z') K(z, z') dz' \quad (39)$$

If the equations (38) and (39) are formally identified with those for the imperfectly conducting, electric dipole antenna [3, eqs. (7) and (9)], it is observed that μ_0 and I_0^e play the roles of ϵ_0 and V_0^e . King and Wu [3] have developed a three-term solution for the electric current on the imperfectly conducting dipole antenna which can be well applied to the present problem of the ferrite as an imperfect magnetic conductor. The procedure used to obtain the three-term solution will be described here briefly; for a detailed analysis the reader is referred to [3].

The approximate kernel in (39) may be separated into real and imaginary parts,

$$K(z, z') = K_R(z, z') - iK_I(z, z') = e^{ik_0 r}/r$$

so that

$$K_R(z, z') = \frac{\cos k_0 r}{r}, \quad K_I(z, z') = -\frac{\sin k_0 r}{r}$$

with $r = [(z - z')^2 + a^2]^{1/2}$. The vector potential may also be divided into two parts,

$$A_z^e(z) = A_R^e(z) - iA_I^e(z)$$

where

$$A_R^e(z) = \frac{k_0 \varepsilon_0}{4\pi} \int_{-h}^h I_z^*(z') \frac{\cos k_0 r}{k_0 r} dz' \quad (40)$$

$$A_I^e(z) = -\frac{k_0 \varepsilon_0}{4\pi} \int_{-h}^h I_z^*(z') \frac{\sin k_0 r}{k_0 r} dz' \quad (41)$$

The properties of the two integrals are quite different. The kernel in (40) has a sharp peak at $k_0|z - z'| = 0$ and thus greatly magnifies the contribution to the integral due to current elements near $z = z'$. The current vanishes at the end but the vector potential $A_R^e(h)$ has a small finite value so that the difference in vector potential should vary closely like $I_z^*(z)$.

Therefore,

$$(4\pi/\varepsilon_0)[A_R^e(z) - A_R^e(h)] = \Psi(z)I_z^*(z) \pm \Psi I_z^*(z) \quad (42)$$

where Ψ is the approximately constant value of $\Psi(z)$ defined at a suitable reference value of z . However, in the second integral in (41) the rather flat behavior of $(\sin k_0 r)/k_0 r$ with $k_0 r$ allows the following approximation:

$$\frac{\sin k_0 r}{k_0 r} \approx \frac{2 \sin \frac{k_0 r}{2} \cos \frac{k_0 r}{2}}{k_0 r} \approx \cos \frac{k_0 r}{2}$$

which is useful over a range $k_0 r \leq \pi$. This approximation leads to

$$A_I^e(z) = A_I^e(0) \cos \frac{k_0 z}{2} \quad (43)$$

where $A_I^e(0)$ is a constant given by

$$A_I^e(0) \approx \frac{k_0 \varepsilon_0}{4\pi} \int_{-h}^h I_z^*(z') \cos \frac{k_0 z'}{2} dz' \quad (44)$$

If equation (42), rearranged in the form $I_z^*(z) = (4\pi/\varepsilon_0)[A_R^e(z) - A_R^e(h)]$, is substituted in the differential equation (38), one obtains:

$$\left(\frac{d^2}{dz^2} + k_0^2 \right) [A_z^e(z) - A_z^e(h)] = -i4\pi\epsilon_0 k_0 z_m^{-1} [A_R^e(z) - A_R^e(h)] - k_0^2 A_z^e(h) + \frac{i}{\omega} k_0^2 I_0^e \delta(z) \quad (45)$$

A complex constant k may now be defined by

$$k^2 = (\beta + i\alpha)^2 = k_0^2 \left(1 + \frac{i4\pi z_m^{-1} \epsilon_0}{k_0} \right) \quad (46)$$

Using (43) and (46), (45) becomes

$$\begin{aligned} \left(\frac{d^2}{dz^2} + k^2 \right) [A_z^e(z) - A_z^e(h)] &= -i(k^2 - k_0^2) A_I^e(z) - [k_0^2 A_R^e(h) - ik^2 A_I^e(h)] + \frac{i}{\omega} k_0^2 I_0^e \delta(z) \\ &= -i(k^2 - k_0^2) A_I^e(0) \cos \frac{k_0 z}{2} - [k_0^2 A_R^e(h) - ik^2 A_I^e(h)] + \frac{i}{\omega} k_0^2 I_0^e \delta(z) \end{aligned} \quad (47)$$

The integral equation of (39) may now be written in the form

$$[A_z^e(z) - A_z^e(h)] = \frac{\epsilon_0}{4\pi} \int_{-h}^h I_z^*(z') K_d(z, z') dz' \quad (48)$$

where the difference kernel K_d is given by

$$K_d(z, z') = K(z, z') - K(h, z') = \frac{e^{-ik_0 r}}{r} - \frac{e^{-ik_0 r_h}}{r_h}$$

with $r = [(z - z')^2 + a^2]^{1/2}$ and $r_h = [(h - z')^2 + a^2]^{1/2}$. If the differential equation (47) is solved for the vector potential difference and the solution is substituted for the left-hand side of (48), an integral equation for the magnetic current on the ferrite antenna is obtained, viz.,

$$\int_{-h}^h I_z^*(z') K_d(z, z') dz' = \frac{-i4\pi k_0 \epsilon_0}{k \cos kh} \left[(1/2) I_0^e M_{kz} + U_k^e F_{kz} - D \cos kh F_{0z}^e \right] \quad (49)$$

where for ease of reference, the same notation as in King and Wu [3] is employed and the various factors on the right side are given by

$$M_{kz} = \sin k(h - |z|)$$

$$U'_k = U_k + D \cos \frac{k_0 h}{2}$$

$$U_k = (i\omega k/k_0^2) \{ (k_0^2/k^2) A_R^e(h) - iA_I^e(h) \}$$

$$D = -\frac{\omega k}{k_0^2} \left[\frac{k^2 - k_0^2}{k^2 - k_0^2/4} \right] A_I^e(0)$$

$$F_{kz} = \cos kz - \cos kh$$

$$F'_{0z} = \cos \frac{k_0 z}{2} - \cos \frac{k_0 h}{2}$$

Following the procedure as in [3], an approximate formal solution to the integral equation may be written in the form

$$I_z^*(z) = I_V^* M_{kz} + I_U^* F_{kz} + I_D^* F'_{0z} \quad (50)$$

where the coefficients I_V^* , I_U^* and I_D^* are obtained by a numerical procedure.

Letting $T_U^* = I_U^*/I_V^*$, $T_D^* = I_D^*/I_V^*$ and evaluating I_V^* , one may write (50) as

$$I_z^*(z) = \frac{-i2\pi k_0 \epsilon_0 I_0^e}{k \Psi_{dR} \cos kh} \{ \sin k(h - |z|) + T_U^* (\cos kz - \cos kh) + T_D^* (\cos \frac{k_0 z}{2} - \cos \frac{k_0 h}{2}) \} \quad (51)$$

where k is redefined by

$$k^2 = (\beta + i\alpha)^2 = k_0^2 \left(1 + \frac{i4\pi z_0^2 \epsilon_0}{k_0^2 \Psi_{dR}} \right) \quad (52)$$

and Ψ_{dR} is given by the integral expression

$$\int_{-h}^h \sin k(h - |z'|) K_{dR}(z, z') dz' \neq \sin k(h - |z|) \Psi_{dR} \quad (53)$$

Thus, equation (51) is the required expression for the total magnetic current on the antenna from which the admittance can be obtained to be

$$Y = G - iB = I_z^*(0)/I_0^e \quad \text{ohms}$$

$$= \frac{-i2\pi k_0 \epsilon_0}{k_{\psi}^2 \cos kh} [\sin kh + T_U^*(1 - \cos kh) + T_D^*(1 - \cos \frac{k_0 h}{2})] \quad (54)$$

Note that, because of an earlier approximation of the imaginary part of the kernel, equations (51) and (54) are valid representations for the magnetic current and admittance only when $k_0 h \leq 5\pi/4$.

The existing computer programs for the imperfectly conducting dipole antenna due to King, Harrison and Aronson [4] have been modified for use on the IBM 370/155 computer system of the Joint Harvard/M.I.T. Ratch Processing Center. Appendix B includes a listing of the Fortran IV programs that compute the magnetic current distribution and the admittance of the finite ferrite-rod antenna when the ferrite is treated as an imperfect magnetic conductor.

6. THE LIMITATIONS OF THE THEORETICAL FORMULATION

The present formulation is based on an analogy between the ferrite-rod antenna and the conducting cylindrical dipole antenna. Because of the symmetry in Maxwell's equations, a set of scalar magnetic (ϕ^*) and electric vector (\vec{A}^*) potentials was defined and used in formulating the finite ferrite-rod antenna problem. It is considered useful to determine the existence of these potentials for the infinite antenna and thus provide some justification for their use in the finite antenna problem.

The electromagnetic fields in both regions for the case of the infinitely long antenna were determined previously [2] to be:

Region I, $0 \leq \rho \leq a$:

$$\vec{E}_{\phi 1}(\rho, \xi) = i\omega\mu_1 a I_0^e H_1^{(1)}(\gamma_0 a) J_1(\gamma_1 \rho) / D(\xi)$$

$$\begin{aligned}\bar{H}_{z1}(\rho, \xi) &= \frac{1}{i\omega\mu_1} [\partial \bar{E}_{\phi 1}(\rho, \xi) / \partial \rho + \bar{E}_{\phi 1}(\rho, \xi) / \rho] = a I_0^e \gamma_1 H_1^{(1)}(\gamma_0 a) J_0(\gamma_1 \rho) / D(\xi) \\ \bar{H}_{\rho 1}(\rho, \xi) &= (\xi / \omega\mu_1) \bar{E}_{\phi 1}(\rho, \xi) = i a I_0^e \xi H_1^{(1)}(\gamma_0 a) J_1(\gamma_1 \rho) / D(\xi) \\ \bar{H}_{\phi 1}(\rho, \xi) &= \bar{E}_{\rho 1}(\rho, \xi) = \bar{E}_{z1}(\rho, \xi) = 0\end{aligned}\quad (56)$$

Region II, $\rho \geq a$:

$$\begin{aligned}\bar{E}_{\phi 2}(\rho, \xi) &= i\omega\mu_1 a I_0^e J_1(\gamma_1 a) H_1^{(1)}(\gamma_0 \rho) / D(\xi) \\ \bar{H}_{z2}(\rho, \xi) &= a I_0^e \gamma_0 \mu_r J_1(\gamma_1 a) H_0^{(1)}(\gamma_0 \rho) / D(\xi) \\ \bar{H}_{\rho 2}(\rho, \xi) &= i a I_0^e \mu_r \xi J_1(\gamma_1 a) H_1^{(1)}(\gamma_0 \rho) / D(\xi) \\ \bar{H}_{\phi 2}(\rho, \xi) &= \bar{E}_{\rho 2}(\rho, \xi) = \bar{E}_{z2}(\rho, \xi) = 0\end{aligned}\quad (56)$$

where

$$D(\xi) = a[\gamma_1 J_0(\gamma_1 a) H_1^{(1)}(\gamma_0 a) - \gamma_0 \mu_r J_1(\gamma_1 a) H_0^{(1)}(\gamma_0 a)]$$

The actual field quantities may be obtained by applying the Fourier inverse formula to the above transformed fields. It can be verified easily that the above field quantities satisfy the following transformed boundary conditions:

$$\text{i) Tangential } \vec{E}: \quad \bar{E}_{\phi 2}(a^+, \xi) = \bar{E}_{\phi 1}(a^-, \xi) \quad (57a)$$

$$\text{ii) Tangential } \vec{H}: \quad \bar{H}_{z2}(a^+, \xi) - \bar{H}_{z1}(a^-, \xi) = -I_0^e \quad (57b)$$

$$\text{iii) Normal } \vec{B}: \quad \bar{B}_{\rho 2}(a^+, \xi) = \bar{B}_{\rho 1}(a^-, \xi) \quad (57c)$$

$$\text{iv) Normal } \vec{D}: \quad \text{Zero in both regions}$$

ϕ^* is a scalar magnetic potential and has a non-zero value in both regions. For the infinitely long antenna, the only non-zero component of \vec{A}^e is

the z-component so that $\hat{A}^e = \hat{z}A_z^e$. The potentials may be derived either from the already known electromagnetic fields or from an independent solution of the following wave equations with suitable boundary conditions:

$$(\nabla^2 + k^2)\hat{A}^e(\rho, z) = 0 \quad , \quad (\nabla^2 + k^2)\hat{\phi}^*(\rho, z) = 0$$

The equations reduce to

Region I, $0 \leq \rho \leq a$:

$$\left[\frac{\partial^2}{\partial z^2} + \frac{1}{\rho} \frac{\partial}{\partial \rho} \rho \frac{\partial}{\partial \rho} + k_1^2 \right] A_{z1}^e(\rho, z) = 0$$

Region II, $\rho \geq a$:

$$\left[\frac{\partial^2}{\partial z^2} + \frac{1}{\rho} \frac{\partial}{\partial \rho} \rho \frac{\partial}{\partial \rho} + k_0^2 \right] A_{z2}^e(\rho, z) = 0$$

Using a Fourier transform pair, the above equations become

$$\left[\frac{\partial^2}{\partial \rho^2} + \frac{1}{\rho} \frac{\partial}{\partial \rho} + (k_1^2 - \xi^2) \right] \bar{A}_{z1}^e(\rho, \xi) = 0$$

$$\left[\frac{\partial^2}{\partial \rho^2} + \frac{1}{\rho} \frac{\partial}{\partial \rho} + (k_0^2 - \xi^2) \right] \bar{A}_{z2}^e(\rho, \xi) = 0$$

With a change of variable the above equations can be recognized as Bessel equations with the following solutions,

$$\bar{A}_{z1}^e(\rho, \xi) = PJ_0(\gamma_1 \rho) \quad \text{for } 0 \leq \rho \leq a$$

$$\bar{A}_{z2}^e(\rho, \xi) = QH_0^{(1)}(\gamma_0 \rho) \quad \text{for } \rho \geq a$$

where $\gamma_0 = (k_0^2 - \xi^2)^{1/2}$ and $\gamma_1 = (k_1^2 - \xi^2)^{1/2}$

The boundary conditions (57a,b), expressed in terms of the electric vector potential, become

$$(1/\epsilon_1) \partial \bar{A}_{z1}^e(a^-, \xi) / \partial \rho = (1/\epsilon_0) \partial \bar{A}_{z2}^e(a^+, \xi) / \partial \rho \quad (58a)$$

$$(i\omega\gamma_0^2/k_0^2) \bar{A}_{z2}^e(a^+, \xi) - (i\omega\gamma_1^2/k_1^2) \bar{A}_{z1}^e(a^-, \xi) = -I_0^e \quad (58b)$$

By applying the boundary conditions and determining P and Q, the electric vector potential can be written as:

$$\bar{A}_{z1}^e(\rho, \xi) = -i\omega\mu_1\epsilon_1 a I_0^e H_1^{(1)}(\gamma_0 a) J_0(\gamma_1 \rho) / \gamma_1 D(\xi) \quad \text{for } 0 \leq \rho \leq a \quad (59)$$

$$\bar{A}_{z2}^e(\rho, \xi) = -i\omega\mu_1\epsilon_0 a I_0^e J_1(\gamma_1 a) H_0^{(1)}(\gamma_0 \rho) / \gamma_0 D(\xi) \quad \text{for } \rho \geq a$$

Similarly, by solving the wave equation for the scalar magnetic potential ϕ^* , the solution can be obtained as:

$$\bar{\phi}_1^*(\rho, \xi) = ia\xi I_0^e H_1^{(1)}(\gamma_0 a) J_0(\gamma_1 \rho) / \gamma_1 D(\xi) \quad \text{for } 0 \leq \rho \leq a \quad (60)$$

$$\bar{\phi}_2^*(\rho, \xi) = ia\xi I_0^e \mu_r J_1(\gamma_1 a) H_0^{(1)}(\gamma_0 \rho) / \gamma_0 D(\xi) \quad \text{for } \rho \geq a$$

The boundary conditions satisfied by $\bar{\phi}^*(\rho, \xi)$ at the surface $\rho = a$ are:

$$(\omega\mu_1/\xi) \partial \bar{\phi}_1^*(a^-, \xi) / \partial \rho = (\omega\mu_0/\xi) \partial \bar{\phi}_2^*(a^+, \xi) / \partial \rho \quad (61a)$$

$$\gamma_0^2 \bar{\phi}_2^*(a^+, \xi) - \gamma_1^2 \bar{\phi}_1^*(a^-, \xi) = -i\xi I_0^e \quad (61b)$$

It can also be verified that the potentials satisfy the gauge condition,

$$\partial \bar{A}_z^e(\rho, z) / \partial z - i\omega\mu\epsilon\phi^*(\rho, z) = 0 \quad \text{in both regions}$$

The potentials of (59) and (60) can also be obtained from the electromagnetic fields of (55) and (56) by making use of the following relationships in both regions:

$$E_{\phi}(\rho, z) = (1/\epsilon) \partial A_z^e(\rho, z) / \partial z \quad ; \quad H_z(\rho, z) = -\partial \phi^*(\rho, z) / \partial z + i\omega A_z^e(\rho, z)$$

and

$$\partial A_z^e(\rho, z) / \partial z - i\omega \mu \epsilon \phi^*(\rho, z) = 0$$

The above analysis verifies that when the antenna is infinitely long, both the scalar magnetic and electric vector potentials exist. They are both discontinuous across the antenna surface and satisfy respective wave equations, appropriate boundary conditions, and the gauge condition.

In the case of the finite antenna, however, a precise knowledge of the vector potential in the two regions is not necessary to derive an approximate integral equation for the magnetic current. What is required is the electric vector potential on the surface of the antenna. To determine this, an internal impedance per unit length is defined and used to obtain the three-term solution for the magnetic current. Using the computer programs described and listed in Appendix B, the magnetic current was evaluated for a range of parameters. The current distribution was studied as a function of the four independent parameters, viz., μ_r^i ; μ_r'' or $Q = \mu_r^i / \mu_r''$; h/λ_0 or $k_0 h$; and ak_0 or $\Omega = 2 \ln(2h/a)$. In this study the value of the dielectric constant of the ferrite was fixed at 10.

The ranges of the four parameters were as follows: $\mu_r^i = 10, 100, 1000$; $Q = 1$ to $Q = 100$; $h/\lambda_0 = .1$ to $h/\lambda_0 = .5$; and $ak_0 = .001$ to $ak_0 = .1$. Typical results of the computations are shown plotted in Fig. 3. The quantities μ_r^i , ak_0 , h/λ_0 and Q are varied, respectively, in Fig. 3a-d, while in each case the remaining three parameters are kept constant.

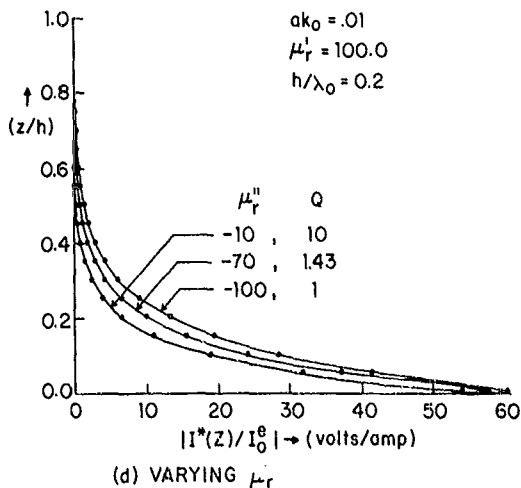
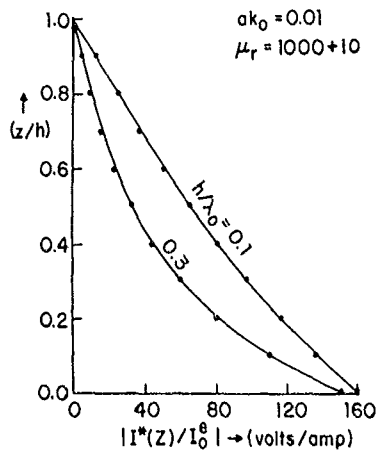
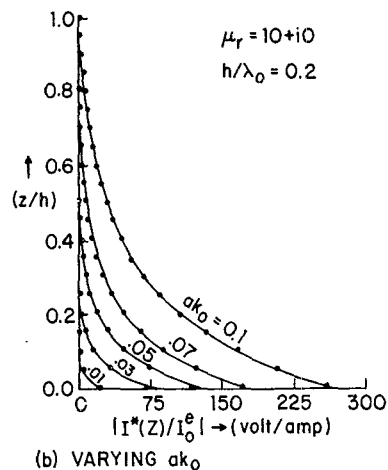
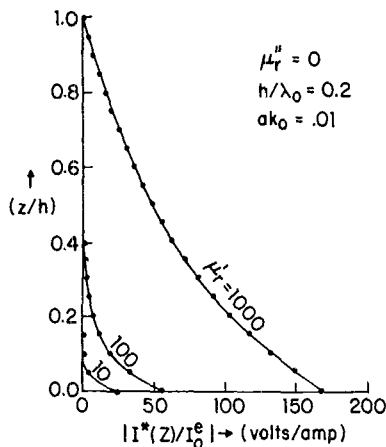


FIG. 3 PLOT OF THE MAGNITUDE OF NORMALIZED MAGNETIC CURRENT ($|I^*(Z)/I_0^e|$) AS A FUNCTION OF NORMALIZED DISTANCE (z/h) FOR VARIOUS PARAMETER RANGES. ($\epsilon_r = 10 + i0$ FOR ALL THE CASES)

In Fig. 3a for fixed height, radius, and ratio Q , the magnetic current on the antenna is seen to increase with the real part of the relative permeability. A similar behavior is observed in Fig. 3b for increasing antenna radius and fixed height, permeability and Q . A comparison between Fig. 3a and Fig. 3d shows that a large value of μ_r^i produces a greater increase in the magnetic current than a high Q ratio; in fact, an increase in Q for $Q < 50$ is seen to reduce the magnitude of the magnetic current. To interpret Fig. 3c, it is useful to examine the behavior of the propagation constant k on the antenna, given by

$$k = \beta + i\alpha = k_0 [1 + i(4\pi z_m^i \epsilon_0 / k_0 \psi_{dR})]^{1/2}$$

If the dimensionless parameter $\phi_1 = (4\pi z_m^i \epsilon_0 / k_0)$ is introduced, this expression becomes

$$k = \beta + i\alpha = k_0 (1 + i\phi_1 / \psi_{dR})^{1/2}$$

Despite the fact that ψ_{dR} is itself a function of k , an efficient iterative method can be used to determine the value of the propagation constant. By substituting for z_m^i from (36) the following expression for ϕ_1 is obtained:

$$\phi_1 = \frac{2iak_1}{(ak_0)^2} \frac{J_0(ak_1)}{J_1(ak_1)}$$

ϕ_1 becomes positive imaginary for the cases plotted in Fig. 3c where ak_1 is real. This makes the propagation constant k on the antenna pure imaginary which leads to an exponentially decreasing magnetic current. For most practical ferrites the positive imaginary part of ϕ_1 dominates, which makes the attenuation constant α significantly larger than the phase constant β . This can also be seen in the experimental results reported in Section 9.

At this stage it is considered useful to summarize all the approximations and assumptions involved in the derivation of the integral equation in (38) with (39). The ferrite was first treated as a perfect magnetic conductor ($\mu_r = \text{infinity}$) and the integral equation in (14) was obtained. This expression was later modified by adding an intrinsic impedance per unit length for a practical ferrite that is an imperfect magnetic conductor and finite. The basic assumption that the radius be small, i.e., $ak_0 \ll 1$, was made. An implied approximation was introduced when the impedance per unit length z_m^i , derived originally for the infinitely long magnetic conductor, was used for the finite antenna. Its use can be justified as follows. For an infinitely long magnetic conductor, the transverse distribution of electric vector potential is independent of the axial distribution. It is reasonable to assume that this remains the case when the conductor length is large compared to the radius, so that the intrinsic impedance per unit length derived for the infinitely long conductor can be used directly for antennas of finite length. A further question arises concerning the discontinuity of the electric vector potential across the antenna surface. It has been established that the electric vector potential is discontinuous across the antenna surface when the antenna is infinitely long. It is reasonable to conclude that the discontinuity exists even when the length of the antenna is finite. The derivation of the integral equation for the magnetic current or the tangential electric field requires a knowledge of the electric vector potential on the surface $\rho = a$, which has apparently two values. This problem is not peculiar to the ferrite-rod antenna but also exists in the analogous resistive electric dipole antenna. In either case, the value of the vector potential used is that obtained by approaching the antenna surface from the surrounding medium. It is believed, however, that the discontinuity in the vector potential is a

consequence of the way in which the vector potential was defined and can be overcome with the introduction of a suitable scale factor in the definition.

The approach of treating the ferrite as an imperfect magnetic conductor relies on the mathematical equivalence of the two analogous problems. One cannot escape the fact, however, that while there are two pieces of conductor separated by a slice voltage or electric field generator in the case of an electric dipole, the magnetic conductor in the ferrite problem is a single continuous rod driven on the outside surface. A delta function, although unphysical, is a mathematical convenience in either case.

In view of the above discussion, a more rigorous analysis which does not invoke the analogy with the electric dipole is developed and presented in the following section.

7. A MORE RIGOROUS TREATMENT OF THE FINITE ANTENNA

Since the total magnetic current $I_z^*(z)$ is linearly related to the tangential electric field $E_\phi(a,z)$ by the relation

$$I_z^*(z) = -2\pi a E_\phi(a,z) \quad ,$$

the following procedure seeks to derive an integral equation for $E_\phi(a,z)$ by solving the ferrite-interior and free space-exterior problems.

Interior Problem. The interior problem consists of a ferrite cylinder of height $2h$ driven at the center by a constant-current loop. The driving condition will be accounted for after the interior and exterior problems are solved. The diameter of the rod and of the loop is $2a$ and the restriction $ak_0 \ll 1$ is satisfied in order to maintain a constant current I_0^e in the driving loop. Given a cylindrical coordinate system (ρ, ϕ, z) and after eliminating \vec{H} from Maxwell's curl equation and imposing azimuthal symmetry, one obtains

for the electric field

$$\left[\frac{\partial^2}{\partial \rho^2} + \frac{1}{\rho} \frac{\partial}{\partial \rho} + (k_1^2 - \frac{1}{2}) + \frac{\partial^2}{\partial z^2} \right] E_\phi(\rho, z) = 0 \quad (62)$$

with $k_1 = k_0(\mu_r \epsilon_r)^{1/2}$, $|z| \leq h$, $0 \leq \rho \leq a$, and $E_\phi(\rho, z) = E_\phi(\rho, -z)$.

Solving (62) by a separation-of-variables technique gives

$$E_\phi(\rho, z) = \sum_{n=-\infty}^{\infty} A_n \cos[(n+1/2)\pi z/h] J_1[\rho \{k_1^2 - (n+1/2)^2 \pi^2/h^2\}^{1/2}] \quad (63)$$

with the coefficients A_n given by

$$A_n = \frac{1}{h J_1[a \{ (n+1/2)^2 \pi^2/h^2 \}^{1/2}]} \int_{-h}^h E_\phi(a, z') \cos[(n+1/2)\pi z'/h] dz'$$

This procedure aims to determine the tangential magnetic field $H_z(a, z)$ from independent treatments of both the interior and exterior problems and then to require that their difference equal $-I_0^e \delta(z)$, the true electric surface current. Thus, $H_z(a^-, z)$ can be obtained from the above by using

$$\begin{aligned} H_z(\rho, z) &= (1/i\omega\mu_1) \{ \partial E_\phi(\rho, z)/\partial \rho + E_\phi(\rho, z)/\rho \} \\ &= (1/i\omega\mu_1 h) \left[\sum_{n=-\infty}^{\infty} \left(\int_{-h}^h dz' E_\phi(a, z') \cos[(n+1/2)\pi z'/h] \right) \right. \\ &\quad \times \cos[(n+1/2)\pi z/h] \frac{J_0[\rho \{k_1^2 - (n+1/2)^2 \pi^2/h^2\}^{1/2}]}{J_1[a \{k_1^2 - (n+1/2)^2 \pi^2/h^2\}^{1/2}]} \\ &\quad \left. \times [k_1^2 - (n+1/2)^2 \pi^2/h^2]^{1/2} \right] \quad (64) \end{aligned}$$

It should be pointed out that, as a first approximation, $E_\phi(a, z)$ is made

to vanish on the top and bottom surfaces defined by $|z| = h$ and $0 \leq \rho \leq a$, thus neglecting all the fringing fields at the ends of the antenna. In practice, this condition nearly prevails for antennas with heights large compared to the radius ($h \gg a$).

Exterior Problem. The exterior problem is concerned with the free space surrounding the ferrite rod which extends from $(0 \leq \rho \leq a)$ and $(-h \leq z \leq h)$ for all ϕ . It is equivalent to solving the problem with the ferrite removed but with the tangential electric field on the surface $E_\phi(a, z)$ for $|z| \leq h$ required to be the same as that used in the interior problem. With an assumed $e^{-i\omega t}$ time dependence, the governing equations are:

$$\nabla \times \vec{H} = -i\omega\epsilon_0 \vec{E} \quad (65a)$$

$$\nabla \times \vec{E} = i\omega\mu_0 \vec{H} \quad (65b)$$

$$\nabla \cdot \vec{H} = 0 \quad (65c)$$

$$\nabla \cdot \vec{D} = 0 \quad (65d)$$

From (65d) in free space, one may define an electric vector potential

$$\vec{D} = -\nabla \times \vec{A}^e$$

so that

$$\vec{E} = -(1/\epsilon_0)\nabla \times \vec{A}^e$$

This leads to

$$\vec{H} = -\nabla\phi^* + i\omega\vec{A}^e$$

The exterior problem may be modeled by a cylindrical surface of radius a

that extends from $z = -h$ to $z = h$. This surface, when immersed in free space, has the following boundary conditions valid for $|z| \leq h$:

$$E_{\phi}(a^+, z) = f^+(z) = E_{\phi}(a, z) \quad (66a)$$

$$E_{\phi}(a^-, z) = f^-(z) = 0 \quad (66b)$$

Substituting for \vec{E} and \vec{H} in (65b), one obtains

$$-\nabla \times \nabla \times \vec{A}^e + i\omega\mu_0\epsilon_0\nabla\phi^* + k_0^2\vec{A}^e = 0 \quad (67a)$$

$$(\nabla^2 + k_0^2)\vec{A}^e = \nabla(\nabla \cdot \vec{A}^e + \mu_0\epsilon_0\dot{\phi}^*) = \nabla\chi \quad (67b)$$

If the Lorentz gauge is satisfied, the Lorentz factor χ [and the right-hand side of (67b)] is zero. The equations may now be specialized to the problem at hand. There is rotational symmetry in the problem and the non-zero quantities are E_{ϕ} , H_{ρ} , H_z , A_z^e and $\dot{\phi}^*$. Equations (65a,b) for the different components become

$$(\partial H_{\rho}/\partial z - \partial H_z/\partial \rho) = -i\omega\epsilon_0 E_{\phi} \quad (68a)$$

$$i\omega\mu_0 H_{\rho} = -\partial E_{\phi}/\partial z \quad (68b)$$

$$i\omega\mu_0 H_z = \frac{1}{\rho} \frac{\partial}{\partial \rho} (\rho E_{\phi}) \quad (68c)$$

These three equations are true everywhere except on the surface $\rho = a$ and $|z| \leq h$. To make the equations valid on the surface, one has to introduce the surface conditions into the above equations. In addition to the conditions in (66a,b), there is an electric current $K_{\phi}(z)$ on the surface as well as a large axial magnetic field. Thus, (68a-c) become

$$(\partial H_\rho / \partial z - \partial H_z / \partial \rho) + \delta(\rho - a) K_\phi(z) = -i\omega\epsilon_0 E_\phi \quad (69a)$$

$$i\omega\mu_0 H_\rho = -\partial E_\phi / \partial z \quad (69b)$$

$$i\omega\mu_0 H_z + \delta(\rho - a) E_\phi = (\partial E_\phi / \partial \rho + E_\phi / \rho) \quad (69c)$$

In terms of the potentials, the fields are given by

$$H_\rho = -\partial \phi^* / \partial z$$

$$H_z = -\partial \phi^* / \partial \rho + i\omega A_z^e$$

$$E_\phi = (1/\epsilon_0) \partial A_z^e / \partial \rho$$

From the preceding equation,

$$A_z^e(\rho, z) = \epsilon_0 \int_0^\infty E_\phi(\rho', z) d\rho' \quad (70)$$

It is now required to set up an equation for $A_z^e(\rho, z)$.

$$\begin{aligned} (v^2 + k_0^2) A_z^e(\rho, z) &= \left[\frac{\partial^2}{\partial \rho^2} + \frac{1}{\rho} \frac{\partial}{\partial \rho} + \frac{\partial^2}{\partial z^2} + k_0^2 \right] \epsilon_0 \int_0^\infty E_\phi(\rho', z) d\rho' \\ &= \epsilon_0 [\partial E_\phi(\rho, z) / \partial \rho + E_\phi(\rho, z) / \rho] + \epsilon_0 \frac{\partial}{\partial z} \int_0^\infty \partial E_\phi(\rho', z) / \partial z d\rho' \\ &\quad + \epsilon_0 k_0^2 \int_0^\infty E_\phi(\rho', z) d\rho' \end{aligned}$$

With (69b,c) this becomes

$$\begin{aligned} (v^2 + k_0^2) A_z^e(\rho, z) &= \epsilon_0 [i\omega\mu_0 H_z(\rho, z) + \delta(\rho - a) E_\phi(\rho, z)] \\ &\quad - i\omega\mu_0 \epsilon_0 \int_0^\infty \partial H_\rho(\rho', z) / \partial z d\rho' + \epsilon_0 k_0^2 \int_0^\infty E_\phi(\rho', z) d\rho' \end{aligned}$$

Using (69a) gives

$$\begin{aligned}
 & (\nabla^2 + k_0^2) A_z^e(\rho, z) \\
 &= i\omega\mu_0\epsilon_0 H_z(\rho, z) + \epsilon_0 \delta(\rho - a) E_\phi(\rho, z) - i\omega\mu_0\epsilon_0 \int_0^\infty [-i\omega\epsilon_0 E_\phi(\rho', z) + \frac{\partial H_z(\rho', z)}{\partial \rho} \\
 &\quad - \delta(\rho' - a) K_\phi(z)] d\rho' + \epsilon_0 k_0^2 \int_0^\infty E_\phi(\rho', z) d\rho' \\
 &= i\omega\mu_0\epsilon_0 H_z(\rho, z) + \epsilon_0 \delta(\rho - a) E_\phi(\rho, z) - \epsilon_0 k_0^2 \int_0^\infty E_\phi(\rho', z) d\rho' \\
 &\quad + i\omega\mu_0\epsilon_0 K_\phi(z) \int_0^\infty \delta(\rho' - a) d\rho' - i\omega\mu_0\epsilon_0 H_z(\rho, z) + \epsilon_0 k_0^2 \int_0^\infty E_\phi(\rho', z) d\rho' \\
 &= \epsilon_0 \delta(\rho - a) E_\phi(\rho, z) + i\omega\mu_0\epsilon_0 K_\phi(z) \int_0^\infty \delta(\rho' - a) d\rho'
 \end{aligned}$$

The ρ' integral may be performed:

$$\int_0^\infty \delta(\rho' - a) d\rho' = H(a - \rho) = \begin{cases} 1 & \text{if } 0 \leq \rho \leq a \\ 0 & \text{if } \rho \geq a^+ \end{cases}$$

Therefore, finally

$$(\nabla^2 + k_0^2) A_z^e(\rho, z) = \epsilon_0 \delta(\rho - a) E_\phi(\rho, z) + i\omega\mu_0\epsilon_0 K_\phi(z) H(a - \rho) \quad (71)$$

If (71) is formally identified with (67b), it is seen that the second term on the right in (71) corresponds to the Lorentz factor term. The Lorentz gauge is satisfied ($\chi = 0$) in the exterior region ($\rho > a$) but is not satisfied in the interior region. Furthermore, by differentiating with respect to ρ

$$\chi = \nabla \cdot \vec{A}^e + \mu_0\epsilon_0 \dot{\phi}^* = \partial A_z^e(\rho, z) / \partial z - i\omega\mu_0\epsilon_0 \dot{\phi}^*(\rho, z)$$

it can be shown that χ is independent of ρ and a function of z only, i.e.,

$\chi = \chi(z)$, which leads to:

$$\chi(z) = \partial A_z^e(\rho, z) / \partial z - i\omega\mu_0\epsilon_0\phi^*(\rho, z) = \begin{cases} i\omega\mu_0\epsilon_0 \int_0^z K_\phi(z') dz' & \text{if } 0 \leq \rho \leq a^- \\ 0 & \text{if } \rho \geq a^+ \end{cases}$$

It is thus seen that the Lorentz condition is satisfied on the exterior but not in the interior. This is because of the presence of the transverse electric current in the ferrite medium. This situation can be contrasted to an electric dipole antenna (thin or thick), where there are no magnetic currents to make the Lorentz condition invalid.

It is now required to solve (71) for the electric vector potential. The equation becomes

$$\left(\frac{\partial^2}{\partial \rho^2} + \frac{1}{\rho} \frac{\partial}{\partial \rho} + \frac{\partial^2}{\partial z^2} + k_0^2 \right) A_z^e(\rho, z) = \epsilon_0 \delta(\rho - a) E_\phi(\rho, z) + i\omega\mu_0\epsilon_0 K_\phi(z) H(a - \rho)$$

This equation can be solved with the use of Green's theorem and the principle of superposition. Thus,

$$A_z^e(\rho, z) = A_{zE}^e(\rho, z) + A_{zK}^e(\rho, z)$$

where

$$\begin{aligned} A_{zE}^e(\rho, z) &= -(\epsilon_0/4\pi) \int_{-\pi}^{\pi} d\phi' / 2\pi \int_0^{\infty} d\rho' 2\pi\rho' \int_{-\infty}^{\infty} dz' E_\phi(\rho, z') \delta(\rho' - a) (e^{ik_0 R} / R) \\ &= -(a\epsilon_0/2) \int_{-h}^h dz' E_\phi(a, z') K(z - z', \rho) \end{aligned}$$

with

$$K(z - z', \rho) = \int_{-\pi}^{\pi} \frac{d\phi'}{2\pi} \frac{e^{ik_0 R}}{R} \quad (72)$$

and $R = [(z - z')^2 + \rho^2 + a^2 - 2\rho a \cos \phi']^{1/2}$. $A_{zE}^e(\rho, z)$ will be used later

to obtain $A_{z1}^e(a, z)$. Similarly,

$$A_{zK}^e(\rho, z) = -(i\omega\mu_0\epsilon_0/4\pi) \int_{-\pi}^{\pi} d\phi' / 2\pi \int_0^{\infty} d\rho' 2\pi\rho' \int_{-\infty}^{\infty} dz' K_{\phi}(z') H(a - \rho) (e^{ik_0 R_1 / R_1})$$

$$= -(i\omega\mu_0\epsilon_0/2) \int_{-h}^h dz' K_{\phi}(z') M_1(z - z', \rho)$$

where

$$M_1(z - z', \rho) = \int_{-\pi}^{\pi} \frac{d\phi'}{2\pi} \int_0^a d\rho' \rho' \frac{e^{ik_0 R_1}}{R_1} \quad (73)$$

$$\text{and } R_1 = [(z - z')^2 + \rho^2 + \rho'^2 - 2\rho\rho' \cos \phi']^{1/2}.$$

Thus, the total electric vector potential is

$$A_z^e(\rho, z) = -(a\epsilon_0/2) \int_{-h}^h dz' E_{\phi}(a, z') K(z - z', \rho)$$

$$-(i\omega\mu_0\epsilon_0/2) \int_{-h}^h dz' K_{\phi}(z') M_1(z - z', \rho) \quad (74)$$

By specializing (74) for $\rho = a^+$ and $\rho = a^-$ and by making use of (70) and (66a,b), one obtains

$$\epsilon_0 E_{\phi}(a, z) = -(a\epsilon_0/2) \int_{-h}^h dz' E_{\phi}(a, z') \partial K(z - z', \rho) / \partial \rho \Big|_{\rho=a^+}$$

$$- (i\omega\mu_0\epsilon_0/2) \int_{-h}^h dz' K_{\phi}(z') \partial M_1(z - z', \rho) / \partial \rho \Big|_{\rho=a^-} \quad (75)$$

Returning to (74), one may now obtain for the tangential magnetic field

$$H_z(\rho, z) = (i\omega/k_0^2) \left(\frac{\partial^2}{\partial z^2} + k_0^2 \right) A_z^e(\rho, z)$$

Thus,

$$H_z(\rho, z) = (a/2)(1/i\omega\mu_0) \left(\frac{\partial^2}{\partial z^2} + k_0^2 \right) \int_{-h}^h dz' E_\phi(a, z') K(z - z', \rho) \\ + (1/2) \left(\frac{\partial^2}{\partial z^2} + k_0^2 \right) \int_{-h}^h dz' K_\phi(z') M_1(z - z', \rho) \quad (76)$$

Once again, on the exterior surface $\rho = a^+$,

$$H_z(a^+, z) = (a/2)(1/i\omega\mu_0) \left(\frac{\partial^2}{\partial z^2} + k_0^2 \right) \int_{-h}^h dz' E_\phi(a, z') K(z - z', a^+) \\ + (1/2) \left(\frac{\partial^2}{\partial z^2} + k_0^2 \right) \int_{-h}^h dz' K_\phi(z') M_1(z - z', a^+) \quad (77)$$

It now remains to use (77) and (64) to obtain the integral equation.

Integral Equation for $E_\phi(a, z)$ and $K_\phi(z)$. The required integral equations for the unknown quantities may be obtained from the results of (64) and (77) for the interior and exterior problems by requiring that

$$H_z(a^+, z) - H_z(a^-, z) = -I_0^e \delta(z)$$

This gives

$$\left\{ (a/2)(1/i\omega\mu_0) \left(\frac{\partial^2}{\partial z^2} + k_0^2 \right) \int_{-h}^h dz' E_\phi(a, z') K(z - z', a) + (1/2) \left(\frac{\partial^2}{\partial z^2} + k_0^2 \right) \right. \\ \times \left. \int_{-h}^h dz' K_\phi(z') M_1(z - z', a) \right\} + \left\{ (1/\omega\mu_1 a h) \sum_{n=-\infty}^{\infty} \left[\int_{-h}^h dz' E_\phi(a, z') \right. \right. \\ \times \left. \left. \cos(pz') \right] \cos(pz) \frac{J_0\{a(k_1^2 - p^2)^{1/2}\}}{J_1\{a(k_1^2 - p^2)^{1/2}\}} \{a(k_1^2 - p^2)^{1/2}\} \right\} = -I_0^e \delta(z) \quad (78a)$$

with $p = (n + 1/2)\pi/h$.

The other equation to be satisfied simultaneously is (75), which is reproduced here for convenience:

$$\begin{aligned} \epsilon_0 E_\phi(a, z) = & -(a\epsilon_0/2) \int_{-h}^h dz' E_\phi(a, z') \frac{\partial K(z - z', \rho)}{\partial \rho} \Big|_{\rho=a} + \\ & - (i\omega\mu_0\epsilon_0/2) \int_{-h}^h dz' K_\phi(z') \frac{\partial M_1(z - z', \rho)}{\partial \rho} \Big|_{\rho=a} \quad (78b) \end{aligned}$$

The two kernels $K(z - z', \rho)$ and $M_1(z - z', \rho)$ appearing in the coupled integral equations above are defined by (72) and (73) respectively.

It can be verified easily that in the limit $h \rightarrow \infty$ the integrals in (78a,b) become convolution integrals, that the two equations decouple and that the expression for $E_\phi(\rho, z)$ on the surface $\rho = a$ is in complete agreement with the results presented in Part I [2, Eqs. (17) or (18)].

Returning to the coupled integral equations in (78a,b), it is seen that there are three kernels. First of all, the kernel on the right-hand side of (78a) will be examined carefully. The kernel is made up of an infinite series which is clearly divergent since, for large values of n , it behaves like n . Although strictly not valid, the operations of summation and integration will be interchanged for the purpose of examining the series. The interchange is reversed at a later stage so that, in effect, all the steps are valid.

It is convenient to define the kernel $M(z, z')$ on the left-hand side of (78a) as:

$$M(z, z') = \sum_{n=-\infty}^{\infty} \cos(pz') \cos(pz) \frac{J_0[a(k_1^2 - p^2)^{1/2}]}{J_1[a(k_1^2 - p^2)^{1/2}]} [a(k_1^2 - p^2)^{1/2}]$$

where $p = (n + 1/2)\pi/h$.

As was pointed out earlier, this series is divergent and, hence, it is useful to write it as the sum of two series, using the first two terms in the

asymptotic form. For large values of n , the series behaves like

$$\begin{aligned} \int \cos(pz') \cos(pz) \frac{J_0(iap)}{J_1(iap)} (iap) &\simeq \int \cos(pz') \cos(pz) \frac{I_0(ap)}{I_1(ap)} (ap) \\ &\simeq \int \cos(pz') \cos(pz) \frac{1 + \frac{1}{8ap}}{1 - \frac{3}{8ap}} (ap) \simeq \int \cos(pz') \cos(pz) \left[1 + \frac{1}{2ap} \right] (ap) \end{aligned}$$

We now write

$$M(z, z') = P(z, z') + Q(z, z') \quad (79)$$

with

$$P(z, z') = \sum_{n=-\infty}^{\infty} \left[\frac{J_0[a(k_1^2 - p^2)^{1/2}]}{J_1[a(k_1^2 - p^2)^{1/2}]} [a(k_1^2 - p^2)^{1/2}] - ap - \frac{1}{2} \right] \cos(pz') \cos(pz) \quad (80)$$

and

$$Q(z, z') = \sum_{n=-\infty}^{\infty} (ap + 1/2) \cos(pz') \cos(pz) \quad (81)$$

Equation (79) along with (80) and (81) is exact because it only adds and subtracts the first two terms in the asymptotic form. Now $P(z, z')$ can be written as:

$$P(z, z') = \sum_{n=-\infty}^{\infty} A_n \cos(pz') \cos(pz)$$

with A_n given by the term in the square brackets in (80).

If all the coefficients A_n were equal, $P(z, z')$ would be a delta function; but this is not the case. In view of the differential operator on the left-hand side of (78a), it is helpful to remove a similar factor from $P(z, z')$. This is easily accomplished by solving an equation of the form:

$$(\partial^2/\partial z^2 + k_0^2)f(z) = \cos(pz)$$

Through the use of Green's function (or by any other method), one can obtain:

$$f(z) = a_1 \cos(k_0 z) + a_2 \sin(k_0 z) + (1/k_0) \int_0^z \sin[k_0(z - z')] \cos(pz') dz'$$

Note that, without any loss of generality, the constants a_1 and a_2 can be set equal to zero and the integral on the right performed to obtain:

$$f(z) = [\cos(pz) - \cos(k_0 z)] / (k_0^2 - p^2)$$

so that

$$P(z, z') = \left(\frac{\partial^2}{\partial z^2} + k_0^2 \right) \sum_{n=-\infty}^{\infty} A_n \left[\frac{\cos(pz) - \cos(k_0 z)}{k_0^2 - p^2} \right] \cos(pz') \quad (82)$$

In (82) it appears that one of the terms in the series will be equal to infinity if $p = k_0$. This condition is equivalent to $h/\lambda = 1/4, 3/4, 5/4, \dots$.

This is not the case, however, because of the numerator and the fact that, as $p \rightarrow k_0$, the term in the square brackets in (82) approaches $[z \sin(k_0 z)]/2k_0$.

Returning to (81), it is found that, since $Q(z, z')$ is an odd series, its most divergent part is identically equal to zero, so that

$$Q(z, z') = (1/2) \sum_{n=-\infty}^{\infty} \cos(pz') \cos(pz) = (h/2) \delta(z - z') \quad (83)$$

Using (82) and (83) with (79) in the integral equation (78a), one obtains

$$\begin{aligned} & \left(\frac{\partial^2}{\partial z^2} + k_0^2 \right) \left[\int_{-h}^h dz' E_{\phi}(a, z') K(z - z', a) + \frac{i\omega\mu_0}{a} \int_{-h}^h K_{\phi}(z') M_1(z - z', a) dz' \right] \\ & = -\frac{2}{a} \left\{ i\omega\mu_0 I_0^e(z) - \frac{1}{a\mu_r} \frac{1}{2} E_{\phi}(a, z) - \frac{1}{a\mu_r} \frac{1}{h} \left(\frac{\partial^2}{\partial z^2} + k_0^2 \right) \int_{-h}^h dz' E_{\phi}(a, z') \right\} \end{aligned}$$

(Continued)

$$\times \left(\sum_{n=-\infty}^{\infty} A_n \left[\frac{\cos(pz) - \cos(k_0 z)}{k_0^2 - p^2} \right] \cos(pz') \right) \Bigg\}$$

Rearranging terms gives

$$\begin{aligned} & \left(\frac{\partial^2}{\partial z^2} + k_0^2 \right) \left[\int_{-h}^h dz' E_{\phi}(a, z') K_1(z - z') + \frac{i\omega\mu_0}{a} \int_{-h}^h K_{\phi}(z') M_1(z - z', a) dz' \right] \\ & = -\frac{2}{a} \left[i\omega\mu_0 I_0^0 \delta(z) - \frac{1}{a\mu_r} \frac{1}{2} E_{\phi}(a, z) \right] \end{aligned} \quad (84)$$

where the combined kernel $K_1(z - z')$ is defined as

$$K_1(z - z') = \int_{-\pi}^{\pi} \frac{d\phi'}{2\pi} \frac{e^{ik_0 R_s}}{R_s} - \frac{2}{a^2 \mu_r h} \sum_{n=-\infty}^{\infty} A_n \left[\frac{\cos(pz) - \cos(k_0 z)}{k_0^2 - p^2} \right] \cos(pz') \quad (85)$$

with the coefficients A_n given by

$$A_n = \frac{J_0[a(k_1^2 - p^2)^{1/2}]}{J_1[a(k_1^2 - p^2)^{1/2}]} [a(k_1^2 - p^2)^{1/2}] - ap - \frac{1}{2}$$

and $p = (n + 1/2)\pi/h$.

The second integral equation from (78b) is:

$$\begin{aligned} & -\frac{a}{2} \int_{-h}^h dz' E_{\phi}(a, z') \frac{\partial}{\partial \rho} K(z - z', \rho) \Big|_{\rho=a^+} - \frac{i\omega\mu_0}{2} \int_{-h}^h dz' K_{\phi}(z') \frac{\partial}{\partial \rho} M_1(z - z', \rho) \Big|_{\rho=a^-} \\ & = E_{\phi}(a, z) \end{aligned}$$

The coupled integral equations can now be written in a short-hand notation

suitable for numerical evaluation:

$$\left(\frac{\partial^2}{\partial z^2} + k_0^2 \right) \left[\int_{-h}^h dz' E_{\phi}(z') K_1(z - z') + C_1 \int_{-h}^h dz' I_{\phi}(z') M_1(z - z') \right] = C_2 \delta(z) + C_3 E_{\phi}(z) \quad (86a)$$

$$C_4 \int_{-h}^h dz' E_{\phi}(z') K_2(z-z') + C_5 \int_{-h}^h dz' I_{\phi}(z') M_2(z-z') = \frac{1}{2} F_{\phi}(z) \quad (86b)$$

where the electric surface current $I_{\phi}(z) = 2\pi a K_{\phi}(z)$. Also, the kernel $K_1(z-z')$ has been defined previously in (85), and

$$C_1 = i\omega\mu_0/2\pi a^2 \quad ; \quad C_2 = -2i\omega\mu_0 I_0^e/a \quad ; \quad C_3 = 1/a^2 \mu_r \quad ;$$

$$C_4 = -a/2 \quad ; \quad C_5 = -i\omega\mu_0/4\pi a$$

The factor (1/2) on the right-hand side of (86b) comes from the discontinuity in the derivative of the $K_2(z-z')$ kernel, viz.,

$$K_2(z-z') = \frac{\partial}{\partial \rho} K(z-z', \rho) \Big|_{\rho=a^+} \neq \frac{\partial}{\partial \rho} K(z-z', \rho) \Big|_{\rho=a^-}$$

$$M_2(z-z') = \frac{\partial}{\partial \rho} M_1(z-z', \rho) \Big|_{\rho=a^+} = \frac{\partial}{\partial \rho} M_1(z-z', \rho) \Big|_{\rho=a^-}$$

8. NUMERICAL SOLUTION BY THE MOMENT METHOD OF THE COUPLED INTEGRAL EQUATIONS

The differential equation (86a) can be solved to obtain:

$$\begin{aligned} & \int_{-h}^h dz' E_{\phi}(z') K_1(z-z') + C_1 \int_{-h}^h dz' I_{\phi}(z') M_1(z-z') \\ & = C_6 \cos(k_0 z) + C_7 \sin(k_0 |z|) + C_8 \int_0^z dz' E_{\phi}(z') \sin[k_0(z-z')] \end{aligned} \quad (87a)$$

Similarly, from (86b)

$$\int_{-h}^h dz' E_{\phi}(z') K_2(z-z') + C_9 \int_{-h}^h dz' I_{\phi}(z') M_2(z-z') = C_{10} F_{\phi}(z) \quad (87b)$$

where C_6 is unknown and determined numerically by employing the end condition

$$I_{\phi}(h) = 0, \text{ and}$$

$$C_1 = i\omega\mu_0/2\pi a^2 \quad ; \quad C_7 = C_2/2k_0 = -i\omega\mu_0 I_0^e/ak_0$$

$$C_8 = C_3/k_0 = 1/a^2 \mu_r k_0 \quad ; \quad C_9 = C_5/C_4 = i\omega\mu_0/2\pi a^2 \quad ; \quad C_{10} = 1/2C_4 = -1/a$$

It is now considered useful to examine the four kernels in (37a,b) and to obtain their Fourier transforms. Thus,

$$K_1(z - z') = K(z - z') - \frac{2}{a^2 \mu_r h} \sum_{n=-\infty}^{\infty} A_n \left\{ \frac{\cos(pz) - \cos(k_0 z)}{k_0^2 - p^2} \right\} \cos(pz')$$

with $p = (n + 1/2)\pi/h$. The Fourier transform of $K(z - z')$ is given by $\bar{K}(\xi) = i\pi J_0(a\gamma_0)H_0^{(1)}(a\gamma_0)$ where $\gamma_0^2 = k_0^2 - \xi^2$.

$$M_1(z - z', \rho) = \int_{-\pi}^{\pi} \frac{d\phi'}{2\pi} \int_0^a d\rho' \rho' \frac{ik_0 [(z - z')^2 + \rho^2 + \rho'^2 - 2\rho\rho' \cos \phi']^{1/2}}{[(z - z')^2 + \rho^2 + \rho'^2 - 2\rho\rho' \cos \phi']^{1/2}}$$

$$\bar{M}_1(\xi, \rho) = i\pi \int_0^a H_0^{(1)}(\rho > \gamma_0) J_0(\rho < \gamma_0) \rho' d\rho'$$

where

$$\rho_> = \text{larger of } \rho \text{ and } \rho'$$

$$\rho_< = \text{smaller of } \rho \text{ and } \rho'$$

which leads to

$$\bar{M}_1(\xi, \rho) = \begin{cases} (i\pi a/\gamma_0) J_0(\rho\gamma_0) H_1^{(1)}(a\gamma_0) & \text{if } \rho > \rho' \\ (i\pi a/\gamma_0) H_0^{(1)}(\rho\gamma_0) J_1(a\gamma_0) & \text{if } \rho < \rho' \end{cases}$$

It is easily seen that

$$\bar{M}_2(\xi) = \frac{\partial}{\partial \rho} \bar{M}_1(\xi, \rho) \Big|_{\rho=a^+} - \frac{\partial}{\partial \rho} \bar{M}_1(\xi, \rho) \Big|_{\rho=a^-} = -i\pi a J_1(a\gamma_0) H_1^{(1)}(a\gamma_0)$$

Finally,

$$\bar{K}_2(\xi) = \frac{\partial}{\partial \rho} \bar{K}(\xi, \rho) \Big|_{\rho=a} +$$

where

$$\bar{K}(\xi, \rho) = i\pi J_0(\rho < \gamma_0) H_0^{(1)}(\rho > \gamma_0)$$

with

$\rho < =$ smaller of ρ and a

$\rho > =$ larger of ρ and a

so that

$$\bar{K}(\xi, \rho) = \begin{cases} i\pi J_0(\rho \gamma_0) H_0^{(1)}(a \gamma_0) & \text{for } \rho < a \\ i\pi J_0(a \gamma_0) H_0^{(1)}(\rho \gamma_0) & \text{for } \rho > a \end{cases}$$

Therefore,

$$\bar{K}_2(\xi) = -i\pi \gamma_0 J_0(a \gamma_0) H_1^{(1)}(a \gamma_0)$$

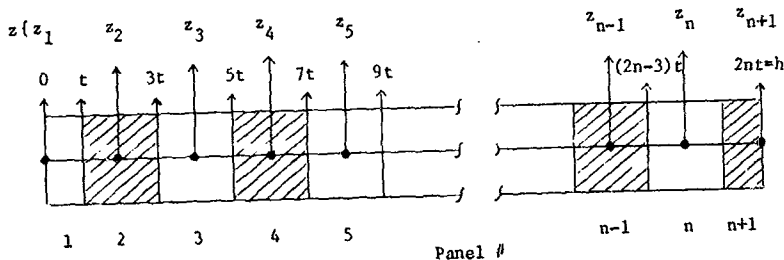
To begin the numerical procedure, it is recognized that, because of the evenness of $E_\phi(z)$ and $I_\phi(z)$, the integrals ranging from $-h$ to h may be converted as follows:

$$\int_{-h}^h E_\phi(z') K_{1,2}(z - z') dz' = \int_0^h E_\phi(z') [K_{1,2}(z - z') + K_{1,2}(z + z')] dz'$$

Similarly,

$$\int_{-h}^h I_\phi(z') M_{1,2}(z - z') dz' = \int_0^h I_\phi(z') [M_{1,2}(z - z') + M_{1,2}(z + z')] dz'$$

Now the interval from 0 to h can be subdivided into $n+1$ panels. Within each panel the unknown quantities $E_\phi(z)$ and $I_\phi(z)$ are approximated by constants and the constant value is assigned to a location z which corresponds to the center of the panel. With the length $h = 2nt$, each panel is of width $2t$ except the first and last panels which are of width t .



The locations at which the unknown quantities are determined are given by $z_I = (2I - 2)t$ with $I = 1, 2, 3, \dots, (n+1)$. Typically,

$$\int_0^h E_\phi(z') [K_1(z - z') + K_1(z + z')] dz' = \left\{ \int_0^t + \int_t^{3t} + \int_{3t}^{5t} + \dots + \int_{(2n-3)t}^{(2n-1)t} + \int_{(2n-1)t}^{2nt} \right\} E_\phi(z') [K_1(z - z') + K_1(z + z')] dz'$$

In each of these intervals $E_\phi(z)$ is approximated by a constant value so that

$$K_1(I, J) = \int_{\Delta z_j} [K_1(z_I + z') + K_1(z_I - z')] dz' = \frac{(2J-1)t}{(2I-3)t} \int dz' \left\{ \frac{1}{2\pi} \int_{-\infty}^{\infty} \bar{K}(\xi) e^{i\xi z_I} \left(e^{i\xi z'} + e^{-i\xi z'} \right) d\xi \right\} - \frac{1}{a^2 v_r h} \frac{(2J-1)t}{(2J-3)t} \int dx' \left\{ \sum_{n=-\infty}^{\infty} A_n \left[\frac{\cos(pz_I) - \cos(k_0^2 z_I)}{k_0^2 - p^2} \right] \cos(pz') \right\}$$

By substituting for $\bar{K}(\xi)$ and carrying out the z' integration, one obtains

$$K_1(I, J) = K(I, J) + B(I, J)$$

where

$$K(I, J) = (4/\pi) \int_{-\infty}^{\infty} [i\pi J_0(a\gamma_0) H_0^{(1)}(a\gamma_0)] \{(\sin \xi t)/\xi\} \{\cos[2\xi(I+J-2)t] + \cos[2\xi(I-J)t]\} d\xi$$

$$B(I, J) = -\frac{4}{\pi k_r} \sum_{n=0}^{\infty} A_n \left[\frac{\cos[2pt(I-1)] - \cos[2k_0 t(I-1)]}{a^2(k_0^2 - p^2)} \right] + \left[\frac{\sin[pt(2J-1)] - \sin[pt(2J-3)]}{(h/\pi)p} \right]$$

The integral in $K(I, J)$ is evaluated by suitably deforming the contour from the real axis to a contour that wraps around the branch cut. When this is done, $K(I, J)$ for $I \neq J$ can be written in the form

$$K(I, J) = \int_0^{\infty} f(x) e^{-x} dx$$

where $f(x)$ is a complex function of a real variable x . The integrals are evaluated using a 10-point Gauss-Laguerre quadrature method. The special case of diagonal elements ($I=J$) can be written in the form

$$K(I, I) = \frac{1}{\pi} \int_{-\infty}^{\infty} \bar{K}(\xi) \{(\sin \xi t)/\xi\} (e^{2i\xi z_I} + 1) d\xi = (1/2)K(1, 1) + T(I)$$

where

$$T(I) = \frac{1}{\pi} \int_{-\infty}^{\infty} \bar{K}(\xi) \{(\sin \xi t)/\xi\} e^{2i\xi z_I} d\xi$$

with $z_I = 2(I-1)t$, $I = 1, 2, \dots, (n+1)$. $K(1,1)$ is evaluated as an integral on the real axis because of the absence of the exponential decay factor, using 10-point Gauss quadrature routines. $T(I)$ can once again be put in a form suitable for Gauss-Laguerre quadrature by a deformation of the contour that wraps around the branch cut at $\xi = k_0$. Care is taken in evaluating the first and last panels' integrations because of their half normal width. What is discussed for kernel $K(z - z')$ or $\bar{K}(\xi)$ is essentially true with the calculation of the elements corresponding to the three other kernels.

Referring back now to the three terms on the right-hand side of (87a), viz.,

$$C_6 \cos(k_0 z_I) + C_7 \sin(k_0 |z_I|) + C_8 \int_0^{z_I} dz' E_\phi(z') \sin[k_0(z_I - z')],$$

the first and last terms, containing respectively the unknowns C_6 and $E_\phi(z)$, are moved to the left-hand side. For example,

$$C_6 \cos(k_0 z_I) = C_6 \cos[k_0(2I-2)t]$$

$$C_8 \int_0^{z_I} dz' [\quad] = C_8 \int_0^{(2I-2)t} dz' [\quad] = C_8 \left\{ \int_0^t + \int_t^{2t} + \dots + \int_{(2I-3)t}^{(2I-2)t} \right\} dz' [\quad]$$

We now define

$$A(I,P) = \int_{(P-1)t}^{Pt} \sin[k_0(z_I - z')] dz' = (1/k_0) \{ \cos[k_0 t(2I - P - 2)] - \cos[k_0 t(2I - P - 1)] \}$$

It is seen that when the term associated with C_8 is moved to the left-hand side, it affects only the lower triangle elements of $K_1(1,1)$ and not the upper triangle elements, thus rendering the $K_1(1,J)$ matrix elements not equal

to $K_1(J, I)$. Extending these calculating principles to (87b), and using the fact that $I_\phi(h) = I_\phi(I=n+1) = 0$, one can finally set up the following matrix equation:

$$\begin{bmatrix}
 a_{11} & a_{12} & \cdots & a_{1,n+1} & a_{1,n+2} & \cdots & a_{1,2n+1} & a_{1,2n+2} \\
 \vdots & & I & \vdots & \vdots & & II & \vdots & \vdots & V \\
 a_{n+1,1} & \cdots & a_{n+1,n+1} & a_{n+1,n+2} & \cdots & a_{n+1,2n+1} & a_{n+1,2n+2} \\
 \hline
 a_{n+2,1} & \cdots & a_{n+2,n+1} & a_{n+2,n+2} & \cdots & a_{n+2,2n+1} & a_{n+2,2n+2} \\
 \vdots & & III & \vdots & \vdots & & IV & \vdots & \vdots & VI \\
 a_{2n+2,1} & \cdots & a_{2n+2,n+1} & a_{2n+2,n+2} & \cdots & a_{2n+2,2n+1} & a_{2n+2,2n+2}
 \end{bmatrix}
 \begin{bmatrix}
 E_1 \\
 \vdots \\
 F_{n+1} \\
 I_1 \\
 \vdots \\
 I_n \\
 C_6
 \end{bmatrix}
 =
 \begin{bmatrix}
 G_1 \\
 \vdots \\
 G_{n+1} \\
 0 \\
 0 \\
 \vdots \\
 0 \\
 0
 \end{bmatrix}$$

where the elements on the right-hand side are given by $G(I) = C_7 \sin[k_0(2I-2)\epsilon]$ with $I = 1, 2, \dots, (n+1)$.

The magnetic current $I_z^*(z)$ is easily obtained from the solution of the system of linear equations by using $I_z^*(z) = -2\pi a E_\phi(z)$ volts. The computer programs are included in Appendix C and the results are plotted and discussed in the next section.

9. EXPERIMENTAL MEASUREMENT OF THE MAGNETIC CURRENT

The magnetization current is essentially the time rate of change of the magnetization vector (\vec{M}) integrated over the antenna cross section. The experimental procedure, however, determines the total axial magnetic flux with the use of a shielded loop placed coaxially over a driven loop which is loaded by a ferrite cylinder. Suitable modifications to the theory have to be made, therefore, before the computations can be compared with the experimental results. These modifications and the assumption of azimuthal symmetry on which they are based are discussed in detail in Appendix D.

Ferrite materials that are available commercially have been used in this experimental investigation. Table 1 lists the initial permeability μ_r' (i.e., the slope of the B-H curve for small H) and the applicable frequency range for a variety of ferrite materials, grouped under their respective suppliers. Ferrites #C-2050 of Ceramic Magnetics, Inc. and #Q-3 of Indiana General were selected for use in the 5-100 MHz frequency range. Toroidal samples of the #C-2050 material were obtained and its properties (μ_r' and Q) measured as a function of frequency by means of a Q-meter. The quality factor Q of the ferrite material is defined by

$$Q = \frac{1}{\text{loss factor}} = \mu_r' / \mu_r'' = \frac{2\pi \times \text{stored energy}}{\text{energy dissipated per period, } 2\pi/\omega} \quad (88)$$

The measured values of Q and μ_r' for the ferrite material #C-2050 are shown plotted in Fig. 4(a) as a function of frequency together with the values supplied by the manufacturer. Fair agreement is observed between the two. The imaginary part μ_r'' of the relative permeability can be calculated easily using (88) and measured values of μ_r' and Q. The manufacturer-supplied values of μ_r' and Q for the ferrite material #Q-3 are shown in Fig. 4(b). The values of the relative permittivity ϵ_r used in the theoretical calculations were

TABLE 1. List of Commercially Available Ferrite Materials

Source #1: Ceramic Magnetics, Inc., Fairfield, N.J.

Type of Ferrite Material	Manufacturer Code #	Initial Permeability μ_r	Frequency Range
Mn-Zn	MN-31 DC-10	2800	Up to 10 MHz
Mn-Zn	MN-31 DC-20	3300	Up to 10 MHz
Ni	CN-20	800	300 KHz - 2 MHz
Ni	CM-2002	1500	1 KHz - 1 MHz
Mn	MN-30	4000	Up to 500 KHz
Mn	MN-60	6000	Up to 600 KHz
Mn	MN-100	9500	Below 1 MHz
	C-2010	200-300	Below 15 MHz
	C-2025	150-200	Below 15 MHz
	C-2050	100-150	Below 20 MHz
	C-2075	25-50	Below 50 MHz
	CMD-5005	1400	Up to 10 MHz
	N-40	15-20	Up to 100 MHz

Source #2: Indiana General, Keasbey, N.J.

Ni-Zn	Q-1	125	Up to 10 MHz
Ni-Zn	Q-2	40	Up to 50 MHz
Ni-Zn	Q-3	18	Up to 200 MHz

Source #3: Fair-Rite Products Corp., Wallkill, N.Y.

Ni-Zn	30-61	125	200 KHz - 10 MHz
-------	-------	-----	------------------

Source #4: Ferroxcube Corp., Saugerties, N.Y.

Ni-Zn	4C4	125	Up to 50 MHz
Mn-Zn	3B3	750	Up to 5 MHz
	3B9	1800	Up to 5 MHz
Mn-Zn	3B7	2300	Up to 1 MHz

Source #5: National Moldite Co., Inc., Newark, N.J.

M-Grade	125 @ 1 MHz	Up to 20 MHz
---------	-------------	--------------

Source #6: Stackpole-Carbon Co., St. Marys, Pa.

Grade 24	2500	Up to 100 KHz
Grade 27A	1000	Up to 800 KHz
Grade 9	190	Up to 2 MHz
Grade 11	125	Up to 6 MHz
Grade 12	35	Up to 80 MHz
Grade 2285A	7.5	Up to 300 MHz

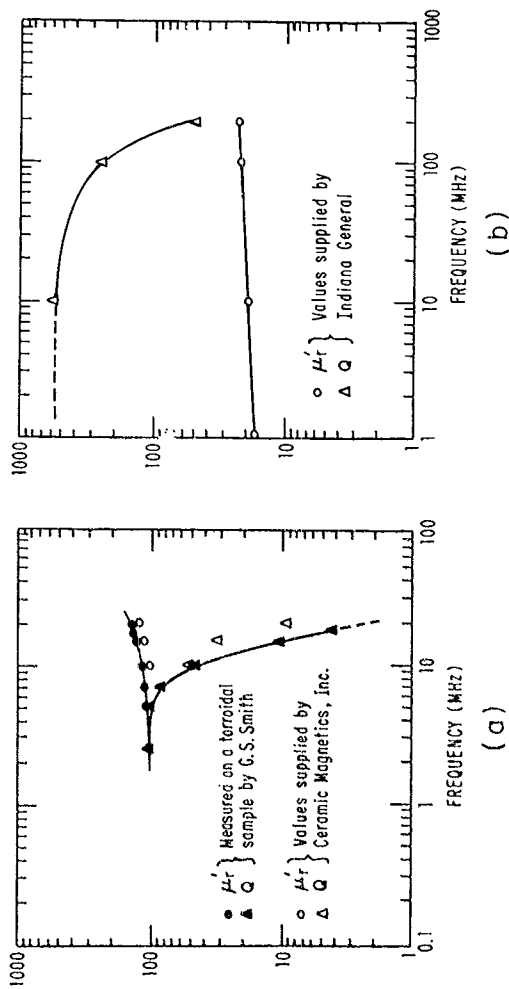


FIG. 4 MAGNETIC PROPERTIES OF FERRITE MATERIAL AS A FUNCTION OF FREQUENCY

(a) MATERIAL #C-2050 ; SOURCE — CERAMIC MAGNETICS INC.

(b) MATERIAL #Q-3 ; SOURCE — INDIANA GENERAL.

also supplied by the manufacturers. It can be seen from Fig. 4(a) that the value of Q for the ferrite material #C-2050 is nearly constant (≈ 100) up to about 2 MHz and then falls off rapidly to less than 10% of this value at 20 MHz. Similarly for the material #Q-3, Fig. 4(b) indicates a nearly constant value of Q (≈ 500) up to about 15 MHz, beyond which it decays to ≈ 50 at 200 MHz.

Three antenna cores were fabricated, as photographed in Fig. 5(a)-(c). Cores (a) and (b) are made of material #C-2050, while core (c) is made of material #Q-3. Cylindrical rods of 5/16" diameter and 5.25" height were used along with adhesive tape to fabricate core (a) of 2" overall diameter and 21" height. Core (b) has the same height as core (a) but is comprised of five cylindrical rods of 1" diameter and varying lengths. Core (c) is formed from three cylindrical rods of .625" diameter and 7.5" length for a total height of 22.5". As was pointed out earlier, cores (a) and (b) are useful for frequencies up to about 20 MHz, core (c) up to 200 MHz.

The three cores were used in various antenna configurations in which an electrically small loop antenna is loaded by a finite cylindrical ferrite rod. The antenna parameters for the eleven different cases are tabulated in Table 2. For antennas numbered 1 through 3, measurements were made at frequencies of 10, 50 and 100 MHz, respectively. The electrical radius ak_0 of the driven loop ranges from .00166 to .01662. Antennas numbered 4 through 7 were operated at frequencies of 5, 10, 15 and 20 MHz, respectively; the electrical radius ranged from .00132 to .00531. The operating frequencies for antennas numbered 8 through 11 were the same as for the previous set but the radius was doubled.

It can be seen in Table 2 that the value of ak_0 does not exceed 0.017 for any of the eleven antennas. This ensures the validity of the assumption



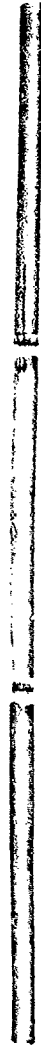
(a)

Dia. $2a = 2"$, height $2h = 21"$



(b)

Dia. $2a = 1"$, height $2h = 21"$



(c)

Dia. $2a = .625"$, height $2h = 22/5"$

FIGURE 5

FERRITE RODS USED IN THE EXPERIMENT

TABLE 2. Antenna Parameters

#Q-3 Material (Supplier: Indiana General)

$$2a = 0.625", 2h = 22.5", \Omega = 2 \ln(2h/a) = 8.5534$$

Antenna #	$\mu_r = \mu'_r - j\mu''_r$	h/λ_0	ak_0	$z_m^i = r_m^i + jx_m^i$
1	18 - j.036	.00952	.00166	.00797 - j3.7637
2	19 - j.0544	.04762	.00831	.00214 - j.70979
3	20 - j.0890	.09525	.01662	.001577 - j.33443

#C-2050 Material (Supplier: Ceramic Magnetics, Inc.)

$$i) 2a = 1", 2h = 21", \Omega = 2 \ln(2h/a) = 7.4754$$

4	100 - j1.0	.00444	.00132	.0051 - j.50479
5	115 - j2.55	.00889	.00265	.0049 - j.21892
6	125 - j12.50	.01333	.00398	.01341 - j.13270
7	135 - j67.5	.01778	.00531	.03747 - j.07394

$$ii) 2a = 2", 2h = 21", \Omega = 2 \ln(2h/a) = 6.089$$

8	105 - j0.63	.00444	.00265	.001275 - j.12611
9	120 - j2.4	.00889	.005319	.001225 - j.05456
10	150 - j15.	.01333	.007979	.003352 - j.03292
11	140 - j42.	.01778	.01064	.009368 - j.01815

that the driven loop be electrically thin in the theoretical calculation of antenna currents. The height of the monopole antenna (h/λ_0) ranges from .00444 to .09525 so that the longest dipole is nearly (1/5)-wavelength long. The value of the relative permeability $\mu_r = \mu_r' - j\mu_r''$ from Fig. 4 and the internal impedance z_m^i per unit length calculated using equation (36) are also listed in Table 2. In this section an $e^{j\omega t}$ time dependence is implicit and is more convenient. Due account of this change in notation has been taken in using (36) to calculate z_m^i . It is observed that for all antennas considered, the internal impedance is largely reactive.

For each of the three ferrite cylindrical cores described above, a set of driven and measuring loops was fabricated. A photograph and representative line drawing showing the construction of the loops are shown in Fig. 6. The six loops were all constructed from commercially available microcoaxial cables ending in a modified BNC connector. The driven and measuring loops are placed coaxially in the experimental setup, as can be seen in the photograph in Fig. 7 and the block diagram in Fig. 8. The short lengths of microcoaxial transmission lines leading away from the two loops are at right angles to one another in the horizontal plane so that any inductive coupling between the two is minimized. The signal source used in this experiment was either a GR-1001A (5-50 MHz) or an HP-3200B (10-500 MHz) oscillator. When the GR-1001A oscillator was used for measurements with antennas #4 through #11, the power amplifier was not needed. The HP-230B power amplifier was used only in conjunction with the HP-3200B oscillator for measurements on antennas #1 through #3. The source frequency was accurately measured using an HP-5240 electronic counter. A signal proportional to the total axial magnetic field was induced in the receiving loop. An HP-8405A vector voltmeter was used to detect and record this signal (B). The reference signal (A) to the

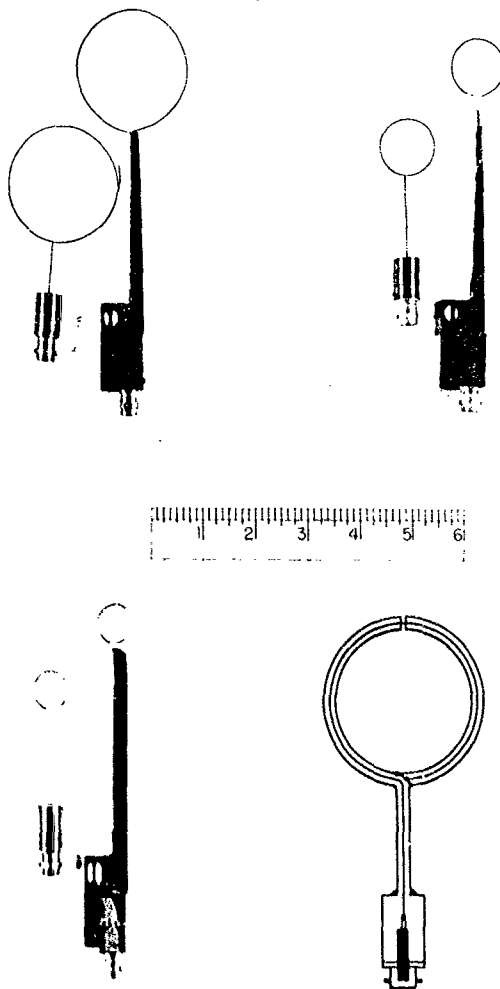


FIGURE 6

THREE PAIRS OF DRIVEN AND MEASURING LOOPS ALONG
WITH A LINE DIAGRAM SHOWING THE CONSTRUCTIONAL
DETAILS OF A REPRESENTATIVE LOOP.

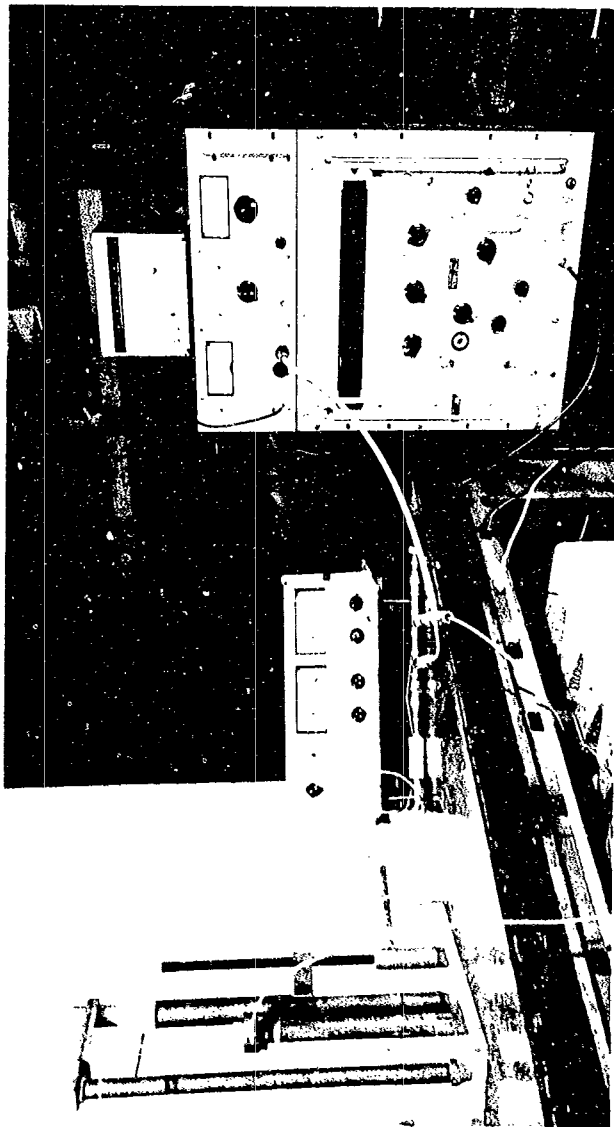


FIGURE 7
PHOTOGRAPH OF THE EXPERIMENTAL SET-UP

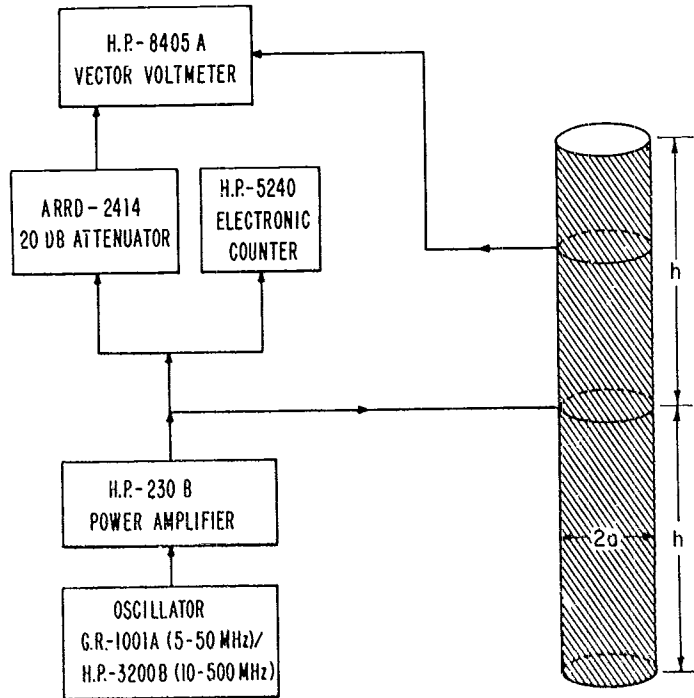


FIG. 8 BLOCK DIAGRAM OF THE EXPERIMENTAL SETUP FOR MEASUREMENT OF MAGNETIC CURRENT ON THE FERRITE ROD ANTENNA .

vector voltmeter was provided from a coaxial T. The vector-voltmeter readings were recorded as a function of the axial distance z from the driving loop. In this manner the amplitude and phase of the magnetic current distribution were obtained for the eleven antenna configurations described in Table 2. The unnormalized data are given in Table C-2 of Appendix C.

Computer programs, described and listed in Appendices A and B, were utilized in calculating the magnetic current distributions for the eleven cases. As discussed earlier, the theoretical calculations are based on a treatment of the ferrite rod as an imperfect magnetic conductor. The theoretical and experimental current distributions are shown graphically in Figs. 9 through 11. Also appearing in Figs. 9 - 11 are Tables 3, 4 and 5, respectively; these show the calculated values of input admittance $Y^* = I_z^*(0)/I_0^* = (G + jB)^*$ ohms and input impedance $Z^* = 1/Y^*$ mhos. The antenna numbering scheme used in the figures and tables corresponds to that given in Table 2. The values of $\Omega = 2 \ln(2h/a)$ for the antennas in Figs. 9 - 11 are, respectively, 8.5534, 7.4754 and 6.089.

The agreement between the theory and experiment is seen to be good. The antennas used here are relatively short and, consequently, the current distribution is seen to be nearly triangular. As may be expected, the largest deviation of the experimental values from the theoretical computations occurs at either end of the antenna ($z/h = 0, 1$) and especially at the driving point. For this reason the raw experimental data were normalized in most cases to the theoretical calculations at a point nearly a third the distance from the driving point to the end of the antenna. In the case of antennas #1 and #2, there appears to be a kink in the experimental values for the phase of the current distribution. This is believed to be due to the stacking of individual ferrite rods by means of adhesive tape. This is not seen in the magnitude

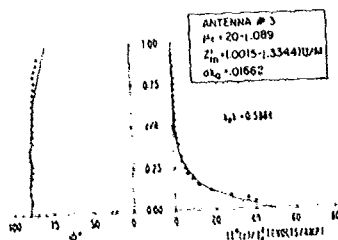
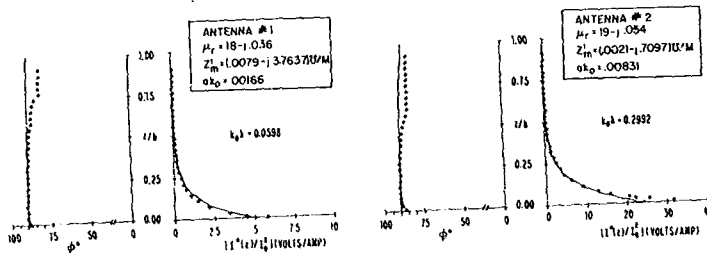


TABLE-3 CALCULATED (3-TERM THEORY)
 Y^* AND Z^* FOR THE THREE
 ANTENNAS.

ANTENNA #	INPUT ADMITTANCE $Y^* = 1/Z_m^* = G_m - jB_m \Omega$	INPUT IMPEDANCE $Z^* = 1/Y^* = R_m + jX_m \Omega$
1	0.0340 - j 4.80036	30.015 - j 20.831
2	0.2347 - j 2.64292	6.5004 - j 0.6018
3	0.8734 - j 4.87834	0.0004 - j 0.0004

— THEORETICAL (3-TERM THEORY)
 ... EXPERIMENTAL

(FERRITE SOURCE, MATERIAL Q#3 SUPPLIED BY INDIANA GENERAL)

FIG 9 PLOT OF MAGNITUDE AND PHASE OF THE MAGNETIC CURRENT ALONG
 THE ANTENNA ($\Omega + 2 \ln(2h/a) = 8.5534$)

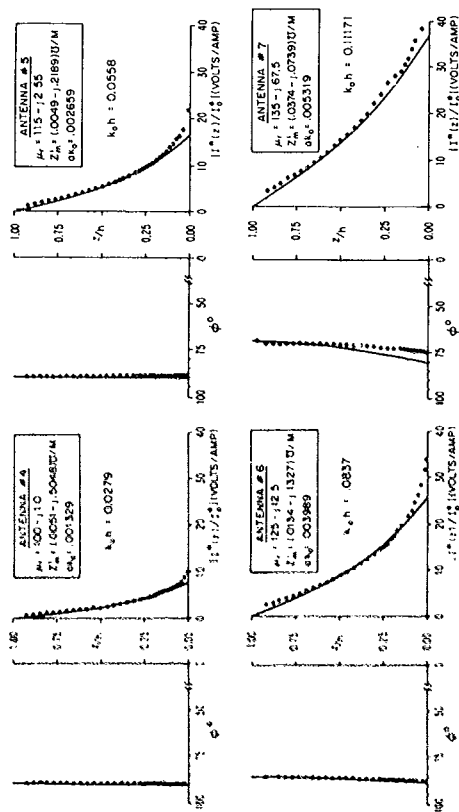


TABLE 4
 Calculated (3-term Theory) Z^* and Z^* for the above four antennas

ANTENNA #	INPUT ADMITTANCE $Y^* = \frac{1}{Z^*} = (G + jB) \Omega$	INPUT IMPEDANCE $Z^* = \frac{1}{Y^*} = (R + jX) \Omega$
4	$0.306 + j7.831$	$.00090 - j.12769$
5	$.1387 + j16.545$	$.00051 - j.06043$
6	$9560 + j25.675$	$.0045 - j.03880$
7	$6.127 + j36.637$	$.00444 - j.02655$

— THEORETICAL (3-TERM THEORY)

..... EXPERIMENTAL

(FERRITE SOURCE : MATERIAL # 2050 SUPPLIED BY CERAMIC MAGNETICS)

FIG 10 PLOT OF MAGNITUDE AND PHASE OF THE MAGNETIC CURRENT ALONG THE ANTENNA.

($\Omega = 2\pi \cdot (2h/a) = 7.4754$)

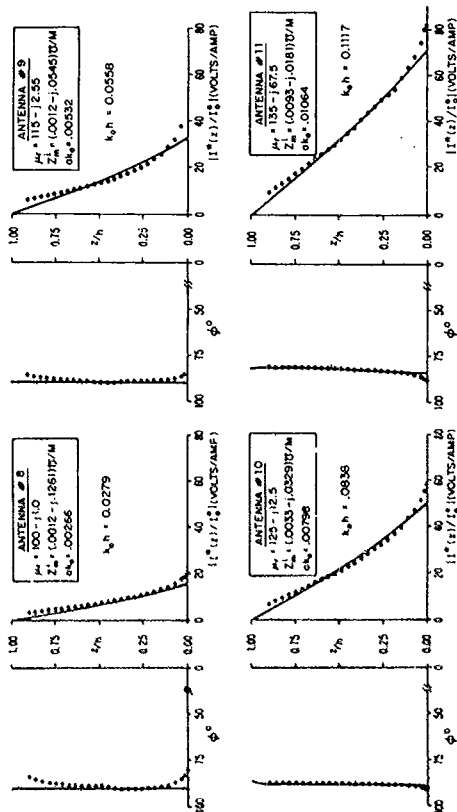


TABLE 5
 Calculated (3-term Theory) Y^0 and Z^0 for the above four antennas

ANTENNA #	INPUT ADMITTANCE $Y^0 = \frac{I_0}{V_0} = (G + jB) \Omega$	INPUT IMPEDANCE $Z^0 = \frac{V_0}{I_0} = (R + jX) \Omega$
8	$.041 + j15.805$	$.0017 - j0.0327$
9	$.176 + j32.807$	$.0016 - j0.03048$
10	$1.160 + j50.373$	$.00046 - j0.01984$
11	$6.749 + j70.870$	$.00133 - j0.01398$

— THEORETICAL (3-TERM THEORY)

..... EXPERIMENTAL

(FERRITE SOURCE: MATERIAL C#2050 SUPPLIED BY
 CERAMIC MAGNETICS)

FIG. 11 PLOT OF MAGNITUDE AND PHASE OF THE MAGNETIC CURRENT ALONG THE ANTENNA.
 ($\Omega = 2\pi \times 10^9$ Hz)

curves because of the relatively low magnitude values. The overall agreement of the theory and experiment was used in deciding the point of normalization.

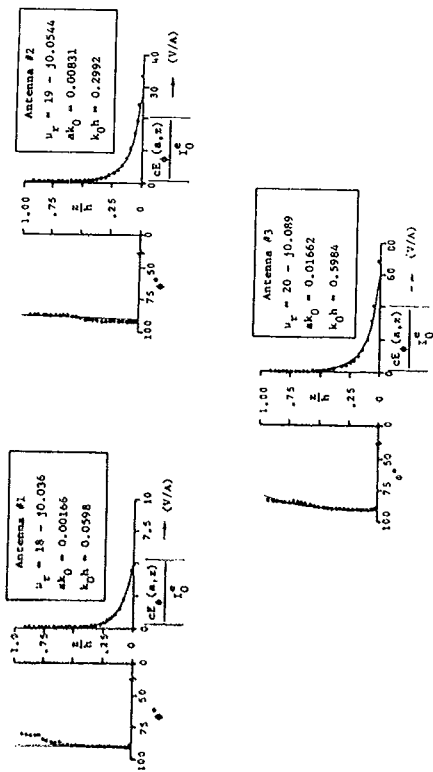
The coupled integral equations in (86a,b) in the two variables, the tangential electric field $E_\phi(z)$ and circumferential electric current $I_\phi(z)$, were solved numerically by the moment method on a Sigma-7 computer system. The method itself has been discussed in Section 8; the computer programs are listed in Appendix C. Table 6 contains a description of all the subroutines used in this computation. The basic philosophy of this method is to reduce the set of coupled integral equations to a system of linear algebraic equations. The standard routines [6] for solving a system of linear equations were modified to handle complex variables. The results of these computations are plotted in Figs. 12 through 14. As before, the experimental data have been normalized at a point approximately one third the distance from the driving point ($z = 0$) to the end.

The magnetic current $I_z^*(z)$ is easily obtained from the solution for the tangential electric field using the relation $I_z^*(z) = -2\pi a E_\phi(z)$ volts per unit current in the driving loop. The input parameters Y^* and Z^* are also tabulated and the tables are included in the figures showing the magnitude and phase of the magnetic current. In all eleven cases the phase is nearly constant, since the antennas are electrically short in free space, and most of the magnetic current is in phase quadrature. The agreement between the experiment and the theoretical calculations is very good including near the source. This was to be expected because the coupled integral equations (86a,b) in two variables comprise a far more accurate and independent theoretical formulation of the problem than the approximate integral equation (39) which relies rather heavily on an analogy between the ferrite rod antenna and the resistive cylindrical dipole antenna.

TABLE 6

LIST OF SUBROUTINES USED IN SOLVING THE COUPLED INTEGRAL EQUATIONS (86a,b)

<u>PROGRAM NAME</u>	<u>PURPOSE</u>
MAIN	Computes $E_\phi(z)$ and $I_\phi(z)$ by solving the coupled integral equations (86a,b).
BSLSML	Computes Bessel functions $J_0(z)$ and $J_1(z)$ for $ z \leq 10.0$ with 5 figure accuracy.
BESH	Computes Hankel functions $H_0^{(1)}(z)$, $H_0^{(2)}(z)$, $H_1^{(1)}(z)$ and $H_1^{(2)}(z)$.
QGL10	10-point Gauss-Laguerre quadrature routine.
QG10	10-point Gauss quadrature routine.
<div> <div>FCTK</div> <div>FK11R, FK11I</div> <div>FK11</div> </div>	<p>Computes the integrand for $K(z - z')$ for $I \neq J$.</p> <p>The same, for $I = J = 1$.</p> <p>The same, for $I = J \neq 1$.</p>
<div> <div>FCTM1, FM11R,</div> <div>FM11I, FM11I</div> </div>	Computes the integrand for $M_1(z - z')$ for $I \neq J$, $I = J = 1$, and $I = J \neq 1$, respectively.
<div> <div>FCTK2, FK21R,</div> <div>FK21I, FK21I</div> </div>	Computes the integrand for $K_2(z - z')$ for $I \neq J$, $I = J = 1$, and $I = J \neq 1$, respectively.
<div> <div>FCTM2, FM21R,</div> <div>FM21I, FM21I</div> </div>	Computes the integrand for $M_2(z - z')$ for $I \neq J$, $I = J = 1$, and $I = J \neq 1$, respectively.
AUX	Auxiliary function used in computing the above integrands.
SERIES	Computes the infinite series part of the kernel $K_1(z - z')$.
<div> <div>DECOMP, SOLVE,</div> <div>IMPRUV, SING</div> </div>	Programs used in solving the linear system of algebraic equations.
ANGLE	Computes the phase angle of complex variables $I_\phi(z)$ and $E_\phi(z)$.



— Calculated
 (Coupled Integral Equations)
 Experimental

(Ferrite source: Material #3 supplied by Indiana General)

Fig. 12. Plot of magnitude and phase of the magnetic current along the antenna; $n = 2$ $\ln(2h/a) = 8.5534$.
 (Uncorrected; see Appendix D.)

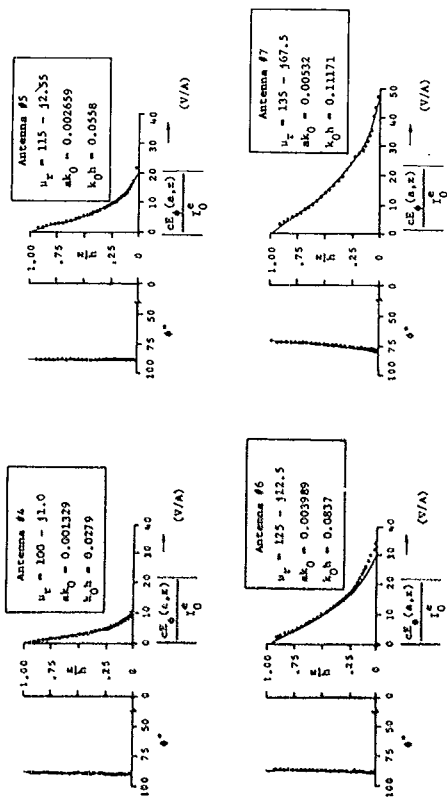


Fig. 13. Plot of magnitude and phase of the magnetic current along the antenna; $\Omega = 2 \ln(2h/a) = 7.4754$.

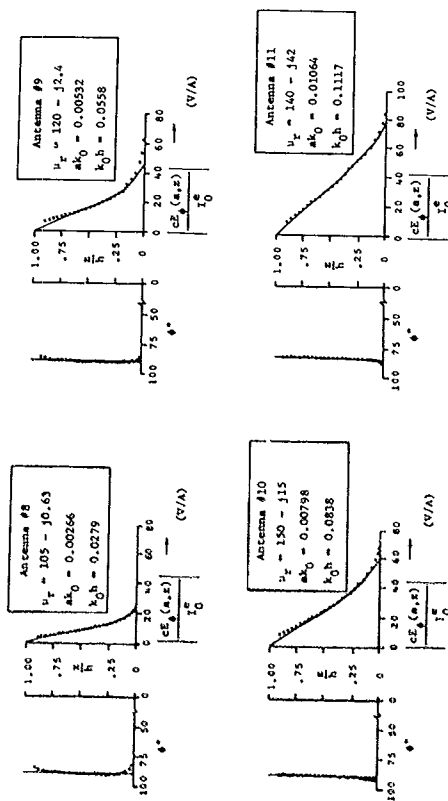


Fig. 14. Plot of magnitude and phase of the magnetic current along the antenna; $\Omega = 2 \ln(2h/a) = 6.089$.

TABLE 7

INPUT ADMITTANCES AND IMPEDANCES OF THE ELEVEN ANTENNAS OBTAINED FROM SOLVING
THE COUPLED INTEGRAL EQUATIONS (86a,b)

Antenna #	Input Admittance (ohms)	Input Impedance (mhos)
1	.003 + j 4.99	.00012 - j.20040
2	.03 + j30.22	.00003 - j.03309
3	.10 + j62.32	.00003 - j.01605
4	.03 + j 9.23	.00035 - j.10834
5	.14 + j20.13	.00035 - j.04967
6	.97 + j29.81	.00109 - j.03351
7	6.21 + j45.62	.00293 - j.02152
8	.92 + j23.55	.00004 - j.04246
9	.16 + j44.27	.00008 - j.02259
10	1.06 + j60.02	.00029 - j.01666
11	4.26 + j75.32	.00075 - j.01323

10. SUMMARY

An electrically small loop that carries a constant current and is loaded by a homogeneous and isotropic ferrite rod has been called the ferrite-rod antenna. In Part I [2] of this report the ferrite rod was assumed to be of infinite length and the problem was treated using a boundary-value approach. In a practical situation, however, the antenna is necessarily finite and often electrically short so that a new mathematical formulation was needed, along with an experimental investigation, for the problem of a finite ferrite rod antenna. With this current distribution known precisely, other quantities of interest can be derived from it.

Although, in terms of physical mechanisms, the ferrite-rod antenna can be compared with the dielectric rod antenna, there exists a complete analogy between the ferrite antenna and the conducting cylindrical dipole antenna. This analogy is based on the dual property of electric and magnetic vectors in Maxwell's equations. The electric dipole antenna has received considerable attention from researchers in the past and, therefore, a treatment of the 'magnetic analog' of the dipole antenna is considered useful. Based on this analogy, an integral equation has been derived for the magnetic current on the finite ferrite-rod antenna. As expected, the integral equation is identical in form to the corresponding equation for the electric current on the dipole antenna. This derivation was based on the assumption that the value of the relative permeability μ_r of the ferrite material equals infinity. In effect, the ferrite is treated as a perfect magnetic conductor as when in the 'electric case' the antenna material is assumed to have an infinite electrical conductivity σ . However, in practice, a material with μ_r equal to infinity does not exist and, furthermore, over a useful frequency range the μ_r value is not high enough to justify using the perfect conductor approximation.

For this reason, the integral equation had to be modified. The modification was achieved by defining the internal impedance per unit length of the magnetic conductor to be the ratio of the tangential magnetic field to the total magnetic current flowing in the magnetic conductor. An approximate, 3-term expression for the magnetic current was then obtained in a manner paralleling the procedure used by King and Wu to solve for the electric current on the imperfectly conducting dipole antenna. It was found that for commercially available ferrites the internal impedance per unit length was largely reactive so that the propagation constant k ($= \beta + i\alpha$) on the antenna had a large imaginary part. The predominance of the attenuation constant α makes the magnetic current very small and, thus, one is led to conclude that the practical ferrite-rod antenna is not a very efficient radiator.

The treatment of the ferrite-rod antenna as an analog of the resistive electric dipole antenna relies rather heavily on the mathematical equivalence of the two problems under idealized driving conditions. For this reason, an alternative derivation of the integral equation for the tangential electric field on the ferrite surface was developed. This derivation led to a pair of coupled integral equations in terms of the tangential electric field and tangential electric surface current. The coupled integral equations were solved numerically by the moment method and the magnetic current obtained from the tangential electric field. It was also verified that in the limit $h \rightarrow \infty$ the equations decouple and are in complete agreement with the results of the theory for the infinite antenna.

Since the magnetic current is proportional to the total axial magnetic field, a simple experimental apparatus was built to measure the magnetic current distribution on several antenna configurations. A graphical comparison of the theoretical and experimental results has been presented. Although the

three-term solution has been shown to give good results for antenna lengths $k_0 h \leq 5\pi/4$, the antennas used in the experiment were much shorter and the near-triangular distribution of currents was verified. The frequency response of the properties of available ferrite materials and the practical limitations on the size of the ferrite rods made it difficult to construct antennas of longer length.

In conclusion, while ferrites have been used extensively at microwave frequencies and up to several Megahertz, the fact that ferrites are now becoming commercially available in the range 30 - 300 MHz should lead to useful applications. In situations in which the physical size of the antenna must be kept small, a loop antenna has limited usefulness because of its low efficiency and radiation resistance. The insertion of a suitable ferrite core offers the advantage of both improved efficiency and increased radiation resistance. Although, in theory, an increased radiation resistance should simplify the problem of matching the antenna to its associated circuit, in practice there remains a severe problem. This has been discussed by Dropkin, Metzger and Cacheris [7] who made measurements of the receiving characteristics of a cylindrical ferrite-rod antenna at a frequency of 75 MHz. They conclude that both ferrite-core and air-core loops can be described by similar equivalent circuits. These circuits have resonant properties and each of the lumped circuit elements can be identified with a physical quantity characterizing the antenna. The improved efficiency and the increased radiation resistance which were determined experimentally can be attributed directly to an increased magnetic flux passing through the loop. They also make the interesting observation that with a dielectric cylinder ($\epsilon_r = 10$, $\mu_r = 1$), the size of the ferrite used had no effect on the air-loop properties. This was because the loop used was small enough to act as a magnetic dipole.

COMPUTATION OF MAGNETIC CURRENT AND ADMITTANCE OF FERRITE ROD ANTENNA

The approximate magnetic current distribution as given by (51) is

$$I_z^*(z) = \frac{-12\pi k_0 \zeta_0 I_0^e}{k_{DR} \cos kh} [\sin k(h - |z|) + T_U^*(\cos kz - \cos kh) + T_D^*(\cos \frac{k_0 z}{2} - \cos \frac{k_0 h}{2})]$$

where T_U^* and T_D^* are given by

$$T_U^* = (C_V E_D - C_D E_V) / (C_U E_D - C_D E_U)$$

$$T_D^* = (C_U E_V - C_V E_U) / (C_U E_D - C_D E_U)$$

with

$$C_U = [1 - (k^2/k_0^2)](\Psi_{dUR} - \Psi_{dR})(1 - \cos kh) - (k^2/k_0^2)\Psi_{dUR} \cos kh - i\Psi_{dUI}(\frac{3}{4} - \cos \frac{k_0 h}{2}) + \Psi_U(h)$$

$$C_D = \Psi_{dD}(\frac{3}{4} - \cos \frac{k_0 h}{2}) - [1 - (k^2/k_0^2)]\Psi_{dR}(1 - \cos \frac{k_0 h}{2}) + \Psi_D(h)$$

$$C_V = -[i\Psi_{dI}(\frac{3}{4} - \cos \frac{k_0 h}{2}) + \Psi_V(h)]$$

$$E_U = -(k^2/k_0^2)\Psi_{dUR} \cos kh + (i/4)\Psi_{dUI} \cos \frac{k_0 h}{2} + \Psi_U(h)$$

$$E_D = -(i/4)\Psi_{dD} \cos \frac{k_0 h}{2} + \Psi_D(h)$$

$$E_V = -(i/4)\Psi_{dI} \cos \frac{k_0 h}{2} - \Psi_V(h)$$

The Ψ functions appearing in the above expressions are defined as follows:

$$\Psi_{dR} = \begin{cases} \Psi_{dR}(0) & k_0 h \leq \pi/2 \\ \Psi_{dR}(h - \lambda/4) & \pi/2 \leq k_0 h \leq 3\pi/2 \end{cases}$$

$$\Psi_{dR}(z) = \csc k(h - |z|) \int_{-h}^h \sin k(h - |z'|) \left[\frac{\cos k_0 r_0}{r_0} - \frac{\cos k_0 r_h}{r_h} \right] dz'$$

$$\Psi_{dUR} = [1 - \cos kh]^{-1} \int_{-h}^h (\cos kz' - \cos kh) \left[\frac{\cos k_0 r_0}{r_0} - \frac{\cos k_0 r_h}{r_h} \right] dz'$$

$$\Psi_{dD} = [1 - \cos \frac{k_0 h}{2}]^{-1} \int_{-h}^h (\cos \frac{k_0 z'}{2} - \cos \frac{k_0 h}{2}) \left[\frac{e^{ik_0 r_0}}{r_0} - \frac{e^{ik_0 r_h}}{r_h} \right] dz'$$

$$\Psi_{dI} = -[1 - \cos \frac{k_0 h}{2}]^{-1} \int_{-h}^h \sin k(h - |z'|) \left[\frac{\sin k_0 r_0}{r_0} - \frac{\sin k_0 r_h}{r_h} \right] dz'$$

$$\Psi_{dUI} = -[1 - \cos \frac{k_0 h}{2}]^{-1} \int_{-h}^h (\cos kz' - \cos kh) \left[\frac{\sin k_0 r_0}{r_0} - \frac{\sin k_0 r_h}{r_h} \right] dz'$$

where the propagation constant k is given by

$$k = k_0 [1 + (i4\pi\epsilon_0 z_m^1 / k_0 \Psi_{dR})]^{1/2}$$

with $\epsilon_0 = 376.7 \Omega$ the characteristic impedance of free space. However, since

Ψ_{dR} is dependent on k , an iteration procedure is used. To begin with, k_1 as given by

$$k_1 = k_0 [1 + (i4\pi\epsilon_0 z_m^1 / k_0 \Psi_{dR0})]^{1/2}$$

is determined. With k_1 substituted for k , Ψ_{dR1} is computed and then k is evaluated using

$$k = k_0 [1 + (i4\pi\epsilon_0 z_m^1 / k_0 \Psi_{dR1})]^{1/2}$$

This new value of k is used in evaluating all the Ψ functions and the current distributions.

APPENDIX B

This appendix contains a listing of the main program and all associated subroutines. The main program accepts as inputs h/λ_0 , Ω and z_m^i , and computes the input impedance Z^* , admittance Y^* , and magnetic current distribution as a function of distance (z/h) along the antenna. Subroutine NINTG employs Simpson's rule for integration to evaluate the functions. The various integrands are calculated using the subroutines FCTH(Y), FCTO(Y) and FCTI(Y).


```

C
C
SUBROUTINE FCTIMY)
  COMMON A2,H,EA,Z,CCHNR,CCHN1,SNHNR,SNH1,CCHZ,AA1
  IY1=V1,V2,V3,V4,V5,V6,V7,V8,V9,V10,V11,V12
  I=I2P(I)
  I1=I/2
  LA=I2P(I)
  RAO=5*(I+EA)
  ZH=ZAH
  A1=506T(I*(X+I)*2+42)
  A11=I/2
  SPWCS(I)=A11*(X+5LK1)*4
  C/Z=5*IN(I)*K11*(SIN(R1))+R
  U=2R+5
  C=CCHZ(I)
  S=SIN(U)
  L=I2P(I*(X+I))
  I1=I/2
  CH1=U-5*(I+I1)
  CH2=CH1-I1
  SH1=S*CH1
  SH2=C*CH2
  CH1=C*CH1
  CH2=C*CH2
  CHZ=5*CHZ
  E=SNHNR*CH1-SNHNR*CH2-CCHNR*5*H1*CHHNR*5*H2
  SH2=SNHNR*CH2+SNHNR*CH1-CCHNR*SHZ-CCHNR*5*H1
  SH1=I
  CH1=CH1-CCHNR
  CHZ=CHZ-CCHNR
  O=C/L1/2*(R1)-CUMZ
  V1=5*V*CH1
  V2=5*V*CH2
  V3=5*V*V
  V4=5*V*V
  V5=5*V*5*H1
  V6=5*V*5*H2
  V7=5*V*5*CH1
  V8=5*V*5*CH2
  V9=5*H1*5*V*5*H2*5*V
  V10=SH2*5*V-SH1*5*V
  V11=CH1*5*V+CH2*5*V
  V12=CH2*5*V-CH1*5*V
  RETURN
END

```

```

C
C
SUBROUTINE FCTOYI)
  COMMON A2,H,EA,Z,CCHNR,CCHN1,SNHNR,SNH1,CCHZ,AA1
  IY1=V1,V2,V3,V4,V5,V6,V7,V8,V9,V10,V11,V12
  I=I2P(I)
  I1=I/2
  LA=I2P(I)
  RAO=5*(I+EA)
  ZH=ZAH
  A1=506T(I*(X+I)*2+42)
  A11=I/2
  SPWCS(I)=A11*(X+5LK1)*4
  C/Z=5*IN(I)*K11*(SIN(R1))+R
  U=2R+5
  C=CCHZ(I)
  S=SIN(U)
  L=I2P(I*(X+I))
  I1=I/2
  CH1=U-5*(I+I1)
  CH2=CH1-I1
  SH1=S*CH1
  SH2=C*CH2
  CH1=C*CH1
  CH2=C*CH2
  CHZ=5*CHZ
  E=SNHNR*CH1-SNHNR*CH2-CCHNR*5*H1*CHHNR*5*H2
  SH2=SNHNR*CH2+SNHNR*CH1-CCHNR*SHZ-CCHNR*5*H1
  SH1=I
  CH1=CH1-CCHNR
  CHZ=CHZ-CCHNR
  O=C/L1/2*(R1)-CUMZ
  V1=5*V*CH1
  V2=5*V*CH2
  V3=5*V*V
  V4=5*V*V
  V5=5*V*5*H1
  V6=5*V*5*H2
  V7=5*V*5*CH1
  V8=5*V*5*CH2
  V9=5*H1*5*V*5*H2*5*V
  V10=SH2*5*V-SH1*5*V
  V11=CH1*5*V+CH2*5*V
  V12=CH2*5*V-CH1*5*V
  RETURN
END

```

```

C
C
SUBROUTINE FCTIYI)
  COMMON A2,H,EA,Z,CCHNR,CCHN1,SNHNR,SNH1,CCHZ,AA1
  IY1=V1,V2,V3,V4,V5,V6,V7,V8,V9,V10,V11,V12
  I=I2P(I)
  I1=I/2
  LA=I2P(I)
  RAO=5*(I+EA)
  ZH=ZAH
  A1=506T(I*(X+I)*2+42)
  A11=I/2
  SPWCS(I)=A11*(X+5LK1)*4
  C/Z=5*IN(I)*K11*(SIN(R1))+R
  U=2R+5
  C=CCHZ(I)
  S=SIN(U)
  L=I2P(I*(X+I))
  I1=I/2
  CH1=U-5*(I+I1)
  CH2=CH1-I1
  SH1=S*CH1
  SH2=C*CH2
  CH1=C*CH1
  CH2=C*CH2
  CHZ=5*CHZ
  E=SNHNR*CH1-SNHNR*CH2-CCHNR*5*H1*CHHNR*5*H2
  SH2=SNHNR*CH2+SNHNR*CH1-CCHNR*SHZ-CCHNR*5*H1
  SH1=I
  CH1=CH1-CCHNR
  CHZ=CHZ-CCHNR
  O=C/L1/2*(R1)-CUMZ
  V1=5*V*CH1
  V2=5*V*CH2
  V3=5*V*V
  V4=5*V*V
  V5=5*V*5*H1
  V6=5*V*5*H2
  V7=5*V*5*CH1
  V8=5*V*5*CH2
  V9=5*H1*5*V*5*H2*5*V
  V10=SH2*5*V-SH1*5*V
  V11=CH1*5*V+CH2*5*V
  V12=CH2*5*V-CH1*5*V
  RETURN
END

```

APPENDIX C

This appendix opens with two tables containing experimental information. The first, Table C-1, lists the values of the various antenna constants (dimensions, ferrite characteristics, frequency, etc.) for the eleven antenna configurations studied experimentally. Table C-2 gives the raw measured data (unnormalized) for the magnetic current distributions on the eleven antennas as a function of z .

The appendix concludes with a listing of the computer programs used to solve the coupled integral equations in (86a,b). The procedure used, i.e., the moment method, was discussed briefly in Section 8. The coupled integral equations are reduced to a system of linear algebraic equations which are then solved for the unknown variables. An unknown constant in the integral equation is also determined in the numerical procedure by imposing the end condition at $z = h$. The magnetic current $I_z^*(z)$ is easily computed from the solution of the tangential electric field $E_\phi(z)$ by using $I_z^*(z) = -2\pi a E_\phi(z)$ volts per unit current in the driving loop.

#	F MHz	ϵ_r	ν_r	$2a$ inches	$2h$ inches	b/a	Ω	ak_o	k_{1h}	ak_1
1	10	11	18-j.036	.625	22.5	36	8.5534	.00166	.80-j.0008	.022-j.0002
2	50	11-j.11	19-j.054	.625	22.5	36	8.5534	.00831	4.12-j.0059	.114-j.0002
3	100	11-j.3	20-j.089	.625	22.5	36	8.5534	.01662	8.46-j.0188	.235-j.0005
4	5	11	100-j.1	1	21	21	7.4754	.00133	.88-j.0044	.042-j.0002
5	10	11	115-j2.55	1	21	21	7.4754	.00266	1.89-j.021	.090-j.001
6	15	10.5	125-j12.5	1	21	21	7.4754	.00399	2.96-j.1479	.141-j.007
7	20	10.25	135-j67.5	1	21	21	7.4754	.00532	4.22-j.9970	.201-j.0475
8	5	11	105-j.63	2	21	10.5	6.089	.00266	.90-j.0027	.086-j.0002
9	10	11	120-j2.4	2	21	10.5	6.089	.00532	1.93-j.0193	.184-j.001
10	15	11	150-j15	2	21	10.5	6.089	.00798	3.25-j.1620	.309-j.015
11	20	11.1	140-j42	2	21	10.5	6.089	.01064	4.22-j.6202	.402-j.059

TABIE C-1 Antenna Constants

TABLE C-2 Unnormalized experimental data (Refer to
Table C-1 for the numbering scheme and antenna constants).

Z cms	Antenna #1		Antenna #2		Antenna #3	
	Mag	Phase	Mag	Phase	Mag	Phase
0.1	-	-	38	-50	-	-
0.2	130.0	30.4	-	-	-	-
0.3	100.0	30.2	31.5	-48.8	-	-
0.5	-	-	-	-	-	-
0.6	-	-	25.5	-47.9	-	-
0.8	-	-	22.0	-47.5	-	-
1.0	77.0	30	20.5	-47.2	82.5	-
1.5	-	-	16	-47.0	57.0	-
2.0	49.0	30	13	-46.6	44	-169.2
3.0	33.0	30	9.1	-46.4	28.5	-178
4.0	23.0	30	6.4	-46.5	19.0	-182
5.0	17.0	30	4.7	-46.5	13.5	-184
6.0	12.5	30	3.5	-46.5	10.0	-185
7.0	9.25	30	2.65	-46.5	7.7	-185
8.0	7.0	30	2.0	-46.5	6.2	-185
9.0	5.3	30	1.45	-46.8	5.6	-183.5
10.0	4.0	30	1.0	-47	?	?
11.0	3.30	30.5	.8	-47.5	3.1	-184
12.0	2.65	30.6	.63	-48.0	2.35	-185.5
13.0	1.95	30.6	.51	-48.5	1.85	-186
14.0	1.75	30.6	.41	-49	1.45	-186
15.0	1.45	31.2	.34	-50.2	1.20	-186
16.0	1.10	31.6	.285	-51.0	1.02	-186
17.0	.9	32.8	.240	-52	.86	-186
18.0	.75	32.6	.205	-52	.70	-186
19.0	.62	33.0	.175	-52	.59	-186
20.0	.51	33.6	.140	-52	.50	-186
21.0	.42	35			.41	-187
22.0	.36	38.2			.35	-186
23.0	.31	38			.30	-186.5
24.0	.27	38			.26	-188.5
25.0	.22	38			.23	-188
26.0	.19	38			.205	-190

TABLE C-2 (Continued)

Z cms	Antenna #4		Antenna #5		Antenna #6		Antenna #7	
	Mag	Phase	Mag	Phase	Mag	Phase	Mag	Phase
.1	-	-	16.0	-129.2	33	-130	5.7	-70
.3	-	-	14.5	-129.2	30.5	-130.2	5.3	-70.2
.5	4.0	-130	13.5	-128.3	28.5	-130.2	4.9	-70.4
1.0	3.5	-130.4	12.0	-129.3	25.5	-130.4	4.5	-70.8
1.5	3.2	-130.4	11.0	-129.4	23.5	-130.5	4.2	-71.2
2.0	3.05	-130.4	10.5	-129.4	22.0	-130.6	3.7	-71.4
2.5	2.85	-130.4	9.8	-129.4	20.5	-130.7	3.5	-71.6
3.0	2.70	-130.2	9.3	-129.5	19.5	-130.8	3.3	-71.8
3.5	2.55	-130.1	8.7	-129.5	18.5	-130.9	3.15	-72.0
4.0	2.45	-130	8.3	-129.6	17.5	-131	3.0	-72.2
4.5	2.30	-130	7.9	-129.6	16.5	-131.0	-	-
5.0	2.15	-130	7.5	-129.6	15.5	-131.2	2.9	-72.2
5.5	2.05	-129.9	7.1	-129.6	15	-131.2	-	-
6.0	1.95	-129.9	6.8	-129.6	14	-131.3	2.75	-72.5
6.5	1.85	-129.8	6.5	-129.7	13.5	-131.4	-	-
7.0	1.80	-129.7	6.2	-129.7	13	-131.4	2.50	-72.8
7.5	-	-	5.9	-129.7	-	-	-	-
8.0	1.65	-129.7	5.7	-129.7	12	-131.5	2.30	-73.2
9.0	1.50	-129.7	5.2	-129.8	11	-131.6	2.05	-73.6
10	1.37	-129.6	4.7	-129.8	10	-131.7	1.9	-73.8
11	1.25	-129.6	4.3	-129.8	9.2	-131.8	1.75	-74
12	1.15	-129.7	4.0	-129.8	8.5	-131.9	1.60	-74.2
13	1.05	-129.6	3.60	-129.8	7.8	-132.0	1.48	-74.5
14	.95	-129.7	3.30	-129.8	7.1	-132.0	1.35	-74.6
15	.89	-129.5	3.05	-129.9	6.5	-132.1	1.20	-74.6
16	.81	-129.5	2.75	-130	5.9	-132.2	1.08	-74.6
17	.74	-130.0	2.5	-130	5.3	-132.2	1.00	-74.6
18	.66	-129.5	2.2	-130	4.8	-132.2	.89	-75
19	.59	-129.5	2.0	-130	4.2	-132.3	.80	-75
20	.52	-129.3	1.75	-130	3.8	-132.2	.71	-75
21	.46	-129.5	1.55	-130	3.3	-132.3	.66	-75
22	.39	-129.2	1.3	-130	2.9	-132.4	.54	-75
23	.33	-129.2	1.1	-130	2.4	-132.4	.45	-75
24	.26	-129.2	.9	-130	2.0	-132.5	.37	-75

TABLE C-2 (Continued)

2	Antenna #8		Antenna #9		Antenna #10		Antenna #11	
	Mag	Phase	Mag	Phase	Mag	Phase	Mag	Phase
.1	6.3	-60	4.4	-50	89	-80	175	-100
.5	5.7	-62.8	3.8	-51.8	84	-79.5	170	-99.2
1	5.4	-64.6	3.3	-53	78	-79	158	-98.4
2	4.8	-66.8	2.8	-54	71.5	-78.2	145	-97.2
3	4.3	-68	2.5	-54.6	66	-77.8	135	-96.5
4	4.0	-68.6	2.23	-55	60	-77.5	125	-96
5	3.7	-69.1	2.05	-55.2	56	-77.2	115	-95.7
6	3.5	-69.4	1.86	-56	52	-77.2	110	-95.4
7	3.2	-69.8	1.72	-56.2	49	-77	105	-95
8	3.05	-70	1.60	-56.3	46	-77	99	-94.6
9	2.90	-70	1.50	-56.4	43	-76.8	93	-94.4
10	2.75	-70	1.40	-56.4	40	-76.8	87	-94.2
11	2.56	-69.4	1.30	-56.4	37	-76.7	80	-94.0
12	2.40	-68.8	1.20	-56.4	35	-76.6	75	-93.7
13	2.25	-68.0	1.15	-56.3	32	-76.6	69	-93.6
14	2.10	-68.2	1.09	-56.1	30	-76.5	64	-93.3
15	1.96	-68.2	1.01	-55.7	28	-76.4	60	-93.3
16	1.85	-68.3	.95	-55.6	26.2	-76.4	55	-93.3
17	1.70	-68	.90	-55.0	24.2	-76.4	51	-93.2
18	1.60	-67.8	.84	-54.8	22	-76.4	47	-93
19	1.5	-67.4	.79	-54.6	20	-76.3	42	-93.0
20	1.36	-67	.73	-54.4	18	-76.3	38	-92.8
21	1.26	-66.5	.67	-54	16.2	-76.2	33	-92.8
22	1.15	-65.6	.62	-53.6	14	-76.2	29	-92.7
23	1.05	-64.6	.56	-53	12	-76.2	25	-92.6
24	.94	-63	.50	-52.2	10	-76.2	20.5	-92.7

COMPUTER PROGRAMS USED TO SOLVE THE COUPLED INTEGRAL EQUATIONS (86a,b):

FORTRAN IV - LEVEL 21		MAIN	DATE = 75205	14/42/31
C		THIS PROGRAM COMPUTES THE AXIAL MAGNETIC AND AZIMUTHAL ELECTRIC		
C		CONSTANTS ON A FINITE SPHERICAL ROD ANTENNA DRIVEN BY A LOOP CARRY-		
C		ING CONSTANT CURRENT.		
C		SOLUTION BY THE ELEMENT METHOD FOR THE COUPLED		
C		INTEGRAL EQNS. 2.62 OF CHAPTER 2.		
0001		DIMENSION CM(20),CK(20),CT(10),AA(40,40),CR(10,10),CX(20)		
0002		2, CM1(10,10),CM11(10),CY2(10,10),CK2(10),CK21(10,10),CM2(10)		
0003		COMMON TAKO,CM04,TPY,TA,CK1,CAK1,TH,T,TKOT,TKO,TPS		
0004		INT=CK1P		
0005		CY1,CA1,CK11,CK111,CK112,CK12,CK121,CK122,CK211,CK212,CK213,CK214,CK215,		
0006		CK216,CK217,CK218,CK219,CK221,CK222,CK223,CK224,CK225,CK226,CK227,CK228,		
0007		CK229,CK231,CK232,CK233,CK234,CK235,CK236,CK237,CK238,CK239,CK241,CK242,		
0008		CK243,CK244,CK245,CK246,CK247,CK248,CK249,CK251,CK252,CK253,CK254,CK255,		
0009		CK256,CK257,CK258,CK259,CK261,CK262,CK263,CK264,CK265,CK266,CK267,CK268,		
0010		CK269,CK271,CK272,CK273,CK274,CK275,CK276,CK277,CK278,CK279,CK281,CK282,		
0011		CK283,CK284,CK285,CK286,CK287,CK288,CK289,CK291,CK292,CK293,CK294,CK295,		
0012		CK296,CK297,CK298,CK299,CK301,CK302,CK303,CK304,CK305,CK306,CK307,CK308,		
0013		CK309,CK311,CK312,CK313,CK314,CK315,CK316,CK317,CK318,CK319,CK321,CK322,		
0014		CK323,CK324,CK325,CK326,CK327,CK328,CK329,CK331,CK332,CK333,CK334,CK335,		
0015		CK336,CK337,CK338,CK339,CK341,CK342,CK343,CK344,CK345,CK346,CK347,CK348,		
0016		CK349,CK351,CK352,CK353,CK354,CK355,CK356,CK357,CK358,CK359,CK361,CK362,		
0017		CK363,CK364,CK365,CK366,CK367,CK368,CK369,CK371,CK372,CK373,CK374,CK375,		
0018		CK376,CK377,CK378,CK379,CK381,CK382,CK383,CK384,CK385,CK386,CK387,CK388,		
0019		CK389,CK391,CK392,CK393,CK394,CK395,CK396,CK397,CK398,CK399,CK401,CK402,		
0020		CK403,CK404,CK405,CK406,CK407,CK408,CK409,CK411,CK412,CK413,CK414,CK415,		
0021		CK416,CK417,CK418,CK419,CK421,CK422,CK423,CK424,CK425,CK426,CK427,CK428,		
0022		CK429,CK431,CK432,CK433,CK434,CK435,CK436,CK437,CK438,CK439,CK441,CK442,		
0023		CK443,CK444,CK445,CK446,CK447,CK448,CK449,CK451,CK452,CK453,CK454,CK455,		
0024		CK456,CK457,CK458,CK459,CK461,CK462,CK463,CK464,CK465,CK466,CK467,CK468,		
0025		CK469,CK471,CK472,CK473,CK474,CK475,CK476,CK477,CK478,CK479,CK481,CK482,		
0026		CK483,CK484,CK485,CK486,CK487,CK488,CK489,CK491,CK492,CK493,CK494,CK495,		
0027		CK496,CK497,CK498,CK499,CK501,CK502,CK503,CK504,CK505,CK506,CK507,CK508,		
0028		CK509,CK511,CK512,CK513,CK514,CK515,CK516,CK517,CK518,CK519,CK521,CK522,		
0029		CK523,CK524,CK525,CK526,CK527,CK528,CK529,CK531,CK532,CK533,CK534,CK535,		
0030		CK536,CK537,CK538,CK539,CK541,CK542,CK543,CK544,CK545,CK546,CK547,CK548,		
0031		CK549,CK551,CK552,CK553,CK554,CK555,CK556,CK557,CK558,CK559,CK561,CK562,		
0032		CK563,CK564,CK565,CK566,CK567,CK568,CK569,CK571,CK572,CK573,CK574,CK575,		
0033		CK576,CK577,CK578,CK579,CK581,CK582,CK583,CK584,CK585,CK586,CK587,CK588,		
0034		CK589,CK591,CK592,CK593,CK594,CK595,CK596,CK597,CK598,CK599,CK601,CK602,		
0035		CK603,CK604,CK605,CK606,CK607,CK608,CK609,CK611,CK612,CK613,CK614,CK615,		
0036		CK616,CK617,CK618,CK619,CK621,CK622,CK623,CK624,CK625,CK626,CK627,CK628,		
0037		CK629,CK631,CK632,CK633,CK634,CK635,CK636,CK637,CK638,CK639,CK641,CK642,		
0038		CK643,CK644,CK645,CK646,CK647,CK648,CK649,CK651,CK652,CK653,CK654,CK655,		
0039		CK656,CK657,CK658,CK659,CK661,CK662,CK663,CK664,CK665,CK666,CK667,CK668,		
0040		CK669,CK671,CK672,CK673,CK674,CK675,CK676,CK677,CK678,CK679,CK681,CK682,		
0041		CK683,CK684,CK685,CK686,CK687,CK688,CK689,CK691,CK692,CK693,CK694,CK695,		
0042		CK696,CK697,CK698,CK699,CK701,CK702,CK703,CK704,CK705,CK706,CK707,CK708,		
0043		CK709,CK711,CK712,CK713,CK714,CK715,CK716,CK717,CK718,CK719,CK721,CK722,		
0044		CK723,CK724,CK725,CK726,CK727,CK728,CK729,CK731,CK732,CK733,CK734,CK735,		
0045		CK736,CK737,CK738,CK739,CK741,CK742,CK743,CK744,CK745,CK746,CK747,CK748,		
0046		CK749,CK751,CK752,CK753,CK754,CK755,CK756,CK757,CK758,CK759,CK761,CK762,		
0047		CK763,CK764,CK765,CK766,CK767,CK768,CK769,CK771,CK772,CK773,CK774,CK775,		
0048		CK776,CK777,CK778,CK779,CK781,CK782,CK783,CK784,CK785,CK786,CK787,CK788,		
0049		CK789,CK791,CK792,CK793,CK794,CK795,CK796,CK797,CK798,CK799,CK801,CK802,		
0050		CK803,CK804,CK805,CK806,CK807,CK808,CK809,CK811,CK812,CK813,CK814,CK815,		
0051		CK816,CK817,CK818,CK819,CK821,CK822,CK823,CK824,CK825,CK826,CK827,CK828,		
0052		CK829,CK831,CK832,CK833,CK834,CK835,CK836,CK837,CK838,CK839,CK841,CK842,		
0053		CK843,CK844,CK845,CK846,CK847,CK848,CK849,CK851,CK852,CK853,CK854,CK855,		
0054		CK856,CK857,CK858,CK859,CK861,CK862,CK863,CK864,CK865,CK866,CK867,CK868,		
0055		CK869,CK871,CK872,CK873,CK874,CK875,CK876,CK877,CK878,CK879,CK881,CK882,		
0056		CK883,CK884,CK885,CK886,CK887,CK888,CK889,CK891,CK892,CK893,CK894,CK895,		
0057		CK896,CK897,CK898,CK899,CK901,CK902,CK903,CK904,CK905,CK906,CK907,CK908,		
0058		CK909,CK911,CK912,CK913,CK914,CK915,CK916,CK917,CK918,CK919,CK921,CK922,		
0059		CK923,CK924,CK925,CK926,CK927,CK928,CK929,CK931,CK932,CK933,CK934,CK935,		
0060		CK936,CK937,CK938,CK939,CK941,CK942,CK943,CK944,CK945,CK946,CK947,CK948,		
0061		CK949,CK951,CK952,CK953,CK954,CK955,CK956,CK957,CK958,CK959,CK961,CK962,		
0062		CK963,CK964,CK965,CK966,CK967,CK968,CK969,CK971,CK972,CK973,CK974,CK975,		
0063		CK976,CK977,CK978,CK979,CK981,CK982,CK983,CK984,CK985,CK986,CK987,CK988,		
0064		CK989,CK991,CK992,CK993,CK994,CK995,CK996,CK997,CK998,CK999,CK1001,CK1002,		
0065		CK1003,CK1004,CK1005,CK1006,CK1007,CK1008,CK1009,CK1011,CK1012,CK1013,CK1014,		
0066		CK1015,CK1016,CK1017,CK1018,CK1019,CK1021,CK1022,CK1023,CK1024,CK1025,CK1026,		
0067		CK1027,CK1028,CK1029,CK1031,CK1032,CK1033,CK1034,CK1035,CK1036,CK1037,CK1038,		
0068		CK1039,CK1041,CK1042,CK1043,CK1044,CK1045,CK1046,CK1047,CK1048,CK1049,CK1051,		
0069		CK1052,CK1053,CK1054,CK1055,CK1056,CK1057,CK1058,CK1059,CK1061,CK1062,CK1063,		
0070		CK1064,CK1065,CK1066,CK1067,CK1068,CK1069,CK1071,CK1072,CK1073,CK1074,CK1075,		
0071		CK1076,CK1077,CK1078,CK1079,CK1081,CK1082,CK1083,CK1084,CK1085,CK1086,CK1087,		
0072		CK1088,CK1089,CK1091,CK1092,CK1093,CK1094,CK1095,CK1096,CK1097,CK1098,CK1099,		
0073		CK1101,CK1102,CK1103,CK1104,CK1105,CK1106,CK1107,CK1108,CK1109,CK1111,CK1112,		
0074		CK1113,CK1114,CK1115,CK1116,CK1117,CK1118,CK1119,CK1121,CK1122,CK1123,CK1124,		
0075		CK1125,CK1126,CK1127,CK1128,CK1129,CK1131,CK1132,CK1133,CK1134,CK1135,CK1136,		
0076		CK1137,CK1138,CK1139,CK1141,CK1142,CK1143,CK1144,CK1145,CK1146,CK1147,CK1148,		
0077		CK1149,CK1151,CK1152,CK1153,CK1154,CK1155,CK1156,CK1157,CK1158,CK1159,CK1161,		
0078		CK1162,CK1163,CK1164,CK1165,CK1166,CK1167,CK1168,CK1169,CK1171,CK1172,CK1173,		
0079		CK1174,CK1175,CK1176,CK1177,CK1178,CK1179,CK1181,CK1182,CK1183,CK1184,CK1185,		
0080		CK1186,CK1187,CK1188,CK1189,CK1191,CK1192,CK1193,CK1194,CK1195,CK1196,CK1197,		
0081		CK1198,CK1199,CK1201,CK1202,CK1203,CK1204,CK1205,CK1206,CK1207,CK1208,CK1209,		
0082		CK1211,CK1212,CK1213,CK1214,CK1215,CK1216,CK1217,CK1218,CK1219,CK1221,CK1222,		
0083		CK1223,CK1224,CK1225,CK1226,CK1227,CK1228,CK1229,CK1231,CK1232,CK1233,CK1234,		
0084		CK1235,CK1236,CK1237,CK1238,CK1239,CK1241,CK1242,CK1243,CK1244,CK1245,CK1246,		
0085		CK1247,CK1248,CK1249,CK1251,CK1252,CK1253,CK1254,CK1255,CK1256,CK1257,CK1258,		
0086		CK1259,CK1261,CK1262,CK1263,CK1264,CK1265,CK1266,CK1267,CK1268,CK1269,CK1271,		
0087		CK1272,CK1273,CK1274,CK1275,CK1276,CK1277,CK1278,CK1279,CK1281,CK1282,CK1283,		
0088		CK1284,CK1285,CK1286,CK1287,CK1288,CK1289,CK1291,CK1292,CK1293,CK1294,CK1295,		
0089		CK1296,CK1297,CK1298,CK1299,CK1301,CK1302,CK1303,CK1304,CK1305,CK1306,CK1307,		
0090		CK1308,CK1309,CK1311,CK1312,CK1313,CK1314,CK1315,CK1316,CK1317,CK1318,CK1319,		
0091		CK1321,CK1322,CK1323,CK1324,CK1325,CK1326,CK1327,CK1328,CK1329,CK1331,CK1332,		
0092		CK1333,CK1334,CK1335,CK1336,CK1337,CK1338,CK1339,CK1341,CK1342,CK1343,CK1344,		
0093		CK1345,CK1346,CK1347,CK1348,CK1349,CK1351,CK1352,CK1353,CK1354,CK1355,CK1356,		
0094		CK1357,CK1358,CK1359,CK1361,CK1362,CK1363,CK1364,CK1365,CK1366,CK1367,CK1368,		
0095		CK1369,CK1371,CK1372,CK1373,CK1374,CK1375,CK1376,CK1377,CK1378,CK1379,CK1381,		
0096		CK1382,CK1383,CK1384,CK1385,CK1386,CK1387,CK1388,CK1389,CK1391,CK1392,CK1393,		
0097		CK1394,CK1395,CK1396,CK1397,CK1398,CK1399,CK1401,CK1402,CK1403,CK1404,CK1405,		
0098		CK1406,CK1407,CK1408,CK1409,CK1411,CK1412,CK1413,CK1414,CK1415,CK1416,CK1417,		
0099		CK1418,CK1419,CK1421,CK1422,CK1423,CK1424,CK1425,CK1426,CK1427,CK1428,CK1429,		
0100		CK1431,CK1432,CK1433,CK1434,CK1435,CK1436,CK1437,CK1438,CK1439,CK1441,CK1442,		
0101		CK1443,CK1444,CK1445,CK1446,CK1447,CK1448,CK1449,CK1451,CK1452,CK1453,CK1454,		
0102		CK1455,CK1456,CK1457,CK1458,CK1459,CK1461,CK1462,CK1463,CK1464,CK1465,CK1466,		
0103		CK1467,CK1468,CK1469,CK1471,CK1472,CK1473,CK1474,CK1475,CK1476,CK1477,CK1478,		
0104		CK1479,CK1481,CK1482,CK1483,CK1484,CK1485,CK1486,CK1487,CK1488,CK1489,CK1491,		
0105		CK1492,CK1493,CK1494,CK1495,CK1496,CK1497,CK1498,CK1499,CK1501,CK1502,CK1503,		
0106		CK1504,CK1505,CK1506,CK1507,CK1508,CK1509,CK1511,CK1512,CK1513,CK1514,CK1515,		
0107		CK1516,CK1517,CK1518,CK1519,CK1521,CK1522,CK1523,CK1524,CK1525,CK1526,CK1527,		
0108		CK1528,CK1529,CK1531,CK		
C		COMPUTE THE CONSTANTS IN THE TWO INTEGRAL EQNS. CA IS THE ONLY		
C		UNKNOWN CONSTANT WHICH IS DETERMINED AS A COMPONENT OF MATRIX		
C		SOLUTION.		
0019		C1=(C0.1,4)*TPY*IF/(TA**2)		
0019		C1=C1-0.1*TPY*TA*TKO		
0029		C2=1/(TA*0.1*TA*TKO)		
0029		C2=2.*C1		
0039		C10=-1./TA		
C				
C		DIVISION INTO PANELS		
C				
0021		N=2		
0024		CCT1=TH		
0025		KPI=K+1		
0026		TP=TH*0.6*TA*TKO/TKO		
0027		T=TH/(2.*C1*CAT(N))		
0028		TKC1=TKO*Y		
C				
C		COMPUTING THE RIGHT HAND SIDE		
C				

THIS PAGE IS BEST QUALITY PRACTICABLE
FROM COPY FURNISHED TO DDG

```

      FORTSPAN IV G LEVEL 21          MAIN          DATE = 75205          14/4/31

0020      DO 20 I=1,NP1
0030      Y(I)=1/WAT(I) *-1.
0040      20      CG(I)=C7*OSIN(2*Y(I)*TKGT)
0050      K2=2*NP1
0060      NP2=NP1+1
0070      P1=1K 1=EP2,K2
0080      10      G(I,2)=(0.,0.)
0090      10      I=1
0100      20      K(I,1)=(6,21) 1,CG(I)
0110      21      10=KAT (5X,1G(1,12,1) = 1,7C0.5,2X,F20.5)
0120      1=1+1
0130      10      11,1F,M2) GO TO 22
0140      C
0150      C      COMPUTING THE ELEMENTS OF REGION 1.
0160      C
0170      C      COMPUTING K(I,1) BY 10 POINT GAUSS QUADATURE.
0180      C      CALL GQ10(1G,50.,FK11,Y)
0190      C      CALL GQ10(1G,50.,FK11,Y1)
0200      C      CK(I,1)=CMPLX(X(YP,Y1)
0210      C
0220      C      COMPUTING K(I,1) FOR I=2,N+1
0230      C
0240      DO 24 I=2,NP1
0250      J=1
0260      CALL GQ10(1J,J,FK11,IR,11)
0270      C      FK11=CMPLX(FK,1)
0280      24      CK(I,2)=CK(I,1)*.5+CT(I)
0290      C
0300      C      COMPUTING K(I,J) FOR I=1,N+1 AND J=1+1,N+1
0310      C
0320      DO 30 I=1,NP1
0330      DO 30 J=1+1,NP1
0340      CALL GQ10(1J,J,FK1K,IR,11)
0350      CK(I,J)=CMPLX(FK,11)
0360      30      CK(J,1)=CK(I,J)
0370      C
0380      C      MODIFYING THE LOWER TRIANGLE ELEMENTS TO OBTAIN THE
0390      C      KRAE ELEMENTS. THE FIRST COLUMN ELEMENTS ARE HALVED.
0400      C
0410      DO 40 I=1,NP1
0420      CK(I,1)=.5*CK(I,1)
0430      DO 45 I=2,NP1
0440      11X2*2*1=2
0450      DO 45 P=1,11P2
0460      A(I,1)= (1./1X0)*(COS(1X0I*(2*1-P-1))-COS(1X0I*(2*1-P-1)))
0470      C
0480      C      COMPUTING 0(I,J) FROM THE SERIES
0490      C
0500      DO 48 I=1,NP1
0510      DO 48 J=1,NP1
0520      CALL SPTK5(1,J,16C)

```

THIS PAGE IS BEST QUALITY PRACTICABLE
FROM COPY FURNISHED TO DDG

FORTRAN IV G LEVEL 21		MAIN	DATE = 75205	14/42/31
0063	48	CR(I,J)=CRC		
	C	THE FIRST COLUMN ELEMENTS		
0064		DC 50 I=2,NP1		
0065	50	CR(I,1)=CR(I,1)-AA(I,1)*C3		
	C	THE DIAGONAL ELEMENTS		
	C			
0066		DC 55 I=2,N		
0067	55	CR(I,1)=CR(I,1)-AA(I,(2*I-2))*C3		
	C	THE ELEMENTS IN THE LOWER TRIANGLE BUT NOT IN THE FIRST		
	C	COLUMN OR THE DIAGONAL.		
	C			
0068		DC 60 I=3,NP1		
0069		I=I-1		
0070		DC 60 J=2,IM		
0071	60	CV(I,J)=CR(I,J)- (3*(AA(I,2*J-2)+AA(I,2*J-1)))		
	C			
	C	COMPUTING K(I,J) ELEMENTS.		
	C			
0072		DC 62 I=1,NP1		
0073		DC 62 J=1,NP1		
0074	62	CR(I,J)=CR(I,J)+CR(I,J)		
	C			
	C	BY NOW ALL THE ELEMENTS IN REGION I ARE COMPUTED.		
	C			
	C	COMPUTING ELEMENTS OF REGION II.		
	C			
0075		CALL UG1010(.50,(K211),Y0)		
0076		CALL UG1010(.50,(K211),Y1)		
0077		CV(1,1)=CPLX(Y0,Y1)		
0078		DC 65 I=2,N		
0079		J=1		
0080		CALL UG1011(J,(K211),Y0,T1)		
0081		CV(1,1)=CPLX(T0,T1)		
0082	65	CV(1,1)=CV(1,1)+.5*CV(1,1)		
0083		DC 70 I=1,NP1		
0084		I=I+1		
0085		DC 70 J=1,NP1		
0086		CALL UG1011(J,(K211),Y0,T1)		
0087		CV(1,1)=CPLX(T0,T1)		
0088	70	CV(1,1)=CV(1,1)+J		
0089		DC 75 I=1,NP1		
0090	75	CV(1,1)=0.5*CV(1,1)		
	C			
	C	BY NOW ALL THE ELEMENTS IN REGION II ARE COMPUTED.		
	C			
	C	COMPUTING ELEMENTS IN REGION III.		
	C			
0091		CALL UG1010(.50,(K211),Y0)		
0092		CALL UG1010(.50,(K211),Y1)		
0093		CV(1,1)=CPLX(Y0,Y1)		
0094		DC 80 I=2,NP1		
0095		J=1		
0096		CALL UG1011(J,(K211),Y0,T1)		

THIS PAGE IS BEST QUALITY PRACTICABLE
FROM COPY FURNISHED TO DDC

FORTRAN IV G LEVEL 21		MAIN	DATE = 75205	14/42/31
0077		CK2(1,1)=CMPLX(TR,TI)		
0086	90	CK2(1,1)=CK2(1,1)+.5*CK2(1,1)		
0099		DC 85 1=1,NP1		
0100		1P1=1+1		
0101		DC 85 J=1P1,NP1		
0102		CALL OG10(1,J,FCR2,TR,TI)		
0103		CK2(1,1)=CMPLX(1P1,TI)		
0104	85	CK2(1,1)=CK2(1,1)		
0105		DC 90 1=1,NP1		
0106	90	CK2(1,1)=0.5*CK2(1,1)		
	C			
	C	BY NOW ALL THE ELEMENTS IN REGION III ARE COMPUTED.		
	C			
	C	COMPUTING ELEMENTS OF REGION IV.		
	C			
0107		CALL OG10(1,50,FCR2,1P1,YI)		
0108		CALL OG10(1,50,FCR2,1P1,YI)		
0109		CK2(1,1)=CMPLX(YI,YI)		
0110		DC 95 1=1,NP1		
0111		1P1=1+1		
0112		CALL OG10(1,J,FCR2,1P1,YI,TI)		
0113		CK2(1,1)=CMPLX(1P1,TI)		
0114	95	CK2(1,1)=CK2(1,1)+.5*CK2(1,1)		
0115		DC 100 1=1,NP1		
0116		1P1=1+1		
0117		DC 100 J=1P1,NP1		
0118		CALL OG10(1,J,FCR2,1P1,TI)		
0119		CK2(1,1)=CMPLX(1P1,TI)		
0120	100	CK2(1,1)=CK2(1,1)		
0121		DC 105 1=1,NP1		
0122	105	CK2(1,1)=0.5*CK2(1,1)		
	C			
	C	BY NOW ALL THE ELEMENTS IN REGION IV ARE COMPUTED.		
	C			
	C	COMPUTING ELEMENTS OF REGION V		
	C			
0123		CALL OG10(1,110,FCR2,1P1,YI)		
0124		DC 110 1=1,NP1		
0125	110	CK2(1,1)=CK2(1,1)+.5*CK2(1,1)		
	C			
	C	COMPUTING ELEMENTS OF REGION VI.		
	C			
0126		CALL OG10(1,115,FCR2,1P1,YI)		
0127		DC 115 1=1,NP1		
0128	115	CK2(1,1)=CK2(1,1)+.5*CK2(1,1)		
	C			
	C	BY NOW ALL THE ELEMENTS IN REGION V AND VI ARE DONE.		
	C			
	C	SETTING UP THE FINAL MATRIX FOR		
	C			
0129		N2P1=2*N2P1		
0130		DC 120 1=1,NP1		
0131		DO 120 J=N2P1,N2P1		

14/42/31

```

0132 120 CK(I,J)=CM(I,I,J-NP1)
C
0133 DO 125 I=NP2,N2P2
0134 DO 125 J=1,NP1
0135 CK(I,J)=CK2(I-NP1,J)
C
0136 DO 130 I=NP2,N2P1
0137 DO 130 J=NP2,N2P1
0138 CK(I,J)=CM2(I-NP1,J-NP1)
C
0139 C
C
0140 DO 142 I=1,N2P2
0141 CK(I,NP1)=0.5*CK(I,NP1)
C
0142 BY NEW SIZE, THE INVERSE MATRIX IS COMPUTED. NEXT WE
C
C
C
C
C
0143 N=N2
0144 CALL DECOMPM,CK,CUL)
0145 CALL SOLVE(4,CUL,CG,EX)
0146 WRITE (6,66) (CX(I),I=1,N2)
0147 FORMAT (12F10.5)
0148 CALL IMPROVEM,CK,CUL,CG,EX,DIGITS)
0149 WRITE (6,66) (CX(I),I=1,N2)
0150 CX(N2)=0.,0.)
0151 C(N,N2)=PM(I2)-10**18(I2)
C
0152 TAPR=(2.*TYP*1000/TKO)
0153 DO 17 I=1,NP1
0154 CX(I)=CX(I)+TAPR*P
C
C
C
C
0155 PRINTOUT OF THE SOLUTION.
C
0156 I=1
0157 T1=PM(1,CX(I))
0158 T2=PM(1,CX(I+1))
0159 T3=PM(1,CX(I+2))
0160 T4=PM(1,CX(I+3))
0161 T5=PM(1,CX(I+4))
0162 T6=PM(1,CX(I+5))
0163 T7=PM(1,CX(I+6))
0164 T8=PM(1,CX(I+7))
0165 T9=PM(1,CX(I+8))
0166 T10=PM(1,CX(I+9))
0167 T11=PM(1,CX(I+10))
0168 T12=PM(1,CX(I+11))
0169 T13=PM(1,CX(I+12))
0170 T14=PM(1,CX(I+13))
0171 T15=PM(1,CX(I+14))
0172 T16=PM(1,CX(I+15))
0173 T17=PM(1,CX(I+16))
0174 T18=PM(1,CX(I+17))
0175 T19=PM(1,CX(I+18))
0176 T20=PM(1,CX(I+19))
0177 T21=PM(1,CX(I+20))
0178 T22=PM(1,CX(I+21))
0179 T23=PM(1,CX(I+22))
0180 T24=PM(1,CX(I+23))
0181 T25=PM(1,CX(I+24))
0182 T26=PM(1,CX(I+25))
0183 T27=PM(1,CX(I+26))
0184 T28=PM(1,CX(I+27))
0185 T29=PM(1,CX(I+28))
0186 T30=PM(1,CX(I+29))
0187 T31=PM(1,CX(I+30))
0188 T32=PM(1,CX(I+31))
0189 T33=PM(1,CX(I+32))
0190 T34=PM(1,CX(I+33))
0191 T35=PM(1,CX(I+34))
0192 T36=PM(1,CX(I+35))
0193 T37=PM(1,CX(I+36))
0194 T38=PM(1,CX(I+37))
0195 T39=PM(1,CX(I+38))
0196 T40=PM(1,CX(I+39))
0197 T41=PM(1,CX(I+40))
0198 T42=PM(1,CX(I+41))
0199 T43=PM(1,CX(I+42))
0200 T44=PM(1,CX(I+43))
0201 T45=PM(1,CX(I+44))
0202 T46=PM(1,CX(I+45))
0203 T47=PM(1,CX(I+46))
0204 T48=PM(1,CX(I+47))
0205 T49=PM(1,CX(I+48))
0206 T50=PM(1,CX(I+49))
0207 T51=PM(1,CX(I+50))
0208 T52=PM(1,CX(I+51))
0209 T53=PM(1,CX(I+52))
0210 T54=PM(1,CX(I+53))
0211 T55=PM(1,CX(I+54))
0212 T56=PM(1,CX(I+55))
0213 T57=PM(1,CX(I+56))
0214 T58=PM(1,CX(I+57))
0215 T59=PM(1,CX(I+58))
0216 T60=PM(1,CX(I+59))
0217 T61=PM(1,CX(I+60))
0218 T62=PM(1,CX(I+61))
0219 T63=PM(1,CX(I+62))
0220 T64=PM(1,CX(I+63))
0221 T65=PM(1,CX(I+64))
0222 T66=PM(1,CX(I+65))
0223 T67=PM(1,CX(I+66))
0224 T68=PM(1,CX(I+67))
0225 T69=PM(1,CX(I+68))
0226 T70=PM(1,CX(I+69))
0227 T71=PM(1,CX(I+70))
0228 T72=PM(1,CX(I+71))
0229 T73=PM(1,CX(I+72))
0230 T74=PM(1,CX(I+73))
0231 T75=PM(1,CX(I+74))
0232 T76=PM(1,CX(I+75))
0233 T77=PM(1,CX(I+76))
0234 T78=PM(1,CX(I+77))
0235 T79=PM(1,CX(I+78))
0236 T80=PM(1,CX(I+79))
0237 T81=PM(1,CX(I+80))
0238 T82=PM(1,CX(I+81))
0239 T83=PM(1,CX(I+82))
0240 T84=PM(1,CX(I+83))
0241 T85=PM(1,CX(I+84))
0242 T86=PM(1,CX(I+85))
0243 T87=PM(1,CX(I+86))
0244 T88=PM(1,CX(I+87))
0245 T89=PM(1,CX(I+88))
0246 T90=PM(1,CX(I+89))
0247 T91=PM(1,CX(I+90))
0248 T92=PM(1,CX(I+91))
0249 T93=PM(1,CX(I+92))
0250 T94=PM(1,CX(I+93))
0251 T95=PM(1,CX(I+94))
0252 T96=PM(1,CX(I+95))
0253 T97=PM(1,CX(I+96))
0254 T98=PM(1,CX(I+97))
0255 T99=PM(1,CX(I+98))
0256 T100=PM(1,CX(I+99))
0257 T101=PM(1,CX(I+100))
0258 T102=PM(1,CX(I+101))
0259 T103=PM(1,CX(I+102))
0260 T104=PM(1,CX(I+103))
0261 T105=PM(1,CX(I+104))
0262 T106=PM(1,CX(I+105))
0263 T107=PM(1,CX(I+106))
0264 T108=PM(1,CX(I+107))
0265 T109=PM(1,CX(I+108))
0266 T110=PM(1,CX(I+109))
0267 T111=PM(1,CX(I+110))
0268 T112=PM(1,CX(I+111))
0269 T113=PM(1,CX(I+112))
0270 T114=PM(1,CX(I+113))
0271 T115=PM(1,CX(I+114))
0272 T116=PM(1,CX(I+115))
0273 T117=PM(1,CX(I+116))
0274 T118=PM(1,CX(I+117))
0275 T119=PM(1,CX(I+118))
0276 T120=PM(1,CX(I+119))
0277 T121=PM(1,CX(I+120))
0278 T122=PM(1,CX(I+121))
0279 T123=PM(1,CX(I+122))
0280 T124=PM(1,CX(I+123))
0281 T125=PM(1,CX(I+124))
0282 T126=PM(1,CX(I+125))
0283 T127=PM(1,CX(I+126))
0284 T128=PM(1,CX(I+127))
0285 T129=PM(1,CX(I+128))
0286 T130=PM(1,CX(I+129))
0287 T131=PM(1,CX(I+130))
0288 T132=PM(1,CX(I+131))
0289 T133=PM(1,CX(I+132))
0290 T134=PM(1,CX(I+133))
0291 T135=PM(1,CX(I+134))
0292 T136=PM(1,CX(I+135))
0293 T137=PM(1,CX(I+136))
0294 T138=PM(1,CX(I+137))
0295 T139=PM(1,CX(I+138))
0296 T140=PM(1,CX(I+139))
0297 T141=PM(1,CX(I+140))
0298 T142=PM(1,CX(I+141))
0299 T143=PM(1,CX(I+142))
0300 T144=PM(1,CX(I+143))
0301 T145=PM(1,CX(I+144))
0302 T146=PM(1,CX(I+145))
0303 T147=PM(1,CX(I+146))
0304 T148=PM(1,CX(I+147))
0305 T149=PM(1,CX(I+148))
0306 T150=PM(1,CX(I+149))
0307 T151=PM(1,CX(I+150))
0308 T152=PM(1,CX(I+151))
0309 T153=PM(1,CX(I+152))
0310 T154=PM(1,CX(I+153))
0311 T155=PM(1,CX(I+154))
0312 T156=PM(1,CX(I+155))
0313 T157=PM(1,CX(I+156))
0314 T158=PM(1,CX(I+157))
0315 T159=PM(1,CX(I+158))
0316 T160=PM(1,CX(I+159))
0317 T161=PM(1,CX(I+160))
0318 T162=PM(1,CX(I+161))
0319 T163=PM(1,CX(I+162))
0320 T164=PM(1,CX(I+163))
0321 T165=PM(1,CX(I+164))
0322 T166=PM(1,CX(I+165))
0323 T167=PM(1,CX(I+166))
0324 T168=PM(1,CX(I+167))
0325 T169=PM(1,CX(I+168))
0326 T170=PM(1,CX(I+169))
0327 T171=PM(1,CX(I+170))
0328 T172=PM(1,CX(I+171))
0329 T173=PM(1,CX(I+172))
0330 T174=PM(1,CX(I+173))
0331 T175=PM(1,CX(I+174))
0332 T176=PM(1,CX(I+175))
0333 T177=PM(1,CX(I+176))
0334 T178=PM(1,CX(I+177))
0335 T179=PM(1,CX(I+178))
0336 T180=PM(1,CX(I+179))
0337 T181=PM(1,CX(I+180))
0338 T182=PM(1,CX(I+181))
0339 T183=PM(1,CX(I+182))
0340 T184=PM(1,CX(I+183))

```


THIS PAGE IS BEST QUALITY PRACTICABLE
FROM COPY FURNISHED TO DDC

```

1. SUBROUTINE BSLSM(L(NERO,XYO,XYL)
2. C SUBROUTINE BSLSM
3. C BSLSM COMPUTES BESSEL J FUNCTION WITH COMPLEX ARGUMENTS
4. C AND ORDER AND 1. ACCURACY UPTO 6TH DECIMAL PLACE OR MORE IS
5. C OBTAINED FOR ABS(Z) LESS THAN 20.
6. C IMPLICIT COMPLEX*16(D), REAL*8(T)
7. COMPLEX XYO,XYL
8. DZZ=XYO
9. A=NDKO
10. TX=REAL(DZZ)
11. TY=AIMAG(DZZ)
12. X=TX
13. Y=TY
14. TX=C.500*TX
15. TY=C.500*TY
16. TR=TX*TX+TY*TY
17. TF=C.D0*TX*TY
18. R=N
19. ETC=10.C
20. L=(C.D0*TR+R+10.0*(X*X+Y*Y))-R)*ETC
21. TFR=1.C0
22. TFI=C.00
23. I1=(L+1)*(N+L+1)
24. J1=(2*L+N+2)
25. D0=C.400*(1/L)
26. TF=I1*(J1+K1)*K
27. TGR=TR/TP
28. TG1=TF/TP
29. TD=TFR
30. TFR=1.C0-TGR*TFN+TG1*TFI
31. 400 TF1=-(TGR*TF1+TG1*TC)
32. IF (N-ET.0) GO TO 401
33. IF (N-ET.0) GO TO 402
34. 401 CONTINUE
35. D0SLJ=D0CMPLX(TFR,TFI)
36. XYL=D0SLJ
37. RETURN
38. 402 TGR=1.C0
39. TG1=C.D0
40. N=N
41. 403 TC=TGR
42. TGR=TGR+TX*TG1*TY
43. TG1=TC*TY+TG1*TX
44. IF (N-ET.0) GO TO 403
45. TC=1.C0
46. TGR=C.400*(1/N)
47. TD=TGR
48. 404 TFI=TGR*TD
49. TGR=TFN/TF
50. TG1=TFI/TF
51. TD=TFR
52. TFR=TFN+TGR*TF1+TG1
53. TF1=TD*TG1+TFI+TGR
54. GO TO 401
55.
56. END

```

THIS PAGE IS BEST QUALITY PRACTICABLE
FROM COPY FURNISHED TO DDC

```

1. SUBROUTINE RESH(XYL,N,KIND,XYL,IER)
2. C SUBROUTINE RESH
3. C 'RESH' COMPUTES HANKEL FUNCTION WITH COMPLEX ARGUMENTS.
4. IMPLICIT COMPLEX*16(D),REAL*8(T)
5. COMPLEX XY0,XYL
6. DIMENSION DT(12),DTT(6),DTX(6)
7. DX=XYL
8. IF(N.EQ.0.AND.KIND.EG.1) GO TO 300
9. IF(N.EQ.0.AND.KIND.EG.2) GO TO 400
10. IF(N.EG.1.AND.KIND.EG.1) GO TO 300
11. IF(N.EG.1.AND.KIND.EG.2) GO TO 400
12. 300 CX=DX*DCMPLX(0.DC,-1.D0)
13. GO TO 500
14. 400 CX=DX*DCMPLX(0.DC,1.D0)
15. GO TO 500
16. 500 TRX=REAL(DX)
17. TIX=AIMAG(DX)
18. TMAG=DSQRT(TRX**2+TIX**2)
19. DBK=DCMPLX(0.D0,C.D0)
20. TP1=3.14159265
21. IF(N) 10,20,20
22. 10 IER=1
23. RETURN
24. 20 IF (TMAG-17C.D0) 22,22,21
25. 21 IER=3
26. RETURN
27. 22 IER=0
28. IF (TMAG-1.D0) 36,36,25
29. 25 CA=CDEXP(-DX)
30. DB=1.D0/CX
31. DC=COSGRT(DR)
32. IE=REAL(DC)+100.I01+101
33. 100 DC=DC
34. 101 CONTINUE
35. DT(1)=DB
36. DO 26 LL=2,12
37. 26 DT(LL)=DT(LL-1)*DB
38. DTT(1)=(CX/R.7500)*.2
39. DO 605 LL=2,6
40. 600 DTT(LL)=DTT(LL-1)*DTT(1)
41. DTX(1)=(DX/2.D0)*.2
42. DO 605 LLL=2,6
43. 605 DTX(LLL)=DTX(LLL-1)*DTX(1)
44. IF(N-1) 627,270,627
45. 627 IF(TMAG-2.D00) 610,610,27
46. C COMPUTE 10 AND THEN K0
47. 610 D10=1.D0+3.51562290C*DTT(1)+3.0899*2*CO*DTT(2)
48. 1+1.2067*920C*DTT(3)+.265973200*DTT(4)+.036076800*DTT(5)
49. 2+0.4561300*DTT(6)
50. 000=C1LL0(DX/2.C0)+.10+.577215600+.2278+2000*DTX(1)
51. 1+.270697500C*DTX(2)+.038859000C*DTX(3)+.002626980C*DTX(4)
52. 2+.000107500C*DTX(5)+.000007*000C*DTX(6)
53. IF(N) 20,628,629
54. 628 DBK=DBK
55. GO TO 200
56. C
57. C COMPUTE K0 USING POLYNOMIAL APPROXIMATION
58. C
59. 27 D00=CA*(1.25331+1.D0+.1866+1800*DT(1)+.088111278C0*DT(2)
60. +.09139095C0*DT(3)+.1344596200*DT(4)+.2299850300*DT(5)
61. +.379249700*DT(6)+.52727300*DT(7)+.55753684C0*DT(8)
62. +.26767270*DT(9)+.21845181C0*DT(10)+.06889767C0*DT(11)

```

THIS PAGE IS BEST QUALITY PRACTICABLE
FROM COPY FURNISHED TO DDC

```

63.      5+.009189383D0*DT(12))*DC
64.      IF(N)20,28,29
65.      28 DBK=DG0
66.      GO TO 200
67.      C COMPUTE J1 AND THEN K1
68.      270 IF (IMAG-2.00D0)-629,629,29
69.      629 DI1=DX*(.5CJ+.87890594D0*DTT(1)+.51498869D0*DTT(2)
70.      1+.1508434D0*DTT(3)+.02658733D0*DTT(4)+.00301532D0*DTT(5)
71.      2+.0032411D0*DTT(6))
72.      DG1=CCLUG(DX/2.00)*DI1+(1.00/DX)*(1.00+.1543144C0*DTX(1)
73.      1+.67278579D0*DTX(2)+.18156897D0*DTX(3)+.01919402C0*DTX(4)
74.      2+.0110404D0*DTX(5)+.00004686D0*DTX(6))
75.      IF (N=1) 20,630,31
76.      630 DBK=DG1
77.      GO TO 200
78.      C
79.      C COMPUTE K1 USING POLYNOMIAL APPROXIMATION
80.      29 DG1=DA*(1.2533141D0+.46999270D0*DT(1)+.14685830D0*DT(2)
81.      2+.12804266C0*DT(3)+.17364316D0*DT(4)+.28476181C0*DT(5)
82.      3+.45943421C0*DT(6)+.62833807D0*DT(7)+.66322954D0*DT(8)
83.      4+.50502386C0*DT(9)+.25813038C0*DT(10)+.07880C612C0*DT(11)
84.      5+.010824177D0*DT(12))*DC
85.      IF(N=1)20,30,31
86.      30 DBK=DG1
87.      GO TO 200
88.      C
89.      C FROM K0,K1 COMPUTE KN USING RECURRENCE RELATION
90.      C
91.      C
92.      31 DB=D0,2,2,4
93.      DGJ=2.00*(FLBAT(J)-1.00)*DG1/DX+DGO
94.      IF(CDABS(DGJ)-1.070) 33,33,32
95.      32 IER=4
96.      GO TO 34
97.      33 CGG=DG1
98.      35 DG1=CGJ
99.      34 DBK=CGJ
100.      GO TO 200
101.      36 DB=DX/2.00
102.      IF (REAL(DB)) 70,71,70
103.      71 IF (AJMAG(DB)) 72,70,73
104.      72 TANG=IP1/2.00
105.      GO TO 75
106.      73 TANG=TP1/2.00
107.      75 TABS=CDABS(DB)
108.      TAR=C.57721600*OLUG(TABS)
109.      DA=DCHPLX(TAR,TANG)
110.      GO TO 76
111.      70 DA=C.5772156600*CCLUG(DB)
112.      76 DC=DB*GB
113.      IF(N=1)37,43,37
114.      C
115.      C COMPUTE K0 USING SERIES EXPANSION
116.      C
117.      37 CGO=DA
118.      DX2J=DCHPLX(1.00,7.00)
119.      TFACT=1.00
120.      THJ=C.D0
121.      DR=0 J=1,6
122.      TRJ=1-D0,FLBAT(J)
123.      DX2J=DX2J*DC
124.      TFACT=TFACT*TRJ*TRJ
125.      THJ=THJ*TRJ

```

```

126.      40 D00=D00+DX2J*TFAC*(THJ-DA)
127.      IF(N143)42,43
128.      42 DBK=D00
129.      GO TO 200
130.      C
131.      C
132.      C      COMPUTE K1 USING SERIES EXPANSION
133.      C
134.      43 DX2J=DB
135.      TFACT=1.00
136.      THJ=1.00
137.      C01=1.00/0X+DX2J*(.500+CA-THJ)
138.      DB 50 J*2.8
139.      DX2J=DX2J+DC
140.      TRJ=1.00/FLB8AT(J)
141.      TFACT=TFACT*TRJ*TRJ
142.      50 C01=C01+DX2J*TFACT*(.500+(DA-THJ)*FLB8AT(J))
143.      IF(N-1)31,52,31
144.      52 DBK=LS1
145.      C
146.      C      COMPUTE HANKEL FUNCTION USING K0 AND K1
147.      C
148.      200 IF(N*EG+0.AND.KIND*EG+1) GO TO 110
149.      IF(N*EG+0.AND.KIND*EG+2) GO TO 115
150.      IF(N*EG+1.AND.KIND*EG+1) GO TO 120
151.      IF(N*EG+1.AND.KIND*EG+2) GO TO 120
152.      110 DBH=-2.00*DCMPLX(0.00+1.00I)*DBK/TP1
153.      GO TO 130
154.      115 DBH=-2.00*DCMPLX(0.00+1.00I)*DBK/TP1
155.      GO TO 130
156.      120 DBH=-2.00*DBK/TP1
157.      130 CONTINUE
158.      XYL=DBH
159.      RETURN
160.      END

```

```

1      SUBROUTINE Q010(XL,YU,F,Y)
2      A=.5*(XU+XL)
3      B=XU-XL
4      C=.4869533*B
5      Y+.03933567*(F(A+C)+F(A-C))
6      C=.4325317*B
7      Y+.07472967*(F(A+C)+F(A-C))
8      C=.3397048*B
9      Y+.1035432*(F(A+C)+F(A-C))
10     C=.2166977*B
11     Y+.1346334*(F(A+C)+F(A-C))
12     C=.07443717*B
13     Y+.1477623*(F(A+C)+F(A-C))
14     RETURN
15     END

```

THIS PAGE IS BEST QUALITY PRACTICABLE
FROM COPY FURNISHED TO DDC

FORTRAN IV G LEVEL	21	FK11	DATE = 75205	14/42/31
0001	SUBROUTINE FK11(MJ,X,TR,T1)			
0002	IMPLICIT COMPLEX*(C),REAL*(4Y)			
0003	COMMON TAKO,CHUR,TPY,TA,CK1,CAL1,TH,T,TKOT,TKO,IPS			
0004	CKOT=(0.,1.)*TKOT			
0005	CY=1.+(0.,1.)*(X/TKOT)			
0006	CY2=CY**2			
0007	CV=TAKO*CSQRT(1.-CY2)			
0008	CALL HSI(SM(TO,CV,CJ))			
0009	CJ2=CJ**2			
0010	T4=4*MI-4			
0011	T14=FLCAT(14)			
0012	CF=CEXP(CKOT*T14)			
0013	CIP=CEXP(CKOT)			
0014	CIM=CEXP(-CKOT)			
0015	T44=4*MI-4			
0016	T14=FLCAT(144)			
0017	T46=4*MI-6			
0018	T16=FLCAT(146)			
0019	T111=EXP(-X*T14)			
0020	T112=EXP(-X*T16)			
0021	CFX=CF*CJ2*(CIP*T111-CIM*T112)/(CKOT*CY)			
0022	TR=PFAL(CFX)			
0023	T1=AIMAG(CFX)			
0024	RETURN			
0025	END			

FORTRAN IV G LEVEL	21	FM11	DATE = 75205	14/42/31
0001	SUBROUTINE FM11(MJ,X,TP,T1)			
0002	IMPLICIT COMPLEX*(C),REAL*(4Y)			
0003	COMMON TAKO,CHUR,TPY,TA,CK1,CAL1,TH,T,TKOT,TKO,IPS			
0004	CKOT=(0.,1.)*TKOT			
0005	CY=1.+(0.,1.)*(X/TKOT)			
0006	CY2=CY**2			
0007	CV=TAKO*CSQRT(1.-CY2)			
0008	CALL HSI(SM(TO,CV,CJ))			
0009	CJ2=CJ**2			
0010	T4=4*MI-4			
0011	T14=FLCAT(14)			
0012	CF=CEXP(CKOT*T14)			
0013	CIP=CEXP(CKOT)			
0014	CIM=CEXP(-CKOT)			
0015	T44=4*MI-4			
0016	T14=FLCAT(144)			
0017	T46=4*MI-6			
0018	T16=FLCAT(146)			
0019	T111=EXP(-X*T14)			
0020	T112=EXP(-X*T16)			
0021	CFX=CF*CJ2*(CIP*T111-CIM*T112)/(CKOT*CY)			
0022	CFX=CFX*TA+IA/CV			
0023	TR=PFAL(CFX)			
0024	T1=AIMAG(CFX)			
0025	RETURN			
0026	END			

FORTRAN IV G LEVFL 21	FK211	DATE = 75205
0001	SUPROUTINE FK211(MI,MJ,X,TR,Y)	
0002	TPM1CTT CCMPCFX*8TC,REAL*4CT	
0003	COMMON TAKO,CHUR,TPY,TA,CK1,CAK1,TH,T,TKOT,TKO,IPS	
0004	CKOT=(0.,1.)*TKOT	
0005	CY=1.+(0.,1.)*(X/TKOT)	
0006	CY2=CY**2	
0007	CV=TAKO+C SORT(1,-CY2)	
0008	CALL DS(SH(0,CV,CJ))	
0009	CJ2=CJ**2	
0010	I4=4*MI-4	
0011	I14=FLPAT(14)	
0012	CF=CFXP(CKOT*I14)	
0013	CIP=CFXP(CKOT)	
0014	C16=CFXP(-CKOT)	
0015	I44=4*MI-4	
0016	I144=FLPAT(144)	
0017	I46=4*MI-4	
0018	I16=FLPAT(146)	
0019	I112=CFXP(-X*I14)	
0020	I112=CFXP(-X*I16)	
0021	CFX=CF*CJ2*(CIP*I11-C16*I12)/CKOT*CV	
0022	CFX=CFX/TA*CV	
0023	TR=REAL(CFX)	
0024	I1=A1MAG(CIX)	
0025	RETURN	
0026	END	

FORTRAN IV G LEVFL 21	FK211	DATE = 75205
0001	SUPROUTINE FK211(MI,MJ,X,TR,Y)	
0002	TPM1CTT CCMPCFX*8TC,REAL*4CT	
0003	COMMON TAKO,CHUR,TPY,TA,CK1,CAK1,TH,T,TKOT,TKO,IPS	
0004	CKOT=(0.,1.)*TKOT	
0005	CY=1.+(0.,1.)*(X/TKOT)	
0006	CY2=CY**2	
0007	CV=TAKO+C SORT(1,-CY2)	
0008	CALL DS(SH(0,CV,CJ))	
0009	CJ2=CJ**2	
0010	I4=4*MI-4	
0011	I14=FLPAT(14)	
0012	CF=CFXP(CKOT*I14)	
0013	CIP=CFXP(CKOT)	
0014	C16=CFXP(-CKOT)	
0015	I44=4*MI-4	
0016	I144=FLPAT(144)	
0017	I46=4*MI-4	
0018	I16=FLPAT(146)	
0019	I112=CFXP(-X*I14)	
0020	I112=CFXP(-X*I16)	
0021	CFX=CF*CJ2*(CIP*I11-C16*I12)/CKOT*CV	
0022	CFX=CFX/TA*TPY	
0023	TR=REAL(CFX)	
0024	I1=A1MAG(CIX)	
0025	RETURN	
0026	END	

THIS PAGE IS BEST QUALITY PRACTICABLE
FROM COPY FURNISHED TO DDC

```

FORTRAN IV G LEVEL 21          FK11R          DATE = 75205

0001      FUNCTION FK11(Y)
0002      IMPLICIT COMMON X*(C),REAL*(Y)
0003      COMMON TAKO,CMUR,TPY,TA,CK1,CAK1,TH,T,TKOT,TKO,IPS
0004      YF2=YF**2
0005      CU=TAKO*CSQRT((1.-YF2)*(1.,0.))
0006      CU1=CU
0007      CALL BSLSM(0,CU,CJ)
0008      CALL BESH(CU1,0.1,CH,TER)
0009      CF=(0.,4.)*CJ*CH*SIN(TKOT*YF)/YF
0010      FK11=REAL(CF)
0011      RETURN
0012      END

FORTRAN IV G LEVEL 21          FK111          DATE = 75205

0001      FUNCTION FK111(Y)
0002      IMPLICIT COMMON X*(C),REAL*(Y)
0003      COMMON TAKO,CMUR,TPY,TA,CK1,CAK1,TH,T,TKOT,TKO,IPS
0004      YF2=YF**2
0005      CU=TAKO*CSQRT((1.-YF2)*(1.,0.))
0006      CU1=CU
0007      CALL BSLSM(0,CU,CJ)
0008      CALL BESH(CU1,0.1,CH,TER)
0009      CF=(0.,4.)*CJ*CH*SIN(TKOT*YF)/YF
0010      FK11=AIMAG(CF)
0011      RETURN
0012      END

FORTRAN IV G LEVEL 21          FM111          DATE = 75205

0001      FUNCTION FM111(Y)
0002      IMPLICIT COMMON X*(C),REAL*(Y)
0003      COMMON TAKO,CMUR,TPY,TA,CK1,CAK1,TH,T,TKOT,TKO,IPS
0004      YF2=YF**2
0005      CU=TAKO*CSQRT((1.-YF2)*(1.,0.))
0006      CU1=CU
0007      CALL BSLSM(1,CU,CJ)
0008      CALL BESH(CU1,0.1,CH,TER)
0009      CF=(0.,4.)*TA*CJ*CH*SIN(TKOT*YF)/(YF*(1.-YF2)*TKO)
0010      FM111=AIMAG(CF)
0011      RETURN
0012      END

FORTRAN IV G LEVEL 21          FM11R          DATE = 75205

0001      FUNCTION FM11R(Y)
0002      IMPLICIT COMMON X*(C),REAL*(Y)
0003      COMMON TAKO,CMUR,TPY,TA,CK1,CAK1,TH,T,TKOT,TKO,IPS
0004      YF2=YF**2
0005      CU=TAKO*CSQRT((1.-YF2)*(1.,0.))
0006      CU1=CU
0007      CALL BSLSM(1,CU,CJ)
0008      CALL BESH(CU1,0.1,CH,TER)
0009      CF=(0.,4.)*TA*CJ*CH*SIN(TKOT*YF)/(YF*(1.-YF2)*TKO)
0010      FM11R=REAL(CF)
0011      RETURN
0012      END

```

```

FORTRAN IV G LEVEL 21          FK211R          DATE = 75205

0001      FUNCTION FK211R(YE)
0002      IMPLICIT COMPLEX*(C), REAL*(4)
0003      COMMON TARKO, CMUR, TPY, TA, CK1, CAK1, TH, T, TKOT, TKO, IPS
0004      YF2 = YE**2
0005      CU = TARKO*CSQRT(1. - YE2)*(1., 0.)
0006      CUI = CU
0007      CALL DSLSM(10, CU, CUI)
0008      CALL DESM(CUI, 1, 1, CH, TPR)
0009      CF = (0., -4.) * TKO * (1. - YE2) * CUI * CH * SIN(TKOT * YE) / YE
0010      FK211R = REAL(CF)
0011      RETURN
0012      END

```

```

FORTRAN IV G LEVEL 21          FK211I          DATE = 75205

0001      FUNCTION FK211I(YE)
0002      IMPLICIT COMPLEX*(C), REAL*(4)
0003      COMMON TARKO, CMUR, TPY, TA, CK1, CAK1, TH, T, TKOT, TKO, IPS
0004      YF2 = YE**2
0005      CU = TARKO*CSQRT(1. - YE2)*(1., 0.)
0006      CUI = CU
0007      CALL DSLSM(10, CU, CUI)
0008      CALL DESM(CUI, 1, 1, CH, TPR)
0009      CF = (0., -4.) * TKO * (1. - YE2) * CUI * CH * SIN(TKOT * YE) / YE
0010      FK211I = AIMAG(CF)
0011      RETURN
0012      END

```

```

FORTRAN IV G LEVEL 21          FK211C          DATE = 75205

0001      FUNCTION FK211C(YE)
0002      COMMON TARKO, CMUR, TPY, TA, CK1, CAK1, TH, T, TKOT, TKO, IPS
0003      IMPLICIT COMPLEX*(C), REAL*(4)
0004      YF2 = YE**2
0005      CU = TARKO*CSQRT(1. - YE2)*(1., 0.)
0006      CUI = CU
0007      CALL DSLSM(11, CU, CUI)
0008      CALL DESM(CUI, 1, 1, CH, TPR)
0009      CF = (0., -4.) * TARKO * CUI * CH * SIN(TKOT * YE) / YE
0010      FK211C = REAL(CF)
0011      RETURN
0012      END

```

```

FORTRAN IV G LEVEL 21          FK211J          DATE = 75205

0001      FUNCTION FK211J(YE)
0002      IMPLICIT COMPLEX*(C), REAL*(4)
0003      COMMON TARKO, CMUR, TPY, TA, CK1, CAK1, TH, T, TKOT, TKO, IPS
0004      YF2 = YE**2
0005      CU = TARKO*CSQRT(1. - YE2)*(1., 0.)
0006      CUI = CU
0007      CALL DSLSM(11, CU, CUI)
0008      CALL DESM(CUI, 1, 1, CH, TPR)
0009      CF = (0., -4.) * TARKO * CUI * CH * SIN(TKOT * YE) / YE
0010      FK211J = AIMAG(CF)
0011      RETURN
0012      END

```


THIS PAGE IS BEST QUALITY PRACTICABLE
FROM COPY FURNISHED TO DDC

FORTRAN IV G LEVEL 21	FCTK	DATE = 75205
0001	SUBROUTINE FCTK(MI,MJ,X,TP,TI)	
0002	IMPLICIT COMPLEX*(C),REAL*(I)	
0003	COMMON TAKO,CMUR,TPY,TA,CKI,CAKI,TH,T,TKOT,TKO,IPS	
0004	CV=1+(0.,1.)*(X/TKOT)	
0005	CV2=CV**2	
0006	CV=TAKO*CSQRT(1.-CV2)	
0007	CALL SSLSM(10,CV,CJ)	
0008	CJ2=CJ**2	
0009	I2=2*MI-2	
0010	I12=I1*AT(I12)	
0011	TKO7=TKOT*TI2	
0012	CKO7=(0.,1.)*TKO7	
0013	CF=CEXP(CKO7)	
0014	CALL AUX(MI,MJ,X,TP,TI)	
0015	C1=CMPLX(TP,TI)	
0016	CFX=CF*CJ2*CI/(CKO7*CV)	
0017	TR=REAL(CFX)	
0018	TI=AIMAG(CFX)	
0019	RETURN	
0020	END	

FORTRAN IV G LEVEL 21	FCTMI	DATE = 75205
0001	SUBROUTINE FCTMI(MI,MJ,X,TP,TI)	
0002	IMPLICIT COMPLEX*(C),REAL*(I)	
0003	COMMON TAKO,CMUR,TPY,TA,CKI,CAKI,TH,T,TKOT,TKO,IPS	
0004	CV=1+(0.,1.)*(X/TKOT)	
0005	CV2=CV**2	
0006	CV=TAKO*CSQRT(1.-CV2)	
0007	CV1=CV	
0008	CV0=CV	
0009	CALL SSLSM(10,CV0,CJ0)	
0010	CALL SSLSM(11,CV1,CJ1)	
0011	CJ2=CJ0*CJ1	
0012	I2=2*MI-2	
0013	I12=I1*AT(I12)	
0014	TKO7=TKOT*TI2	
0015	CKO7=(0.,1.)*TKO7	
0016	CF=CEXP(CKO7)	
0017	CALL AUX(MI,MJ,X,TP,TI)	
0018	C1=CMPLX(TP,TI)	
0019	CFX=CF*CJ2*CI*TA*TA/(CJ0*1.)*TKO7*CV*CV1	
0020	TR=REAL(CFX)	
0021	TI=AIMAG(CFX)	
0022	RETURN	
0023	END	

FORTRAN IV G. LEVEL	21	FCTK2	DATE = 75205
0001	SUBROUTINE FCTK2(MI,MJ,X,TR,II)		
0002	IMPLICIT COMPLEX*8(C),REAL*4(Y)		
0003	COMMON TAKO,CMUR,TPY,TA,CK1,CAK1,TH,T,TKOT,TKO,IPS		
0004	CY=1.+(0.,1.)*(X/TKOT)		
0005	CY2=CY**2		
0006	CV=TAKO*CSQRT(1.-CY2)		
0007	CV1=CV		
0008	CV0=CV		
0009	CALL BSLSM(0,CV0,CJ0)		
0010	CALL BSLSM(1,CV1,CJ1)		
0011	CJ2=CJ0*CJ1		
0012	I2=2*MJ-2		
0013	II2=FLCAT(I2)		
0014	TKO7=TKOT*II2		
0015	CKO2=(0.,1.)*TKO7		
0016	CF=CEXP(CKO2)		
0017	CALL AUX(MI,MJ,X,TR,II)		
0018	C1=CMPLX(TH,II)		
0019	CFX=-CF*CJ2*CV*C1*4./(TA*TKOT*CY)		
0020	TR=REAL(CFX)		
0021	II=AIMAG(CFX)		
0022	RETURN		
0023	END		

FORTRAN IV G. LEVEL	21	FCTM2	DATE = 75205
0001	SUBROUTINE FCTM2(MI,MJ,X,TR,II)		
0002	IMPLICIT COMPLEX*8(C),REAL*4(Y)		
0003	COMMON TAKO,CMUR,TPY,TA,CK1,CAK1,TH,T,TKOT,TKO,IPS		
0004	CY=1.+(0.,1.)*(X/TKOT)		
0005	CY2=CY**2		
0006	CV=TAKO*CSQRT(1.-CY2)		
0007	CALL BSLSM(1,CV,CJ1)		
0008	CJ2=CJ1**2		
0009	I2=2*MJ-2		
0010	II2=FLCAT(I2)		
0011	TKO7=TKOT*II2		
0012	CKO2=(0.,1.)*TKO7		
0013	CF=CEXP(CKO2)		
0014	CALL AUX(MI,MJ,X,TR,II)		
0015	C1=CMPLX(TH,II)		
0016	CFX=-4.*CF*CJ2*C1/(TKOT*CY)		
0017	TR=REAL(CFX)		
0018	II=AIMAG(CFX)		
0019	RETURN		
0020	END		

FORTRAN IV G LEVEL 21		DECOMP	DATE = 75195
0001		SUBROUTINE DECOMP(NN, A, UL)	
0002		DIMENSION SCALES(35), IPS(35)	
0003		COMPLEX A(35,35), UL(35,35), PIVOT, EM	
0004		COMMON TAKO, TPY, TKOT, IPS	
0005		N=NN	
	C		
	C	INITIALIZE IPS, UL AND SCALES	
0006		DO 5 I=1, N	
0007		IPS(I)=I	
0008		ROWNRM=0.0	
0009		DO 2 J=1, N	
0010		UL(I, J)= A(I, J)	
0011		IF(ROWNRM-CABS(UL(I, J))) 1, 2, 2	
0012	1	ROWNRM= CABS(UL(I, J))	
0013	2	CONTINUE	
0014		IF(ROWNRM) 3, 4, 3	
0015	3	SCALES(I)=1.0/ROWNRM	
0016		GO TO 5	
0017	4	CALL SING(1)	
0018		SCALES(I)=0.0	
0019	5	CONTINUE	
	C		
	C	GAUSSIAN ELIMINATION WITH PARTIAL PIVOTING	
0020		NM1=N-1	
0021		DO 17 K=1, NM1	
0022		BIG=0.0	
0023		DO 11 I=K, N	
0024		IP=IPS(I)	
0025		SIZE= CABS(UL(IP, K))*SCALES(IP)	
0026		IF(SIZE-BIG) 11, 11, 10	
0027	10	BIG=SIZE	
0028		INXP=I	
0029	11	CONTINUE	
0030		IF(BIG) 13, 12, 13	
0031	12	CALL SING(2)	
0032		GO TO 17	
0033	13	IF(INXP=K) 14, 15, 14	
0034	14	J=IPS(K)	
0035		IPS(K)=IPS(INXP)	
0036		IPS(INXP)=J	
0037	15	KP = IPS(K)	
0038		PIVOT=UL(KP, K)	
0039		KP1=K+1	
0040		DO 16 I=KP1, N	
0041		IP=IPS(I)	
0042		EM=-UL(IP, K)/PIVOT	
0043		UL(IP, K)=-EM	
0044		DO 16 J=KP1, N	
0045		UL(IP, J)=UL(IP, J)+EM*UL(KP, J)	
	C	INNER LOOP.	
0046	16	CONTINUE	
0047	17	CONTINUE	
0048		KP=IPS(N)	
0049		IF(CABS(UL(KP, N))) 19, 18, 19	
0050	18	CALL SING(2)	
0051	19	RETURN	
0052		END	

FORTRAN IV G LEVEL 21

SOLVE

DATE = 75195

```

0001      SUBROUTINE SOLVE(NN,UL,B,X)
0002      DIMENSION IPS(35)
0003      COMPLEX UL(35,35),B(35),X(35),SUM
0004      COMMON TAKO,TPY,TKOT,IPS
0005      N=NN
0006      NP1= N+1

      C
0007      IP=IPS(1)
0008      X(1)=B(IP)
0009      DO 2 I=2,N
0010      IP=IPS(I)
0011      IM1=I-1
0012      SUM=(0.,0.)
0013      DO 1 J=1,IM1
0014      1 SUM=SUM+UL(IP,J)*X(J)
0015      2 X(I)=B(IP)-SUM

      C
0016      IP=IPS(N)
0017      X(N)= X(N)/UL(IP,N)
0018      DO 4 IBACK=2,N
0019      I=NP1-IBACK
      C 1 GCES (N-1),...,1
0020      IP=IPS(I)
0021      IP1=I+1
0022      SUM=(0.,0.)
0023      DO 3 J=IP1,N
0024      3 SUM=SUM+UL(IP,J)*X(J)
0025      4 X(I)=(X(I)-SUM)/UL(IP,I)
0026      RETURN
0027      END

```

FORTRAN IV G LEVEL 21

ANGLE

DATE = 75195

```

0001      FUNCTION ANGLE(X,Y)
0002      COEFF=57.29577951
0003      IF(X)550,500,450
0004      500 IF(Y) 350,300,250
0005      300 ANGLE=0.0
0006      RETURN
0007      350 ANGLE=270.0
0008      RETURN
0009      250 ANGLE=90.0
0010      RETURN
0011      450 IF(Y) 455,454,453
0012      454 ANGLE=0.0
0013      RETURN
0014      453 ANGLE=COEFF*ATAN(Y/X)
0015      RETURN
0016      455 ANGLE=-COEFF*ATAN(-Y/X)+360.0
0017      RETURN
0018      550 XN=-X
0019      IF(Y)554,553,552
0020      553 ANGLE=180.0
0021      RETURN
0022      552 ANGLE=180.0-COEFF*ATAN(Y/XN)
0023      RETURN
0024      554 ANGLE=180.0+COEFF*ATAN(-Y/XN)
0025      RETURN
0026      END

```

FORTRAN IV G LEVEL 21

IMPRUV

DATE = 75195

```

0001      SUBROUTINE IMPRUV(NN,A,UL,B,X,DIGITS)
0002      CUMMGN TAKO,TPY,TKOT,IPS
0003      COMPLEX A(35,35),UL(35,35),B(35),X(35),R(35),DX(35),T
0004      COMPLEX*16 SUM,AIJ,XJ
0005      C  USES ABS(),AMAX1(),ALOG10()
          N=NN
          C
0006      EPS=1.0E-8
0007      ITMAX=16
          C  **EPS AND ITMAX ARE MACHINE DEPENDENT.
          C
0008      XNORM=0.0
0009      DO 1 I=1,N
0010      1  XNORM=AMAX1(XNORM,CABS(X(I)))
0011      IF(XNORM) 3,2,3
0012      2  DIGITS = -ALOG10(EPS)
0013      GO TO 10
          C
0014      3  DO 9 ITER=1,ITMAX
0015      DO 5 I=1,N
0016      SUM=0.0
0017      DO 4 J=1,N
0018      AIJ=A(I,J)
0019      XJ=X(J)
0020      4  SUM=SUM+AIJ*XJ
0021      SUM=B(I)-SUM
0022      5  R(I)=SUM
          C  **IT IS ESSENTIAL THAT A(I,J)*X(J) YIELD A DOUBLE PRECISION
          C  RESULT AND THAT THE ABOVE + AND - BE DOUBLE PRECISION.**
0023      CALL SOLVE(N,UL,R,DX)
0024      DXNORM=0.0
0025      DO 6 I=1,N
0026      T=X(I)
0027      X(I)=X(I) +DX(I)
0028      DXNORM=AMAX1(DXNORM, CABS(X(I)-T))
0029      6  CONTINUE
0030      IF(ITER-1) 8,7,8
0031      7  DIGITS=-ALOG10(AMAX1(DXNORM/XNORM,EPS))
0032      8  IF(DXNORM-EPS*XNORM) 10,10,9
0033      9  CONTINUE
          C  ITERATION DID NOT CONVERGE
0034      CALL SING(3)
0035      10 RETURN
0036      END

```

THIS PAGE IS BEST QUALITY PRACTICABLE
FROM COPY FURNISHED TO DDG

```

1      SUBROUTINE SERIES(MJ,MJ,C8)
2      IMPLICIT COMPLEX*8(C),REAL*4(T)
3      DIMENSION CSUM(30)
4      COMMON TAKO,CMUR,TPY,TA,CK1,CAK1,TH,T,TKOT,TKO,IPS
5      T1=FLOAT(MJ)-1.
6      T2=FLOAT(MJ)*2.-1.
7      T3=FLOAT(MJ)*2.-3.
8      K=2
9      CSUM(K-1)=(0.,0.)
10     CCOR=-4./(TPY*CMUR)
11     TN=0.
12     5    TP=(TN+.5)*(TPY/TH)
13     CS=1.-((TP/CK1)*2)
14     CZ=CAK1*CSQRT(CS)
15     CZ1=CZ
16     CZO=CZ
17     CALL BSLSML(D,CZO,CJO)
18     CALL BSLSML(1,CZ1,CJ1)
19     TAP=TA*TP
20     COEFT=(CJO*(CZ/CJ1))-TAP-0.5
21     TC1=CO5(2.*TP+T1)
22     TC2=CO5(2.*TKOT+T1)
23     TS1=SIN(TPT+TJL)
24     TS2=SIN(TPT+TJ3)
25     TOR=(TN+.5)*(TAKO*2-TAP*2)
26     IF=((TC1-TC2)*(TS1-TS2))/TOR
27     CSUM(K)=CSUM(K-1)+COEFT*TF
28     T1=CAK1*(CSUM(K))
29     T2=CAK1*(CSUM(K-1))
30     ERR=ABS((T1-T2)/T1)
31     IF (ERR*LE+.1.E-03) GO TO 20
32     K=K+1
33     TN=TN+1
34     IF (K*LE+.26) GO TO 15
35     WRITE (6,16)
36     16    FORMAT (5X,'ERROR CRITERION UNSATISFIED IN 25 TERMS',/)
37     CB=(0.,0.)
38     RETURN
39     15    GO TO 5
40     20    CB=CCOR*CSUM(L)
41     RETURN
42     END

```

```

1      SUBROUTINE AUX(MJ,MJ,X,TR,T1)
2      IMPLICIT COMPLEX*8(C),REAL*4(T)
3      COMMON TAKO,CMW,TPY,TA,CK1,CAK1,TH,T,TKOT,TKO,IPS
4      J1=2*MJ-1
5      T1=FLOAT(J1)
6      J3=2*MJ-3
7      T3=FLOAT(J3)
8      CKOT=(0.,1.)*TKOT
9      MIJ4=CMW*(2*MJ-4)
10     T1=FLOAT(MIJ4)
11     J1=MI-MJ
12     T1=FLOAT(J1)
13     TE2=ABS(T1)*2.
14     MIJ6=CMW*(2*MJ-6)
15     TE3=FLOAT(MIJ6)
16     TE4=TE2*2.
17     T1=EXP(-X*TE1)
18     T2=EXP(-X*TE2)
19     T3=EXP(-X*TE3)
20     T4=EXP(-X*TE4)
21     C1=CEXP(CROT+TJ1)
22     C2=CEXP(-CKOT+TJ3)
23     C3=CEXP(CKOT+TJ3)
24     C4=CEXP(-CKOT+TJ1)
25     CFX=(C1+T1)+C2+T2-C3+T3-C4+T4)
26     TR=REAL(CFX)
27     TI=AIMAG(CFX)
28     RETURN
29     END

```

```

1      SUBROUTINE QGL10(I,J,CT,TGR,TYI)
2      IMPLICIT COMPLEX*8(C),REAL*4(T)
3
4      C
5      10 POINT GAUSS-LAGUERRE QUADRATURE FORMULA OF S.S.P. (IBM)
6      TX=.92070
7      CALL FCT(I,J,TX,TGR,TGI)
8      TYR=.991827E-12 * TGR
9      TYI=.991827E-12 * TGI
10     TX=.21.99659
11     CALL FCT(I,J,TX,TGR,TGI)
12     TYR=TYR+.183565E-8 * TGR
13     TYI=TYI+.183565E-8 * TGI
14     TX=.16.27960
15     CALL FCT(I,J,TX,TGR,TGI)
16     TYR=TYR+.4249314E-6 * TGR
17     TYI=TYI+.4249314E-6 * TGI
18     TX=.11.84379
19     CALL FCT(I,J,TX,TGR,TGI)
20     TYR=TYR+.2825923E-4 * TGR
21     TYI=TYI+.2825923E-4 * TGI
22     TX=.8.330153
23     CALL FCT(I,J,TX,TGR,TGI)
24     TYR=TYR+.7530064E-3 * TGR
25     TYI=TYI+.7530064E-3 * TGI
26     TX=.5.552496
27     CALL FCT(I,J,TX,TGR,TGI)
28     TYR=TYR+.009501517 * TGR
29     TYI=TYI+.009501517 * TGI
30     TX=.3.401434
31     CALL FCT(I,J,TX,TGR,TGI)
32     TYR=TYR+.06268746 * TGR
33     TYI=TYI+.06268746 * TGI
34     TX=.1.608343
35     CALL FCT(I,J,TX,TGR,TGI)
36     TYR=TYR+.2180683 * TGR
37     TYI=TYI+.2180683 * TGI
38     TX=.7294545
39     CALL FCT(I,J,TX,TGR,TGI)
40     TYR=TYR+.4011199 * TGR
41     TYI=TYI+.4011199 * TGI
42     TX=.1377935
43     CALL FCT(I,J,TX,TGR,TGI)
44     TYR=TYR+.3084411 * TGR
45     TYI=TYI+.3084411 * TGI
46     RETURN
47     END

```

```

1      SUBROUTINE GING(I,NHY)
2      11 FORMAT (54HOMATRIX WITH 0 POW IN DECOMPOSE
3      12 FORMAT (54HOSINGULAR MATRIX IN DECOMPOSE. ZERO DIVIDE IN SOLVE)
4      13 FORMAT (54HONG CONVERGENCE IN IMPROV. MATRIX IS NEARLY SINGULAR.
5      00 TO (1,2,3),JNHY
6      1 WRITE (6,11)
7      GO TO 10
8      2 WRITE (6,12)
9      GO TO 10
10     3 WRITE (6,13)
11     10 RETURN
12     END

```

APPENDIX D

BASIS FOR MORE ACCURATE COMPARISON OF THEORETICAL AND EXPERIMENTAL RESULTS

With reference to Fig. 8, the voltage $V(z)$ induced in the receiving loop is proportional to the tangential electric field, viz.,

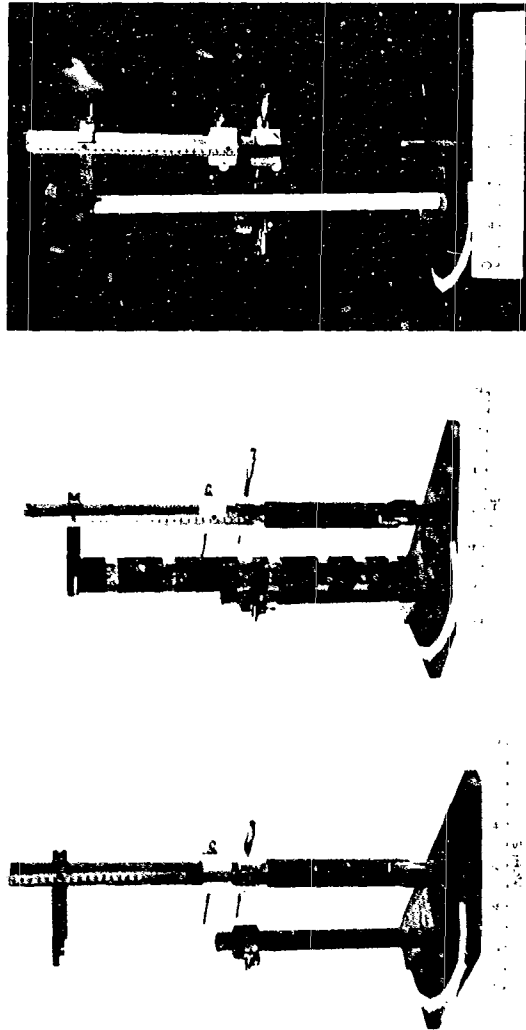
$$V(z) = \int \vec{B}_z \cdot d\vec{S} = -2\pi a E_\phi(a, z)$$

This relation, however, assumes that there is azimuthal symmetry and that the current in the receiving loop is negligible. These assumptions are investigated in detail.

Azimuthal Symmetry. The value of ak_0 for the eleven cases studied in the experiment ranges from .00133 to .01662, whereas $|ak_1|$ has values between .02 to about .41. It is well known that a loop in free space has nearly constant current if $ak_0 \leq .1$. If this criterion is applied, all of the eleven cases are rotationally symmetric. However, if $|ak_1| \leq .1$ is the criterion, rotational symmetry is clearly absent in some of the cases. Because of the unique location of the driving loop on the surface $\rho = a$, a simple analytical criterion on the radius is not possible to ensure rotational symmetry. For this reason, rotational symmetry was ensured experimentally.

As shown in Fig. D-1, a shielded loop of 3/16 in. diameter was fabricated and used to measure the voltage induced by the radial magnetic field as a function of azimuthal coordinate for eight of the eleven cases. The largest deviation from a constant value was found to be less than 5%. The three antennas not tested had lower values of $|ak_1|$ than those tested. The experimental measurements established rotational symmetry conclusively for all of the cases considered in the experimental study.

Measurements were then made of the total axial magnetic current on a



(a) (b) (c)
FIG D-1 PHOTOGRAPH SHOWING THE DRIVEN LOOP AND THE TWO RECEIVING LOOPS. c) AIR CORE
b) LARGEST RADIUS FERRITE CORE c) TEFLON CORE.

dielectric rod made of Teflon, as shown in Fig. D-1(c). The experimental parameters are summarized below:

Diameter of the driven loop = 1.0^+ inch

Diameter of the Teflon rod = 1.0 inch

Diameter of loop for axial measurements = 1.0 inch

Diameter of loop for radial measurements = 3/16 inch

Frequency = 20 MHz

The axial magnetic current distribution was measured with and without the Teflon rod present. The results are tabulated in Table D-1 and plotted in Fig. D-2. As one might expect, the dielectric rod ($\epsilon_r \approx 2.2$) has very little effect, and the measurements taken with it present do not differ significantly from those taken with it absent. In both cases, rotational symmetry was confirmed experimentally. The characteristics of the Teflon rod antenna are similar to those of the air-core antenna because the loop used in the experiment was small enough to act as a magnetic dipole.

Correction to Experimental Data. An answer was then sought to the important question, what is the voltage $V(z)$ induced at the terminals of the receiving loop? The receiving loop is loaded by the vector voltmeter which has a nominal impedance of 100 K-ohms shunted by a 2.5 pf capacitor. The frequency in this experiment varies from 5 to 150 MHz so that the vector voltmeter impedance has a range of values. An analysis based on circuit theory can be carried out to determine accurately the voltage $V_R(z)$ measured by the vector voltmeter. A diagram of the two coupled circuits is in Fig. D-3. The various quantities shown in the figure are:

$V_e^{-i\omega t}$ = Oscillator voltage

TABLE D-1: Unnormalized experimental data of total axial magnetic current with an air core and also a teflon rod. (This data is plotted in Figure D-2).

Z cms	Air Core $ak_o = .00532$		Teflon, $\epsilon_r = 2.2$, $ak_o = .00792$	
	Mag	Phase	Mag	Phase
0.3	11.0	35	11.0	40
0.5	8.4	35	8.5	40
1.0	4.5	35	4.35	40
1.5	2.4	35	2.58	40.1
2.0	1.5	35	1.60	40.2
2.5	.98	35.4	1.02	40.3
3.0	.65	35.5	.695	40.4
3.5	.45	35.6	.500	40.6
4.0	.33	35.6	.365	40.7
4.5	.245	36	.265	40.7
5.0	.18	36	.205	40.7
5.5	.15	36	.155	40.7
6.0	.135	36.2	.130	40.8
6.5	.105	36.2	.10	41
7.0	.085	36	.083	41
7.5	.07	36	.067	41
8.0	.06	36	.056	41
8.5	.05	36	.048	41
9.0	.04	36	.041	41
10.0	.03	36	.03	41

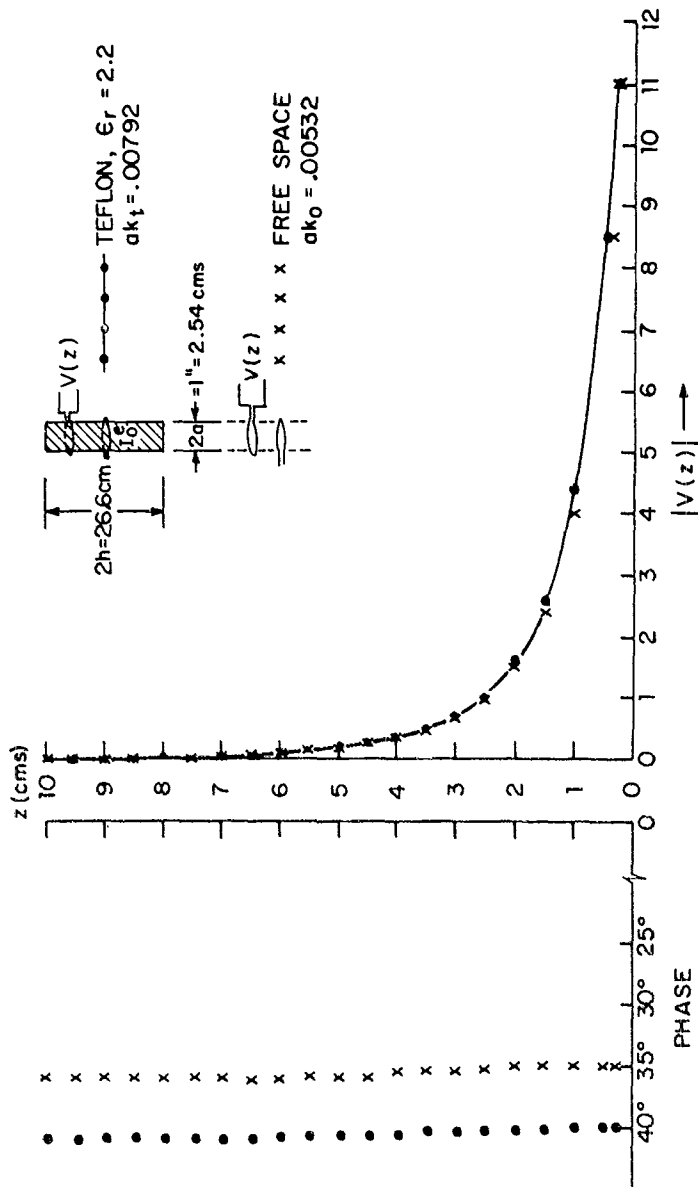


FIG. D-2 PLOT OF MAGNITUDE AND PHASE OF THE RECEIVED VOLTAGE WITH AND WITHOUT A DIELECTRIC ROD. (THE DATA IS IN TABLE D-1)

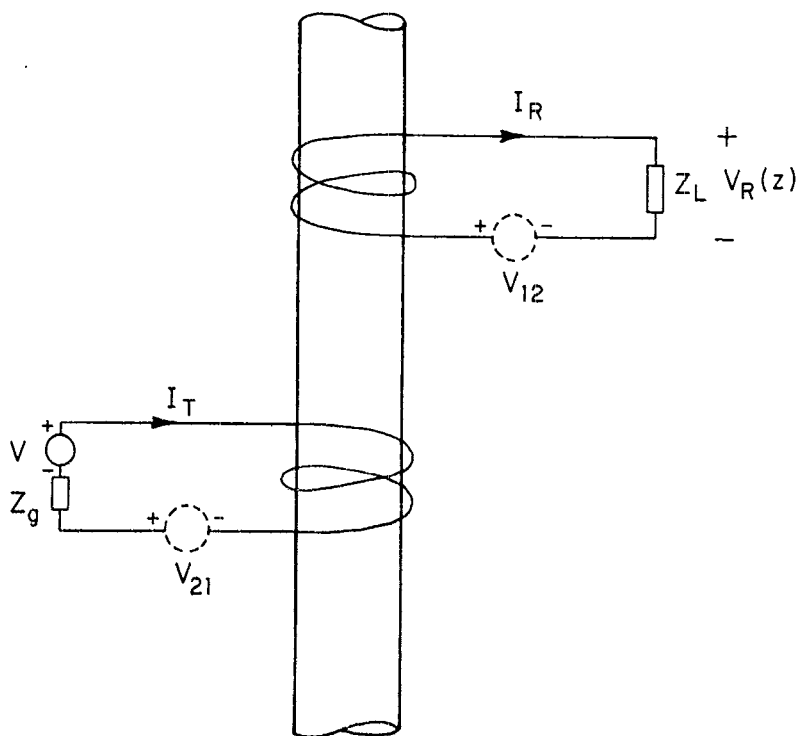


FIG. D-3 THE TWO COUPLED CIRCUITS

Z_g = Generator impedance

I_T = Current in the transmitting loop

$V_{21} = V_{12}$ = Fictitious generator due to coupling

I_R = Current in the receiving loop

Z_L = Vector voltmeter impedance

The two mesh equations can be written as

$$V = I_T(Z_g + Z_r) - I_R Z_M \quad (D-1)$$

$$0 = I_T(-Z_M) + I_R(Z_g + Z_L) \quad (D-2)$$

where Z_M is the mutual impedance, Z_g the self-impedance of the two loops.

From (D-1),

$$I_T = (V + I_R Z_M) / (Z_g + Z_r)$$

Substituting this into (D-2) gives

$$0 = \frac{(V + I_R Z_M)(-Z_M)}{(Z_g + Z_r)} + I_R(Z_g + Z_L)$$

or

$$I_R = \frac{V Z_M}{(Z_g + Z_r)} \frac{1}{[(Z_g + Z_L) - Z_M^2 / (Z_g + Z_r)]}$$

The measured voltage $V_R(z) = I_R Z_L$ in Fig. D-3 is, therefore,

$$\begin{aligned} V_R(z) &= \frac{V Z_M Z_L}{(Z_g + Z_r)} \frac{1}{[(Z_g + Z_L) - Z_M^2 / (Z_g + Z_r)]} \\ &= \frac{V Z_M}{Z_g} \left(\frac{1}{1 + Z_r / Z_g} \right) \left(\frac{1}{1 + Z_g / Z_L} \right) \left[\frac{1}{1 - Z_M^2 / (Z_g + Z_r)(Z_g + Z_L)} \right] \quad (D-3) \end{aligned}$$

The theoretical computations from the integral equation account only for the mutual coupling and ignore the generator impedance Z_g , the loading of the receiver by the vector voltmeter impedance Z_L , and the change in the current in the transmitting loop due to the nearness of the receiving loop. The correction terms can be identified in (D-3) as follows:

$$V_R(z) \Big|_{\text{measured}} = V_R(z) \Big|_{\text{calculated}} \times C_1 \times C_2 \times C_3(z) \quad (D-4)$$

where

C_1 = Correction due to generator impedance.

C_2 = Correction due to the loading of the vector voltmeter.

$C_3(z)$ = Correction due to secondary coupling (Lenz's Law).

It is observed that the correction terms C_1 and C_2 are independent of the separation between the two loops. Since the measured $V_R(z)$ is only relative in the present study, $C_3(z)$ is the only correction factor which is significant. It is [from the right-hand term in (D-3)]:

$$C_3(z) = \left[\frac{1}{1 - Z_M^2(z) / (Z_g + Z_R)(Z_g + Z_L)} \right] \quad (D-5)$$

As a first approximation the generator impedance Z_g is set equal to zero. Z_L is the impedance of the vector voltmeter transferred to the gap in the receiving loop. The impedance of the vector voltmeter is composed of a 100 k-ohm resistor shunted by a 2.5 pf capacitance, viz.,

$$Z_{VVM} = R / (1 + j\omega CR)$$

with $R = 10^5$ ohms and $C = 2.5 \times 10^{-12}$ farads. Z_L can be calculated using

$$Z_L = R_c \left(\frac{Z_{VVM} + jR_c \tan \beta d}{R_c + jZ_{VVM} \tan \beta d} \right) \quad (D-6)$$

where

$R_c = 50 \text{ ohms}$ = Characteristic impedance of the line

$$\beta = \beta_0 \epsilon_{rt}^{1/2}$$

ϵ_{rt} = Dielectric constant of Teflon FEP

d = Distance from the vector voltmeter output terminals to the gap in the receiving loop

An approximate value for $C_3(z)$ can now be computed using (D-5) with Z_g set equal to zero. However, Z_M - the mutual impedance between two loops that are in the near zone of one another - is still unknown. An excellent analysis of the mutual impedance of two loops in air is available [8]. In the present case, however, the mutual impedance is required when the ferrite is present. If the permeability μ_0 in King's analysis [8] is replaced by the permeability μ_1 of the ferrite, an approximate value for the mutual impedance is obtained, viz.,

$$Z_M(z) = (j\omega\mu_1 a^2/2) \{ [4/(z^2 + 4a^2)]^{1/2} [(2/\Lambda^2 - 1)K(\pi/2, a) - (2/\Lambda^2)F(\pi/2, a)] - j\pi a^2 k_1^3/3 \} \quad (D-7)$$

where

ω = Angular frequency; k_1 = Propagation Constant in the ferrite = $\omega\sqrt{\mu_1\epsilon_1}$

μ_1 = Permeability of the ferrite; ϵ_1 = Permittivity of the ferrite

a = Radius of the two loops

z = Distance separating the two loops

$$\Lambda^2 = \sin^2 \alpha = 4a^2/(z^2 + 4a^2)$$

$$K(\pi/2, a) = \int_0^{\pi/2} \frac{d\psi}{(1 - \sin^2 \alpha \sin^2 \psi)^{1/2}} = \text{Elliptic integral of the first kind}$$

and

$$F(\pi/2, \alpha) = \int_0^{\pi/2} (1 - \sin^2 \alpha \sin^2 \psi)^{1/2} d\psi = \text{Elliptic integral of the second kind}$$

Fortran IV computer programs for computing the elliptic functions were available in the Scientific Subroutine Package of IBM 360. Thus, the correction factor $C_3(z)$ was computed as a function of the separation distance z using equations (D-5), (D-6) and (D-7). This factor was then used to correct the experimental data for a comparison with the theoretical results. A typical comparison of the theory with corrected and uncorrected experimental data is shown in Fig. D-4 for the specific case of antenna #6. The uncorrected experimental data depart from the theoretical curve near the driving point, $0 \leq z/h \leq .25$. The vector voltmeter impedance Z_L at the gap for the antenna configuration under consideration (antenna #6) is $Z_L = 2.88 - j534.7$ ohms. The corrected experimental data obtained when this value of Z_L is used to compute the correction factor are plotted in Fig. D-4 and are seen to deviate less from the theory than the uncorrected values. The correction factor does not account for the entire discrepancy, however. This is in part because of the approximations made in computing the correction factor and in part because of the lack of an accurate value for Z_L . For this reason, the correction factor was also computed for a range of real and imaginary parts of Z_L . Two representative cases are shown in Fig. D-4. They illustrate that a precise knowledge of Z_L could improve the accuracy of the correction factor applied to the experimental data and, thus, minimize the discrepancy with theory near the driving point. Away from the driving point ($z/h \geq .25$) the agreement is seen to be very good.

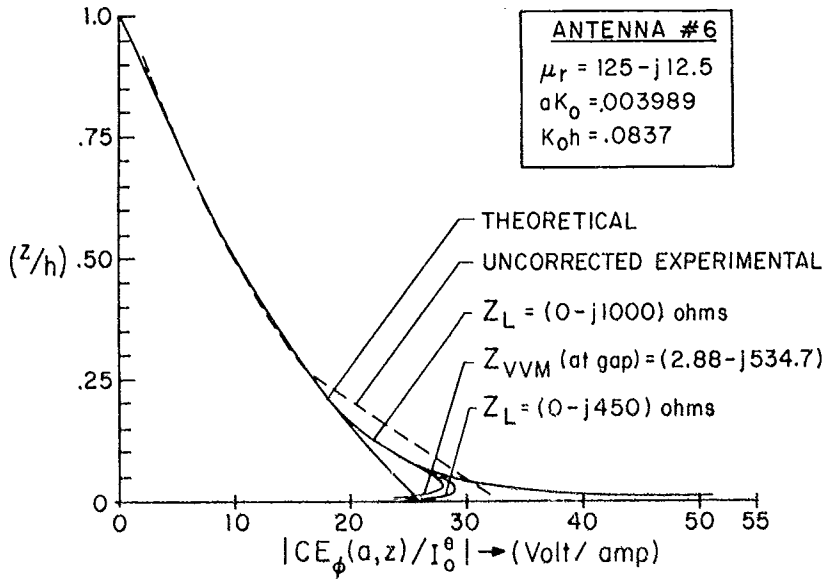


FIG. D-4 MAGNITUDE OF THE VOLTAGE RECEIVED BY THE MEASURING LOOP

ACKNOWLEDGMENT

The authors wish to thank Dr. G. S. Smith and Mr. Neal Whitman for their help in the design and construction of the experimental apparatus. Thanks are also due Dr. D. H. Preis for painstakingly reading the manuscript and Ms. Margaret Owens for her assistance in the preparation of this report.

REFERENCES

- [1] R. W. P. King and C. W. Harrison, Jr., Antennas and Waves: A Modern Approach. Cambridge, Mass.: M.I.T. Press, 1969, pp. 143-149.
- [2] D. V. Giri, "Electrically Small Loop Antenna Loaded by a Homogeneous and Isotropic Ferrite Cylinder - Part I," Technical Report No. 646, Division of Engineering and Applied Physics, Harvard University, Cambridge, Mass., July 1973.
- [3] R. W. P. King and T. T. Wu, "The Imperfectly Conducting Cylindrical Transmitting Antenna," IEEE Trans. Antennas Propagat., vol. AP-14, No. 5, pp. 524-534, May 1966.
- [4] R. W. P. King, C. W. Harrison, Jr., and E. A. Aronson, "The Imperfectly Conducting Cylindrical Transmitting Antenna; Numerical Results," IEEE Trans. Antennas Propagat., vol. AP-14, No. 5, pp. 535-542, May 1966.
- [5] A. Sommerfeld, Electrodynamics. New York, N.Y.: Academic Press, 1966, pp. 177-185, 3rd Edition.
- [6] G. E. Forsyth and C. B. Moler, Computer Solution of Linear Algebraic Systems. New York: Prentice-Hall, 1967.
- [7] H. A. Dropkin, E. Metzger, and J. C. Cacheris, "VHF Ferrite Antenna Radiation Measurements," Diamond Ordnance Fuze Laboratories, Washington, D.C., Tech. Report No. TR-484, July 1957.
- [8] R. W. P. King, Fundamental Electromagnetic Theory. New York: Dover Publications, 1963, Ch. VI, Secs. 13 and 14.

